

Utah State University

DigitalCommons@USU

---

All Graduate Theses and Dissertations

Graduate Studies

---

8-2020

## Soil Health Assessment on Arid Rangeland Soils Impacted by Oil and Gas Exploration, Development, and Extraction

Justin Allred  
*Utah State University*

Follow this and additional works at: <https://digitalcommons.usu.edu/etd>



Part of the [Soil Science Commons](#)

---

### Recommended Citation

Allred, Justin, "Soil Health Assessment on Arid Rangeland Soils Impacted by Oil and Gas Exploration, Development, and Extraction" (2020). *All Graduate Theses and Dissertations*. 7815.

<https://digitalcommons.usu.edu/etd/7815>

This Thesis is brought to you for free and open access by the Graduate Studies at DigitalCommons@USU. It has been accepted for inclusion in All Graduate Theses and Dissertations by an authorized administrator of DigitalCommons@USU. For more information, please contact [digitalcommons@usu.edu](mailto:digitalcommons@usu.edu).



SOIL HEALTH ASSESSMENT ON ARID RANGELAND SOILS IMPACTED BY OIL  
AND GAS EXPLORATION, DEVELOPMENT, AND EXTRACTION

by

Justin Allred

A thesis submitted in partial fulfillment  
of the requirements of the degree

of

MASTER OF SCIENCE

in

Soil Science

Approved:

---

Paul Grossl, Ph.D.  
Major Professor

---

Grant Cardon, Ph.D.  
Committee Member

---

Colleen Jones, Ph.D.  
Committee Member

---

Seth Lyman, Ph.D.  
Committee Member

---

Richard S. Inouye, Ph.D.  
Vice Provost for Graduate Studies

UTAH STATE UNIVERSITY  
Logan, Utah

2020

Copyright © Justin Allred 2020

All Rights Reserved

## ABSTRACT

Soil Health Assessment on Arid Rangeland Soils Impacted by Oil and Gas Exploration,  
Development, and Extraction

by

Justin Allred, Masters of Science

Utah State University, 2020

Major Professor: Dr. Paul Grossl  
Department: Plants, Soils, and Climate

Oil and gas well pad reclamation in arid environments such as in the Uinta Basin of Utah, presents unique challenges, including remote locations, limited water, and elevated soil salinity and sodicity. Successfully reclaimed Plugged and Abandoned (P&A) well pads should resemble the surrounding rangeland once fully reclaimed. Revegetation of native species is the primary indicator of successful reclamation. Still, the lack of water makes it challenging to re-seed native plants, while trying to prevent the encroachment of invasive plant species such as *Bromus tectorum* (cheatgrass), *Salsola tragus* (Russian thistle), and *Halogeton glomeratus* (halogeton). Could successful reclamation be reflective of good soil health? Our objective was to determine if land disturbance negatively impacted soil health and consequently successful revegetation, by performing a soil health assessment on P&A well pads (disturbed soils) and comparing that to the soil health of the surrounding, adjacent rangeland (undisturbed soil). By using



undisturbed rangeland soil as the desired reclamation goal for the P&A well pad, certain soil health indicators were chosen for comparison between the two sites.

Overall, P&A well pads had reduced soil health compared to the undisturbed rangeland. There was a difference in soil texture, with the undisturbed rangeland having a coarser soil texture (sandy loam) and the P&A well pads having a finer soil texture (clay loam, sandy clay loam). Compared to the rangeland, the P&A well pads had higher sodicity levels, measured by sodium adsorption ratio (SAR) and exchangeable sodium percentage (ESP), making the P&A well pads more susceptible to sodic crust formation and reducing aggregate stability. Electromagnetic induction sensing (EMI) was also used, to see if it could quickly identify soil health indicators ( $EC_e$ , SAR, pH, texture, etc.) to aid land managers in a more direct, targeted reclamation strategy. Many different soil properties can impact EMI reading, so while useful, EMI cannot always be relied on for the desired soil health indicators for reclamation.

## PUBLIC ABSTRACT

Soil Health Assessment on Arid Rangeland Soils Impacted by Oil and Gas Exploration,  
Development, and Extraction

by

Justin Allred, Masters of Science

Utah State University, 2020

Oil and gas well pad reclamation in arid environments such as in the Uinta Basin of Utah, presents unique challenges, including remote locations, limited water, and elevated soil salinity and sodicity. Successfully reclaimed Plugged and Abandoned (P&A) well pads should resemble the surrounding rangeland once fully reclaimed. Revegetation of native species is the primary indicator of successful reclamation, but the lack of water makes it challenging to re-seed native plants, while trying to prevent the encroachment of invasive plant species such as *Bromus tectorum* (cheatgrass), *Salsola tragus* (Russian thistle), and *Halogeton glomeratus* (halogeton). Could successful reclamation be reflective of good soil health? Our objective was to determine if land disturbance negatively impacted soil health and consequently successful revegetation, by performing a soil health assessment on P&A well pads (disturbed soils) and comparing that to the soil health of the surrounding, adjacent rangeland (undisturbed soil). By using undisturbed rangeland soil as the desired reclamation goal for the P&A well pad, certain soil health indicators were chosen for comparison between the two sites.

Overall, P&A well pads had reduced soil health compared to the undisturbed rangeland. There was a difference in soil texture, with the undisturbed rangeland having a coarser soil texture (sandy loam) and the P&A well pads having a finer soil texture (clay loam, sandy clay loam). Compared to the rangeland, the P&A well pads had higher sodicity levels, measured by sodium adsorption ratio (SAR) and exchangeable sodium percentage (ESP), making the P&A well pads more susceptible to sodic crust formation and reducing aggregate stability. Electromagnetic induction sensing (EMI) was also used, to see if it could quickly identify soil health indicators ( $EC_e$ , SAR, pH, texture, etc.) to aid land managers in a more direct, targeted reclamation strategy. Many different soil properties can impact EMI reading, so while useful, EMI cannot always be relied on for the desired soil health indicators for reclamation.

## ACKNOWLEDGMENTS

I would like to thank my major advisor, Dr. Paul Grossl, for providing the opportunity for me to work for him as an undergraduate as well as encouraging me to pursue a graduate degree. I would also like to thank my committee members, Dr. Grant Cardon, Dr. Colleen Jones, and Dr. Seth Lyman, for their advice and guidance. I would also thank Bailey Shaffer, Trevor O'Neil, and Anthony Whaley for all of their help, collecting and testing samples, and understanding the data collected.

I would also like to thank the Vernal Field Office of the Bureau of Land Management for support funding this project (BLM #L16AC00126, Reclamation of Lands Impacted by Energy Exploration and Extraction Activities in the Uinta Basin, Utah). Also, thanks to Newfield Exploration, Uinta Basin Office, for their help selected P&A well pad sites used in the study, as well as allowing access to the selected sites.

Most importantly, I would like to thank my family and friends for their support in all my schooling and their encouragement to pursue advanced education.

Justin Allred

## CONTENTS

	Page
ABSTRACT.....	iii
PUBLIC ABSTRACT .....	v
ACKNOWLEDGMENTS .....	vii
LIST OF TABLES .....	x
LIST OF FIGURES .....	xii
ACRONYMS.....	xviii
CHAPTER	
1. INTRODUCTION .....	1
Oil and Gas Exploration, Development, and Extraction .....	2
Soil Health .....	5
Soil Salinity and Sodicity .....	7
Aggregate Stability .....	9
Soil Organic Carbon .....	11
Soil Microbial Activity.....	12
Electromagnetic Induction.....	14
2. SOIL HEALTH ASSESSEMENT ON ARID RANGELAND SOILS IMPACTED BY OIL AND GAS EXPLORATION, DEVELOPMENT, AND EXTRACTION .....	15
Introduction.....	15
Methods and Materials .....	18
Location Selection .....	18
Soil Sampling .....	20
Soil Health.....	22
Electromagnetic Induction.....	31
ArcGIS Modeling .....	33

	ix
Results.....	35
Soil Health .....	35
Electromagnetic Induction.....	45
Discussion.....	50
Soil Health .....	51
Electromagnetic Induction.....	53
3. SUMMARY .....	54
REFERENCES .....	56
APPENDICES .....	60

## LIST OF TABLES

Table		Page
1	The total percent cover from plant counts split into beneficial and invasive for P&A well pads (Pad) and the adjacent rangeland. Also included is the ratio of beneficial vs invasive plant cover .....	42
2	List of pad numbers and their corresponding information .....	60
3	All soil tests performed with mean and error values with corresponding site names. Pad indicates P&A well pad and RL indicates the adjacent rangeland .....	61
4	List of tested soil attributes and the P&A well pad/rangeland, with the associated T-Stat and P-Value, showing significant differences between the P&A well pad and rangeland .....	62
5	List of plants found during plant counts and split into either beneficial or invasive .....	63
6	Site names with corresponding GPS coordinates, dates sampled, and number of days since the start of reclamation. Site 9-18-9-19 has been used for previous studies and has been disturbed multiple times since reclamation was started .....	64
7	SAS Studio software output for multiple regression for $EM_H$ with all 240 sample sites and all soil properties that could impact $EM_H$ . Significant factors include: SAR, soil temperature, soil moisture, soil organic carbon, and soil pH .....	65
8	SAS Studio software output for multiple regression for $EM_H$ , with all 240 sample sites and soil properties that had the greatest influence from the original multiple regression (Table 7). SAR had the greatest influence out of the five soil properties .....	65
9	SAS Studio software output for multiple regression for $EM_H$ , using the ground truthing (101) sample sites and all soil properties that could impact $EM_H$ . Significant factors include: SAR and soil moisture .....	66
10	SAS Studio software output for multiple regression for $EM_H$ , using the ground truthing (101) sites and soil properties that had the greatest influence from the original multiple regression	

(Table 9). SAR had the greatest influence between SAR and soil moisture.....	66
11 Dates, soil moisture, soil temperature, and the number of ground truthing for each location for EMI .....	67



## LIST OF FIGURES

Figure		Page
1	Typical location on Pariette Bench. Taken from site 9-18-9-19_RL with 9-18-9-19 in background .....	17
2	Map showing P&A well pad locations on the Pariette Bench, Utah. Service Layer Credits: Source: Esri, DigitalGlobe, GeoEye, Earthstar Geographics, CNES/Airbus DS, USDA, AeroGRID, IGN, and the GIS User Community.....	20
3	Soil sample taken from 9-18-9-19. Visable physical soil crust.....	21
4	Map showing the soil sampling grid for 12-11-9-18 .....	22
5	Soil textures being determined with hydrometers .....	23
6	Aggregate stability being conducted with sieving apparatus being ran, submerging aggregates .....	25
7	Aggregate stability results after sieving and prior to being placed in oven for final drying. The slake material (unstable aggregate) in the foreground, with the non-aggregate in the background .....	26
8	Soil saturated paste extracts being extracted for pH, EC <sub>e</sub> , and SAR .....	27
9	Dynamic CO <sub>2</sub> flux being measured on 2-35-8-18 with a polycarbonate flux chamber, with the hose running to the trailer containing the LGR greenhouse gas analyzer.....	30
10	Plant counts being performed using a meter squared to measure plant cover on the rangeland adjacent to 12-11-9-18 .....	31
11	Electromagnetic induction sensor (EMI) being carried across rangeland adjacent to 11-12-9-17 .....	32
12	Texture triangle displaying each soil sample with the corresponding P&A well pad and rangeland .....	36
13	Percentage of clay with mean and error at all six locations .....	37
14	Interpolation map displaying EC <sub>e</sub> values from all pads and the corresponding rangelands. Service Layer Credits: Source: Esri,	

	DigitalGlobe, GeoEye, Earthstar Geographics, CNES/Airbus DS,a USDA, AeroGRID, IGN, and the GIS User Community .....	38
15	Electrical conductivity from a saturated paste extract ( $EC_e$ ) mean and error at all six locations .....	38
16	Interpolation map displaying SAR values from all pads and the corresponding rangelands. Service Layer Credits: Source: Esri, DigitalGlobe, GeoEye, Earthstar Geographics, CNES/Airbus DS,a USDA, AeroGRID, IGN, and the GIS User Community .....	39
17	Sodium Adsorption Ratio (SAR) mean and error at all six locations .....	40
18	Percentages of plant cover for beneficial (left) and invasive (right) plants at all six locations with mean and error .....	41
19	Percent plant cover of beneficial and invasive plants at all six locations with mean and error.....	42
20	Aggregate Stability mean and error for the two locations tested.....	43
21	CO <sub>2</sub> Flux mean and error at the two locations measured. CO <sub>2</sub> flux is being used to measure soil CO <sub>2</sub> respiration.....	44
22	Interpolation map displaying the EM <sub>H</sub> (left) and SAR (right) values from pad 7-8-9-18 and its corresponding rangeland. Service Layer Credits: Source: Esri, DigitalGlobe, GeoEye, Earthstar Geographics, CNES/Airbus DS, USDA, AeroGRID, IGN, and the GIS User Community .....	47
23	Interpolation map displaying the EM <sub>H</sub> (left) and SAR (right) values from pad 9-18-9-19 and its corresponding rangeland. Service Layer Credits: Source: Esri, DigitalGlobe, GeoEye, Earthstar Geographics, CNES/Airbus DS,a USDA, AeroGRID, IGN, and the GIS User Community .....	47
24	Interpolation maps displaying the EM <sub>H</sub> , SAR, and other values from P&A well pads; 2-35-8-18, 12-11-9-18, & 9-18-91-9 and the corresponding rangelands. Service Layer Credits: Source: Esri, DigitalGlobe, GeoEye, Earthstar Geographics, CNES/Airbus DS,a USDA, AeroGRID, IGN, and the GIS User Community .....	49
25	Interpolation maps displaying the EM <sub>H</sub> , SAR, and other values from P&A well pads; 7-8-9-18, 14-21-9-18Y, & 11-12-9-17 and the corresponding rangelands. Service Layer Credits:	

	Source: Esri, DigitalGlobe, GeoEye, Earthstar Geographics, CNES/Airbus DS,a USDA, AeroGRID, IGN, and the GIS User Community .....	50
26	Well pad with salvaged topsoil.....	53
27	Exchangeable Sodium Percentage (ESP) mean and error at all six locations .....	68
28	Percentages of sand (top left), silt (top right), and clay (bottom) with mean and error at all six locations .....	69
29	Soil pH mean and error at all six locations.....	70
30	Percentages of total carbon (TC), inorganic carbon (IC), and soil organic carbon (SOC) with mean and error at all six locations.....	71
31	Compilation of mean and error for all soil tests performed between P&A well pad 2-35-8-18 and the adjacent rangeland .....	72
32	Compilation of mean and error for all soil tests performed between P&A well pad 12-11-9-18 and the adjacent rangeland .....	73
33	Compilation of mean and error for all soil tests performed between P&A well pad 9-18-9-19 and the adjacent rangeland .....	74
34	Compilation of mean and error for all soil tests performed between P&A well pad 7-8-9-18 and the adjacent rangeland .....	75
35	Compilation of mean and error for all soil tests performed between P&A well pad 14-21-9-18Y and the adjacent rangeland.....	76
36	Compilation of mean and error for all soil tests performed between P&A well pad 11-12-9-17 and the adjacent rangeland .....	77
37	Interpolation map displaying the EM <sub>H</sub> (left) and SAR (right) values from pad 2-35-8-18 and its corresponding rangeland. Service Layer Credits: Source: Esri, DigitalGlobe, GeoEye, Earthstar Geographics, CNES/Airbus DS, USDA, AeroGRID, IGN, and the GIS User Community .....	78
38	Interpolation map displaying the percent of plant cover of beneficial (left) and invasive (right) plants for pad 2-35-8-18 and its corresponding rangeland. Service Layer Credits: Source: Esri, DigitalGlobe, GeoEye, Earthstar Geographics,	

CNES/Airbus DS, USDA, AeroGRID, IGN, and the GIS User Community .....	78
39 Interpolation map displaying the $EC_e$ values from pad 2-35-8-18 and its corresponding rangeland. Service Layer Credits: Source: Esri, DigitalGlobe, GeoEye, Earthstar Geographics, CNES/Airbus DS, USDA, AeroGRID, IGN, and the GIS User Community .....	79
40 Interpolation map displaying the $EM_H$ (left) and SAR (right) values from pad 12-11-9-18 and its corresponding rangeland. Service Layer Credits: Source: Esri, DigitalGlobe, GeoEye, Earthstar Geographics, CNES/Airbus DS, USDA, AeroGRID, IGN, and the GIS User Community .....	79
41 Interpolation map displaying the percent of plant cover of beneficial (left) and invasive (right) plants for pad 12-11-9-18 and its corresponding rangeland. Service Layer Credits: Source: Esri, DigitalGlobe, GeoEye, Earthstar Geographics, CNES/Airbus DS, USDA, AeroGRID, IGN, and the GIS User Community .....	80
42 Interpolation map displaying the $EC_e$ values from pad 12-11-9-18 and its corresponding rangeland. Service Layer Credits: Source: Esri, DigitalGlobe, GeoEye, Earthstar Geographics, CNES/Airbus DS, USDA, AeroGRID, IGN, and the GIS User Community .....	80
43 Interpolation map displaying the percent of plant cover of beneficial (left) and invasive (right) plants for pad 9-18-9-19 and its corresponding rangeland. Service Layer Credits: Source: Esri, DigitalGlobe, GeoEye, Earthstar Geographics, CNES/Airbus DS, USDA, AeroGRID, IGN, and the GIS User Community .....	81
44 Interpolation map displaying the $EC_e$ values from pad 9-18-9-19 and its corresponding rangeland. Service Layer Credits: Source: Esri, DigitalGlobe, GeoEye, Earthstar Geographics, CNES/Airbus DS, USDA, AeroGRID, IGN, and the GIS User Community .....	81
45 Interpolation map displaying the percent of plant cover of beneficial (left) and invasive (right) plants for pad 7-8-9-18 and its corresponding rangeland. Service Layer Credits: Source: Esri, DigitalGlobe, GeoEye, Earthstar Geographics,	

	CNES/Airbus DS, USDA, AeroGRID, IGN, and the GIS User Community .....	82
46	Interpolation map displaying the $EC_e$ values from pad 7-8-9-18 and its corresponding rangeland. Service Layer Credits: Source: Esri, DigitalGlobe, GeoEye, Earthstar Geographics, CNES/Airbus DS, USDA, AeroGRID, IGN, and the GIS User Community .....	82
47	Interpolation map displaying the $EM_H$ (left) and SAR (right) values from pad 14-21-9-18Y and its corresponding rangeland. Service Layer Credits: Source: Esri, DigitalGlobe, GeoEye, Earthstar Geographics, CNES/Airbus DS, USDA, AeroGRID, IGN, and the GIS User Community .....	83
48	Interpolation map displaying the percent of plant cover of beneficial (left) and invasive (right) plants for pad 14-21-9-18Y and its corresponding rangeland. Service Layer Credits: Source: Esri, DigitalGlobe, GeoEye, Earthstar Geographics, CNES/Airbus DS, USDA, AeroGRID, IGN, and the GIS User Community .....	83
49	Interpolation map displaying the $EC_e$ values from pad 14-21-9-18Y and its corresponding rangeland. Service Layer Credits: Source: Esri, DigitalGlobe, GeoEye, Earthstar Geographics, CNES/Airbus DS, USDA, AeroGRID, IGN, and the GIS User Community .....	84
50	Interpolation map displaying the $EM_H$ (left) and SAR (right) values from pad 11-12-9-17 and its corresponding rangeland. Service Layer Credits: Source: Esri, DigitalGlobe, GeoEye, Earthstar Geographics, CNES/Airbus DS, USDA, AeroGRID, IGN, and the GIS User Community .....	84
51	Interpolation map displaying the percent of plant cover of beneficial (left) and invasive (right) plants for pad 11-12-9-17 and its corresponding rangeland. Service Layer Credits: Source: Esri, DigitalGlobe, GeoEye, Earthstar Geographics, CNES/Airbus DS, USDA, AeroGRID, IGN, and the GIS User Community .....	85
52	Interpolation map displaying the $EC_e$ values from pad 11-12-9-17 and its corresponding rangeland. Service Layer Credits: Source: Esri, DigitalGlobe, GeoEye, Earthstar Geographics, CNES/Airbus DS, USDA, AeroGRID, IGN, and the GIS User Community .....	85

53	Plant counts being performed using a meter squared to measure plant cover on 12-11-9-18. Dynamic CO <sub>2</sub> flux being measured with a polycarbonate flux chamber, with the hose running to the trailer containing the LGR greenhouse gas analyzer .....	86
54	Dynamic CO <sub>2</sub> flux being measured on rangeland adjacent to 2-35-8-18 with a polycarbonate flux chamber .....	86
55	Dynamic CO <sub>2</sub> flux being measured on rangeland adjacent to 2-35-8-18 with a polycarbonate flux chamber .....	87
56	Plant counts being performed using a meter squared to measure plant cover on 2-35-8-18. Dynamic CO <sub>2</sub> flux being measured in the background with a polycarbonate flux chamber .....	87
57	Plant counts being performed using a meter squared to measure plant cover on 12-11-9-18 .....	88
58	Plant counts being performed using a meter squared to measure plant cover on 2-35-8-18 .....	88
59	Electromagnetic induction sensor (EMI) being carried across rangeland adjacent to 11-12-9-17 .....	89
60	Well pad 9-18-9-19 with well marker present .....	89
61	Aggregate stability results after sieving and prior to being placed in oven for final drying. Tins containing non-aggregate fraction which remained after sieving and after stable aggregate was crushed and flushed out .....	90
62	Aggregate stability sieving apparatus, with aggregates being re-hydrated prior to sieving in the foreground .....	90
63	Aggregate stability being conducted with sieving apparatus finished cycle. Slaked material (unstable aggregate) has now been collected in metal tins, while the non-aggregate and stable aggregate remain in the sieve .....	91
64	Depth profile variation of EC <sub>e</sub> at P&A well pad and undisturbed site (Grossl, 2017) .....	91

## ACRONYMS

BLM	Bureau of Land Management
BMP	Best Management Plan
CEC	Cation Exchange Capacity
DD	Decimal Degrees
EC <sub>e</sub>	Soil Electrical Conductivity of a Saturated Paste
EM <sub>H</sub>	Electromagnetic Horizontal Reading
EMI	Electromagnetic Induction
EM <sub>v</sub>	Electromagnetic Vertical Reading
ESP	Exchangeable Sodium Percentage
GPS	Global Positioning System
IC	Inorganic Carbon
ICP	Inductively-coupled Plasma Spectrophotometer
IWD	Inverse Distance Weighted
LGR	Los Gatos Research Greenhouse Gas Analyzer
LOP	Life of Project
NDIR	Nondispersive Infrared
NRCS	Natural Resources Conservation Service
OC	Organic Carbon
P&A	Plugged and Abandoned
RL	Rangeland
SAR	Sodium Adsorption Ratio
SOC	Soil Organic Carbon
TC	Total Carbon

## CHAPTER 1: INTRODUCTION

The Pariette Bench, located in the Uinta Basin, roughly 56 km (35 miles) south of Vernal, Utah, is a typical arid rangeland (remote, expansive, unsuitable for crop production, etc. (Skaggs, 2008)), similar to many managed by the Bureau of Land Management (BLM) of the U.S. Department of the Interior. Along with its remote location, the lack of water in this arid environment makes reclamation challenging to implement. The Ouray, Utah weather station (40.1344°, -109.644°), located 20 km (12 miles) from the Pariette Bench, has recorded an average of 170.5 mm (6.5 in) of annual precipitation from 1985 – 2018.

Arid soils, like those on the Pariette Bench, are prone to higher levels of salinity and sodicity than non-arid soils (USDA – ARS, 1954). Once disturbed, salinity and sodicity levels become exacerbated, making revegetation of native plants challenging, resulting in the establishment of invasive plants (Grossl, 2017; Dose et al., 2015). The use of cover crops to compete against invasive plant species, mainly *Bromus tectorum* (cheatgrass), *Salsola tragus* (Russian thistle), and *Halogeton glomeratus* (halogeton), have proven challenging to implement with success (Grossl, 2017). The lack of consistent moisture in this region makes for uncoordinated planting times, resulting in unsuccessful cover crop germination.

These challenges have led to the need for a better understanding of the soil health (also referred to as soil quality) on plugged and abandoned (P&A) well pads and the influence of soil disturbance from oil and gas exploration, development, and extraction.



## OIL AND GAS EXPLORATION, DEVELOPMENT, AND EXTRACTION

A single oil and gas well pad is typically 1ha (2.5 acres) in size, but can be as large as 2.5 ha (6 acres) for multi-well pads (USDI – BLM, 2012). As of August 2011, in the Uinta Basin, there were 9,636 ha (23,811 acres) of disturbed land from oil and gas development, with a projected 33,177 ha (81,981 acres) (17,654 ha (43,625 acres) for the life of project (LOP)) based on future development plans over the next 15 – 20 years (USDI – BLM, 2012). There were 10,689 oil and gas wells on 9,197 pads (USDI – BLM, 2012). As of August 2011, 176 well pads (178 ha (440 acres)) were considered plugged and abandoned by the Bureau of Land Management, but still unreclaimed.

Prior to pad development, a reclamation plan must be submitted and approved by the BLM. The plan must explain “the complexity of the project, the environmental concerns..., and the reclamation potential for the site” (USDI – BLM, 2011, p.1). The reclamation plan should address a short-term plan that facilitates long term reclamation (USDI – BLM, 2011). “Reclamation is most effective when the ecology of the site is considered” (USDI – BLM, 2007, p. 45). The Green River District, that oversees the Uinta Basin, has a set of reclamation objectives and guidelines, listed in *Green River District Reclamation Guidelines* (2011). These reclamation objectives and guidelines include the following:

1. Establish a desired self-perpetuating plant community.
  - a. Non-native plants can be used, but they should not compete long term with native plants.
  - b. Drill seeding is preferred to broadcast seeding with 148 seeds m<sup>-1</sup> (45 seeds ft<sup>-1</sup>). Seeds should be placed at 6.35 – 12.7 mm (0.25 – 0.5 in)

deep. If broadcast, harrowing, drag bar, or roller should be used to cover seeds to the same depth.

- c. Seeding should happen between August 15 and winter freezing.
  - d. Mulching may be required, depending on the site. Mulching should be applied within 24 hours following seeding and should be weed-free straw or native grass hay. Hydro-mulching may also be used.
2. Ensure slope stability and topographic diversity.
  3. Reconstruct and stabilize altered watercourses and drainage features.
  4. Ensure the biological, chemical, and physical integrity of the topsoil resource during all phases of construction, operation, and reclamation. BMP's (best management practices) designed to minimize and prevent erosion, compaction, and contamination of the topsoil resource should be used to maintain the topsoil resource.
    - a. Topsoil should be segregated from the subsoil without mixing them.
    - b. Topsoil should be integrated, where possible, into the existing production landscape.
    - c. Action should be taken to avoid soil compaction.
  5. Re-establish the visual composition and characteristics to blend with the natural surroundings.
  6. Control the occurrences of noxious weeds and undesirable invasive species by utilizing principles of integrated weed management including prevention, mechanical, chemical, and biological control methods.
  7. Manage all waste materials.
  8. Conduct monitoring that can assess the attainment or failure of reclamation actions.
    - a. 75% basal cover within five years and be comprised of similar species as those of the surrounding, undisturbed rangeland (USDI – BLM, 2011, p. 2-5).

To ensure proper reclamation according to BLM guidelines, a monetary investment, in the form of a bond, must be filed with the BLM (\$10,000 minimum), that can be used as collateral to ensure all operator obligations are performed, including proper reclamation (USDI – BLM, 2007). Complete ecological reclamation is not necessary, but steps for the site to naturally become completely ecological reclaimed is necessary (USDI – BLM, 2007).

Part of well pad development is the removal and off-site storage of the topsoil and subsoil. Topsoil and subsoil are stored independently off-site in 1 – 2 m (3 – 6 ft) piles. Topsoil depths vary depending on location, but typical topsoil depths on the Pariette Bench are only 40 mm (1.5 in) deep and are comprised of only an A horizon (Jones et al., 2017). Subsoil for the Pariette Bench is typically comprised of calcium carbonate rich subsoil (Bk horizons) and soft bedrock (C horizon) (Jones et al., 2017). Once extraction operations at the well pad have ceased and the wellhead is capped and sealed, the compacted soil surface is ripped (deep tillage to break up compacted soils), and the stored topsoil and subsoil are distributed back onto the site (USDI – BLM, 2007). Along with seeding and the addition of mulch, other amendments can be applied at the discretion of the operator (USDI – BLM, 2007). Elemental sulfur and gypsum have been used to reduce soil sodicity but the selection of amendments can vary depending on the site conditions (Mzezewa et al., 2003).

## SOIL HEALTH

Soil health is when a soil's chemical, physical, and biological properties work in conjunction to support plant and animal life and health, as well as improve other environmental qualities (Doran, 2002). It can "provide an overall picture of soil functionality" (Arias et al., 2005, p. 13) and can be "seen as a living system" (Carter et al., 1997, p. 7). Soil health "sustains plants, animals, and humans while maintaining or enhancing water and air quality" (Stott, 2019, p. 26). Soil health can be assessed and compared to a different soil chosen as a standard or benchmark (Carter et al., 1997). Monitoring soil health over time is the best way to monitor sustainable land management (Doran, 2002). While much has been studied and done to improve soil health (also referred to as soil quality) in high-value agricultural soils, very little has been done to improve soil health on low-value rangelands impacted by oil and gas exploration, development, and extraction (Herrick et al., 2001). The majority of rangelands remain undisturbed and do not require any improvement to their soil health.

Soil health is the integration of the three aspects of soil condition: physical, chemical, and biological (Moebius-Clune et al., 2016). Soil health does not only reflect the chemical, physical, and biological properties, but the interactions between those properties (Karlen et al., 2003). Carter et al. (1997) suggests that there are two parts to soil health; the inherent and the dynamic parts. Inherent soil properties (or indicators) change very little over time, while dynamic soil properties can change rapidly, depending on the management practices (Carter et al., 1997). Along these same lines, Doran (2002) stated that soil health can change over time, depending on natural events and human

activity. While dynamic soil properties (soil organic carbon, salinity, etc.) can change more rapidly than inherent soil properties (soil texture, pH, etc.) it is still vital to monitor inherent soil properties (Karlen et al., 2003). By monitoring long-term inherent soil health indicators, agriculture can be sustainable and overall have a smaller environmental impact (Arias et al., 2005). While soil monitoring does not directly change the soil health, it provides insight into those management practices that can be changed to improve soil health (Carter et al., 1997). With many possible soil health indicators, it can be challenging to identify those that will be the most beneficial to monitor. While some soil properties may have a significant, direct impact on plant growth (i.e. soil organic carbon and aggregate stability), others can have no direct impact, but significantly impact other soil properties that do directly impact plant growth (i.e. soil pH impacts the availability of specific plant nutrients, which affects plant growth) (Carter et al., 1997). Some soil health indicators, such as aggregate stability and soil organic carbon (SOC), integrate the physical, chemical, and biological properties, which provide insight into how all three properties work in conjunction. The following are some of the soil health indicators commonly measured and monitored: soil texture, soil organic carbon, aggregate stability, microbial activity, soil pH, salinity, and sodicity (Stott, 2019; Moebius-Clune et al., 2016).

Common issues that negatively impact soil health include: soil compaction, poor aggregation, low soil organic matter content, weed pressure, salinity, and sodicity (Moebius-Clune et al., 2016; Karlen et al., 2008). Many of these issues are linked and affected by other issues. Soil compaction, caused by heavy equipment or traffic, causes poor water infiltration, as well as a reduction in root penetration and growth. Poor water

infiltration can lead to an accumulation of salts. Poor soil aggregation, like soil compaction, causes poor water infiltration, poor seedling emergence, and can lead to increased erosion. Poor aggregation is commonly caused by intensive tillage, lack of organic matter additions, and subsequently low biological activity. Low amounts of organic matter caused by excessive tilling, along with a lack of organic additions to the soil (typically from plant matter), leads to low water and nutrient retention. Low organic matter content can also lead to a reduction in microbial activity and poor soil aggregation. Weed pressure makes it challenging for the desired plants to become established. Salinity and sodicity are often closely related to each other. While salinity causes water stress to plants, sodicity degrades soil structure and soil aggregation. Salinity, sodicity, compaction, and loss of organic matter (lack of organic additions) degrade soils and decrease soil health (Karlen et al., 2008).

### **Soil Salinity and Sodicity**

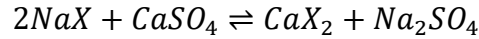
Sodicity and salinity are often referred to and occasionally confused with each other. Salinity refers to any salt, typically those with sodium ( $\text{Na}^+$ ), calcium ( $\text{Ca}^{2+}$ ), and magnesium ( $\text{Mg}^{2+}$ ) cations with either chloride ( $\text{Cl}^-$ ) and sulfate ( $\text{SO}_4^{2-}$ ) anions (USDA – ARS, 1954). The presence of salts (salinity) in soil, change the osmotic potential of soil water and decrease the ability for plants to obtain it (USDA – ARS, 1954; USDA – NRCS, 1998). Sodicity refers to exchangeable sodium ( $\text{Na}^+$ ) in the soil. Exchangeable sodium ions ( $\text{Na}^+$ ) are typically attached to negatively charged clay particles in the soil. Sodicity causes soil particles to disperse and therefore, reduces soil pore space (USDA – ARS, 1954; Heil and Sposito, 1997). This reduction in soil pore space limits air and water

infiltration and reduces soil aggregate stability. The formation of sodic crust can occur on the soil surface, sealing off the soil surface, reducing air and water infiltration (USDA – ARS, 1954; USDA – NRCS, 2001b).

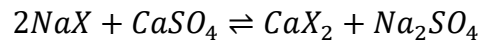
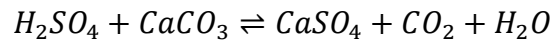
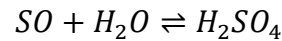
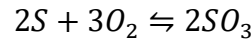
The salinity of a soil is determined by the electrical conductivity of the soil. This is commonly measured via a saturated paste extract ( $EC_e$ ). A soil is deemed saline if the  $EC_e$  is greater than  $4.0 \text{ mS cm}^{-1}$ . The sodicity of a soil is determined by sodium adsorption ratio (SAR) and the exchangeable sodium percentage (ESP). A soil is considered sodic if the SAR is greater than 13 and the ESP is greater than 15. A soil can also be characterized as saline-sodic, if a soil has an  $EC_e$  greater than  $4.0 \text{ mS cm}^{-1}$ , a SAR greater than 13, and the ESP is greater than 15 (USDA – ARS, 1954; Mzezewa et al., 2003).

Water is used to reduce the amount of salts from the root zones of plants. The salts dissolve in the water and the water drains out of the rootzone. Adequate drainage is needed for the water and the dissolved salts to be drawn away from the root zone. To leach salts from the top 305 mm (12 in) of the soil, flushing 152 mm (6 in) of water will reduce soil salinity by 50%, and 305 mm (12 in) will reduce soil salinity by 80%. (Rhoades, 1974). If the soil is sodic or saline-sodic, calcium ( $\text{Ca}^{2+}$ ) can be used to replace sodium ions on the exchange site on the clay particles. With calcium ions replacing sodium ions, water can then flush the sodium ions out of the root zone (Mzezewa et al., 2003). Calcium can be beneficial by promoting the flocculation of the clay particles into aggregates, improving air and water infiltration. (USDA – ARS, 1954). Calcium can be added in the form of gypsum ( $\text{CaSO}_4 \cdot 2\text{H}_2\text{O}$ ) or acid can be used to break apart the calcium carbonate ( $\text{CaCO}_3$ ), if the soil has high amounts present. The following equation

demonstrates how calcium from gypsum replaces sodium ions at soil exchange sites (USDA – ARS, 1954; Armstrong and Tanton, 1992). The variable  $X$  represents the exchange site.



Elemental sulfur can be used in place of acid, allowing for soil microorganisms to break down the elemental sulfur into sulfuric acid. The following equations demonstrate the chemical process for the oxidation of sulfur, mediated by microbial activity, to produce sulfuric acid, which reacts with calcium carbonate, replacing the sodium ion (USDA – ARS, 1954). The variable  $X$  represents the exchange site.



### **Aggregate Stability**

Aggregate stability is when soil particles bind strongly together to create aggregates which are resistant to outside dispersing forces (USDA – NRCS, 2008a). When testing aggregate stability researchers look at the strength of soil aggregates (USDA – NRCS, 2008b; USDA – NRCS, 1999; Tisdall and Oades, 1982). Soil aggregate stability is tested by wet sieving soil aggregates and comparing the slaked material to the remaining stable aggregate (Kemper and Rosenau, 1986; USDA – NRCS, 1996b). A soil with high aggregate stability is desirable, as unstable aggregates slake off leading to the sealing of pores, limiting water and air infiltration, and may lead to hard crust (sodic)



formations (USDA – NRCS, 2008a). The more stable aggregates, the greater the soil health (USDA – NRCS, 2008a). Stable aggregates increase water and air infiltration, increase seed and soil contact to improve seed germination, and improve the root penetration of plants (Karlen et al., 2008; USDA – NRCS, 2008a). Stable aggregates are more resistant to water and wind erosion, as well as other disturbances (USDA – NRCS, 1996b; USDA – NRCS, 2008a). Macroaggregates ( $>0.25$  mm), typically 1 – 2 mm are used to determine aggregate stability (Kemper and Rosenau, 1986; Seybold and Herrick, 2001).

Aggregate stability is an important soil health indicator since it “integrates soil biological, chemical and physical properties” (Stott, 2019). Along with being an important soil health indicator, aggregate stability is an important indicator of overall rangeland health (Herrick et al., 2001). Because aggregate stability is influenced by many different soil properties, as well as being an influence on others, it is a key soil health indicator (Seybold and Herrick, 2001). Many different soil properties impact aggregate stability, but aggregate stability is largely influenced by soil organic matter (Abiven et al., 2009; Ekwue, 1990). Stable soil aggregates are formed and stabilized by soil organic matter (Diaz et al., 1994). This factor leads to aggregate stability being indicative of biological activity and soil organic matter content and cycling (USDA – NRCS, 2008a). The quantity and quality of organic material, as well as timing, is important to take into account when adding organic carbon to the soil, to increase soil aggregate stability (Abiven et al., 2009).

## **Soil Organic Carbon**

Soil organic carbon (SOC) is carbon based biological material in varying degrees of decomposition (USDA – NRCS, 2001a). Soils in ecosystems that produce more biological material tend to have more soil organic carbon. In contrast, those ecosystems that produce lower amounts of biological material (such as arid ecosystems) have lower amounts of soil organic carbon (USDA – NRCS, 2001a). Soil organic carbon can range from 0.5 – 8% in rangeland topsoils (USDA – NRCS, 2001a). Soil organic carbon breaks down over time, but disturbance and the lack of organic additions, lead to a decrease in soil organic carbon (USDA – NRCS, 2001a).

Soil organic carbon, is considered an “important baseline measurement” in soil health (Stott, 2019). This because soil organic carbon is mediated by the microbial community (biological), is key to improving soil structure (physical), and influences many other soil properties (Stott, 2019). Increased levels of soil organic carbon have shown positive correlations with aggregate stability, soil microbial community, and plant nutrients (Gregorich et al., 1997; Stott, 2019).

Soil microbes break down soil organic carbon and release nutrients into the soil, making those nutrients available to plants (USDA – NRCS, 2001a). Changes in soil organic carbon, caused by disturbance, closely impact the overall size of the microbial community and change the activity of soil enzymes, which are produced by the soil microbes (Raiesi and Beheshti, 2015). Soil organic carbon is important to forming stable soil aggregates and storing/suppling plant nutrients (USDA – NRCS, 1996a; USDA – NRCS, 2001a).

Soil organic carbon increases the water retention of the soil and increases water and air infiltration (Gregorich et al., 1997). Soil organic carbon is a chemical soil health indicator, even though it is closely related to biological soil activity, by being microbially mediated (Stott, 2019). The method used in this study to measure soil organic carbon (dry combustion) doesn't differentiate between the different carbon pools and does not distinguish between organic matter and organic carbon (Stott, 2019). Soil organic matter is comprised of the remnants of anything previously living (USDA–NRCS, 1996a), while soil organic carbon is comprised only of the carbon fraction of organic matter.

### **Soil Microbial Activity**

While chemical soil testing has been commonplace for many years, biological soil testing in the past, was rarely used to characterize soil health (Moebius-Clune et al., 2016). It is unfortunate because soil biodiversity is associated with soil resilience (Arias et al., 2005). Measuring the soil respiration by CO<sub>2</sub> evolution methods has traditionally been used as an indicator of microbial metabolic activity (Gregorich et al., 1997). Aerobic organisms (mostly microbes) produce CO<sub>2</sub> by oxidizing organic carbon. Soil respiration correlates with soil organic carbon and microbial activity (Arias et al., 2005). Higher respiration in soil is considered a positive attribute (USDA – NRCS, 1999). The Natural Resources Conservation Service (NRCS) in their Soil Quality Test Kit Guide (1999) suggests measuring soil respiration as mg CO<sub>2</sub>-C m<sup>-2</sup> h<sup>-1</sup> (lbs CO<sub>2</sub>-C acre<sup>-1</sup> d<sup>-1</sup>) evolved. A measurement of 0.0 mg CO<sub>2</sub>-C m<sup>-2</sup> h<sup>-1</sup> (0.0 lbs CO<sub>2</sub>-C acre<sup>-1</sup> d<sup>-1</sup>) evolved would be considered no biological soil activity and a virtually sterile soil. A measurement

150 – 300 mg CO<sub>2</sub>-C m<sup>-2</sup> h<sup>-1</sup> (32 – 64 lbs CO<sub>2</sub>-C acre<sup>-1</sup> d<sup>-1</sup>) evolved is considered ideal for agriculture soils (USDA – NRCS, 1999).

Soil respiration is moisture- and temperature-sensitive (Davidson et al., 2006; Lloyd and Taylor, 1994). As temperature increases, CO<sub>2</sub> evolution rate increases by a constant factor referred to as “Q<sub>10</sub>”. Q<sub>10</sub> is the “factor by which respiration is multiplied when temperature increases by 10 °C” (Davidson et al., 2006, pg. 156).

Soil respiration has traditionally been measured by placing a sample of air-dried soil into an airtight jar, re-wetting the soil, and measuring the amount of CO<sub>2</sub> evolved over several days (Moebius-Clune et al., 2016). However, dynamic gas flux chambers are becoming used more commonly to measure CO<sub>2</sub> flux (Lyman et al., 2017; Lyman et al., 2018; Lyman et al., 2020; Makky et al., 2018).

## ELECTROMAGNETIC INDUCTION

Electromagnetic Induction (EMI) uses electromagnets to induce an electrical current (flow of electrons) through a medium. The induced electrical flow creates a magnetic field. The higher the electrical flow through the medium, the stronger the magnetic field (Adamchuk et al., 2004). The strength of this magnetic field is measured by the instrument and is expressed by  $EM_H$  or  $EM_V$  depending on the polarity of the magnetic field measurement ( $EM_H$  for a horizontal reading, and  $EM_V$  for a vertical reading.)  $EM_H$  and  $EM_V$  are expressed in  $mS\ m^{-1}$ . The strength of the magnetic field can be influenced by many soil factors including: soil moisture, soil temperature, soil mineralogy, salinity, sodicity, pH, soil organic carbon, etc. (Doolittle and Brevik, 2014; Jiang et al., 2016; Adamchuk et al., 2004).

An instrument that measures EMI is comprised of two dipoles, one that measures  $EM_H$  and one that measures  $EM_V$ . Each dipole has a transmitter and a receiver set 1 meter apart (Heil and Schmidhalter, 2017). The transmitter and receiver are the electromagnets which generate the electrical flow. The instrument is combined with a GPS receiver and is carried or dragged over the soil surface while it logs the precise position and  $EM_H$  or  $EM_V$  (Adamchuk et al., 2004). It has been commonly used in precision agriculture as well as in archaeology (Heil and Schmidhalter, 2017; Adamchuk et al., 2004).

Electromagnetic induction is considered noninvasive and is used to collect large amounts of detailed information (Doolittle and Brevik, 2014).

## CHAPTER 2: SOIL HEALTH ASSESSEMENT ON ARID RANGELAND SOILS IMPACTED BY OIL AND GAS EXPLORATION, DEVELOPMENT, AND EXTRACTION

### INTRODUCTION

The Pariette Bench, located in the Uinta Basin, roughly 56 km (35 miles) south of Vernal, Utah, is a typical arid rangeland (remote, expansive, unsuitable for crop production, etc. (Skaggs, 2008)) like many managed by the Bureau of Land Management (BLM) of the U.S. Department of the Interior. Along with its remote location, the lack of water in this arid environment makes reclamation challenging to implement. The Ouray, Utah weather station (Station ID USC00426568) (40.1344°, -109.644°), located 20 km (12 miles) from the Pariette Bench, has recorded an average of 170.5 mm (6.5 in) of annual precipitation from 1985 – 2018.

Arid soils, like those on the Pariette Bench, are prone to having higher levels of salinity and sodicity than non-arid soils. Once disturbed, those higher levels of salinity and sodicity in the soil are exacerbated, making re-vegetation of native plants challenging, resulting in the establishment of invasive plants. Other reclamation techniques, such as using cover crops to compete against invasive plant species, mainly *Bromus tectorum* (cheatgrass), *Salsola tragus* (Russian thistle), and *Halogeton glomeratus* (halogeton), have proven challenging to implement with success (Grossl, 2017). The lack of consistent moisture in this region makes for uncoordinated planting times, resulting in unsuccessful cover crop germination.

These challenges have led to the need for a better understanding of the soil health (also referred to as soil quality) on plugged and abandoned (P&A) well pads and the influence of soil disturbance from oil and gas exploration, development, and extraction.

The objectives for this study were to identify differences of soil health between plugged and abandoned (P&A) well pads and the surrounding, undisturbed rangeland, and to use soil health indicators to describe soil health on rangeland soils.

Using common soil testing methods, soil health data was collected from disturbed P&A well pads and undisturbed rangelands. The effectiveness of electromagnetic induction sensing (EMI) was compared to the common soil testing methods for identifying soil health indicators. A minor objective of this study was to also test the effectiveness of a CO<sub>2</sub> dynamic flux chamber as a method of measuring soil microbial activity via microbial respiration.

This research provided an important understanding of the soil characteristics (physical, chemical, and biological) on plugged and abandoned well pads as well as the surrounding, undisturbed rangeland. This provides key information to land managers when trying to reclaim plugged and abandoned well pads in arid environments, such as the Uinta Basin.

By identifying key soil health differences between disturbed sites requiring reclamation and nearby undisturbed rangeland can provide insight leading to greater reclamation success in arid environments. By understanding what the soil health on the surrounding, undisturbed rangeland as well as the disturbed sites, land managers can spend valuable resources on improving those soil health indicators, which will bring the

disturbed soil sites to more closely resemble the undisturbed rangeland and closer to being fully reclaimed.

Using electromagnetic induction (EMI) (which has been used primarily in high-value agriculture systems and not in rangeland reclamation) can potentially provide essential soil health data for larger landscapes (such as rangelands) faster than traditional soil testing techniques by lowering the amount of lab tests needed to understand the overall system's soil health. Using the data generated by electromagnetic induction, visual soil property maps can be generated through ArcGIS. Land managers can use these maps to understand the soil health of vast landscapes and use them to target specific areas in need of special attention on the landscape, thereby leading to a direct reclamation strategy.



**Fig. 1. Typical location on Pariette Bench. Taken from site 9-18-9-19\_RL with 9-18-9-19 in background.**



## **METHODS AND MATERIALS**

### **Location Selection**

Six plugged and abandoned oil well pads were selected on the Pariette Bench, in Uintah County, Utah. All pads are within 12 km (7.5 miles) of each other (Fig. 2). Five of the pads are presently managed by Newfield Exploration and one pad is presently managed by the Bureau of Land Management (BLM). These pads vary from when they were plugged and abandoned. Four of the six were plugged and abandoned between 2016 – 2018, while the other two were plugged in 2010 and 1989. A portion of undisturbed rangeland adjacent to each of the six well pads were also selected, mirroring the conditions that would best represent a successful reclamation of the well pad. The sections of undisturbed rangeland are currently managed by the Bureau of Land Management, Vernal Field Office.

Pad names are based on the location of the pads within a township and range organized by the Bureau of Land Management. Townships are used to indicate how far north and south a location is from a designated parallel while the range indicates how far east and west a location is from a designated meridian. Townships and ranges are labeled as T#N/S and R#E/W, with the # being the number in order from the designated meridian or parallel (1, 2, 3...) The direction the township or range is related to the designated meridian or parallel and is indicated with N, S, E, or W for north, south, east or west. One section of township and range is 9.7 km (6 miles) by 9.7 km (USDI – USGS, 2018). All pads in this study are located within four adjacent township/range segments: T8S-R18E, T9S-R18E, T9S-R19E, and T9S-R17E. This township/range is then divided into 36

sections (1.6 km (1 mile) by 1.6 km). These 36 sections are then divided into 16 pieces.

Newfield Exploration names pads by listing the piece, then the section, followed by the township and range (2-35-8-18). Newfield Exploration only denotes the number from the township and range. Pad names included in this study are: 2-35-8-18, 12-11-9-18, 9-18-9-19, 7-8-9-18, 14-21-9-18Y, and 11-12-9-17. Well pads 2-35-8-18, 12-11-9-18, 7-8-9-18, and 11-12-9-17 had straw mulch added and mixed into the topsoil as part of the reclamation. Well pad 9-18-9-19 was used in a previous study in 2014 – 2015, which compared different carbon treatments including: biochar, desilt material, wood chips, activated carbon, and compost. Prior to the end of the 2014 – 2015 study, the site was flooded by fall monsoonal rain showers. This caused a mixing of the carbon treatments and was removed from that previous study. These carbon treatments can still be identified in certain areas and should be noted due to soil organic carbon is being measured in this study.

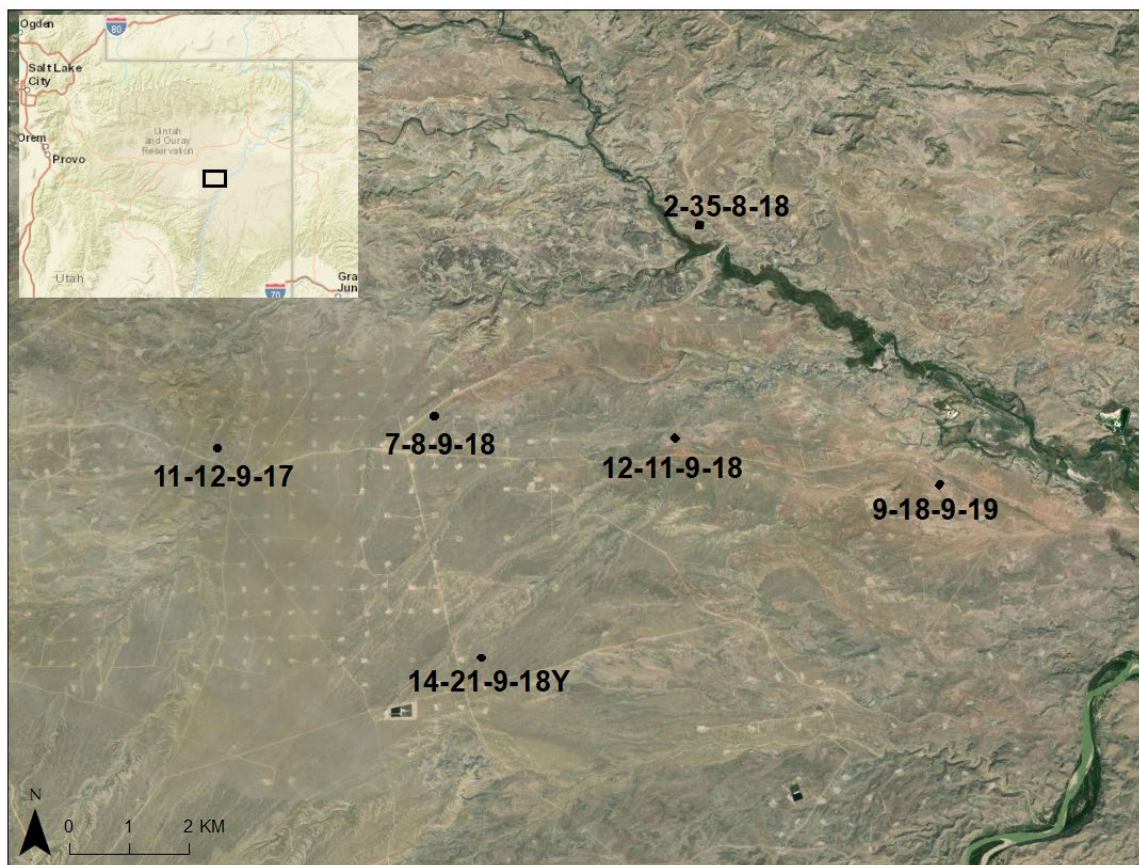


**Fig. 2. Map showing P&A well pad locations on the Pariette Bench, Utah. Service Layer Credits: Source: Esri, DigitalGlobe, GeoEye, Earthstar Geographics, CNES/Airbus DS, USDA, AeroGRID, IGN, and the GIS User Community.**

### Soil Sampling

Twenty soil samples were collected based on a grid system spaced 27.4 m by 48.8 m (90 by 160 ft) at each pad and rangeland location (a total of 240 samples for all pads sampled) (Fig. 4). The soil sample collection sites were spaced 9.1 m by 12.2 m (30 by 40 ft) apart. Soil samples were taken from the top 120 mm (5 in) (at some sites this depth was not be achieved due to rockiness of the soil.) A resealable plastic bag (3.8 L (1 gallon)) was filled with soil at all 240 sample sites, in order to have enough soil to perform all soil health tests. The GPS coordinates were recorded for every soil sample.

Soil sample locations may have been altered by 0.3 m (1 ft) depending on the composite of the site (lack of soil due to rocks).

Soil samples were labeled with the pad number and the grid letter/number combination (A – D and 1 – 5) (example: 2-35-8-18\_A1). If the soil was collected from a rangeland site, a RL was added (example: 2-35-8-18\_RL\_A1). Samples were then air dried for several days, and sieved to 2 mm.



**Fig. 3. Soil sample taken from 9-18-9-19. Visable physical soil crust.**





**Fig. 4. Map showing the soil sampling grid for 12-11-9-18.**

### **Soil Health**

Soil health assessments performed on agriculture soils typically use a scorecard developed by NRCS or a local university (Moebius-Clune, 2016) to evaluate soil health. This study used the adjacent undisturbed rangeland as the scorecard for the desired soil health for successful reclamation. Soil health indicators were split into three groups: physical, chemical, and biological indicators. Physical soil health indicators included soil texture and aggregate stability. Chemical soil health indicators included: pH, electrical conductivity ( $EC_e$ ), sodium adsorption ratio (SAR), exchangeable sodium percentage (ESP), and soil organic carbon (SOC). The biological soil health indicator measured was soil  $CO_2$  respiration.  $CO_2$  respiration was used to measure soil microbial activity. Plant

counts, which are a site evaluation and not a soil health test, were conducted at all sites where soil samples were taken. Plant counts were used to distinguish the percent of plant cover between beneficial and invasive plant species.

#### Physical Soil Health Indicators

Soil texture is fundamental to the movement of air and water, as well as the availability of soil nutrients. Soil texture was determined by using the hydrometer method to calculate the percentage of sand, silt, and clay present. While soil texture is not a dynamic soil health indicator that can quickly be changed, it is still important to know for assessing soil health.



**Fig. 5. Soil textures being determined with hydrometers.**

Two P&A well pads and adjacent rangelands were tested for aggregate stability. Those two locations were 9-18-9-19 and 12-11-9-18. Location 9-18-9-19 was selected to be tested due to the high SAR values found at location while location 12-11-9-18 was chosen randomly. Of the 20 soil samples taken at each location, 10 were chosen from

each location to test aggregate stability. Individual soil sample sites were chosen based on the SAR values. The soil sample sites were ranked by SAR value, with the ten with the highest SAR values selected to be tested for aggregate stability. This was done to test for any correlation between SAR and aggregate stability. All 40 samples (two P&A well pads and two adjacent rangelands with 10 soil samples each) were tested in triplicate for aggregate stability.

After collection, soil samples were air dried. Aggregates between 1 – 2 mm were collected using 2.38 mm and 1.397 mm sieves. The aggregates that passed through the 2.38 mm sieve, but did not pass through the 1.387 sieve were collected and used for testing. Three grams of each sample were weighed, placed in a 105 °C oven for 24 hours to dry. After 24 hours, samples were re-weighed and recorded. Samples were placed into individual cups with a 250  $\mu$ m sieve on the bottom. Samples were then placed on dH<sub>2</sub>O saturated sponges, to slowly rehydrate the aggregates. After 30 minutes, samples were placed onto the sieving apparatus (Wet Sieving Apparatus from Eijkelkamp Soil and Water) and were sieved for 3 minutes, being submerged in dH<sub>2</sub>O 35 times min<sup>-1</sup>. The sieving apparatus submerged the 250  $\mu$ m sieve cups, allowing for the aggregates to slake off and fall through the sieve, being collected in bottom container. After the 3-minute run time, the bottom containers, which the unstable fraction of the aggregates slaked into, were collected and placed in a 105 °C oven for 24 hours, to evaporate the water and dry the unstable aggregate. The 250  $\mu$ m sieve cups containing contained the remaining aggregate, both the stable aggregate as well as non-aggregate (sand and plant material) fractions were removed from the sieving apparatus. The stable aggregate was then gently pulverized and washed through the 250  $\mu$ m sieve and discarded. The non-aggregate that

remained in the cup was collected into a small tin and oven dried at 105 °C for 24 hours.

Once the unstable aggregate (slake material) and the non-aggregate samples were dried, they were weighed and record. Subtracting the mass of the non-aggregate from the total mass (oven dried), the aggregate mass was calculated. Stable aggregate was calculated by subtracting the unstable aggregate from the aggregate. By dividing the stable aggregate from the aggregate and multiplying by 100, the percent of stable aggregate was calculated.

$$Total - NonAggregate = Aggregate$$

$$Aggregate - Unstable Aggregate = Stable Aggregate$$

$$\left( \frac{Stable Aggregate}{Aggregate} \right) \times 100 = Percent Stable Aggregate$$

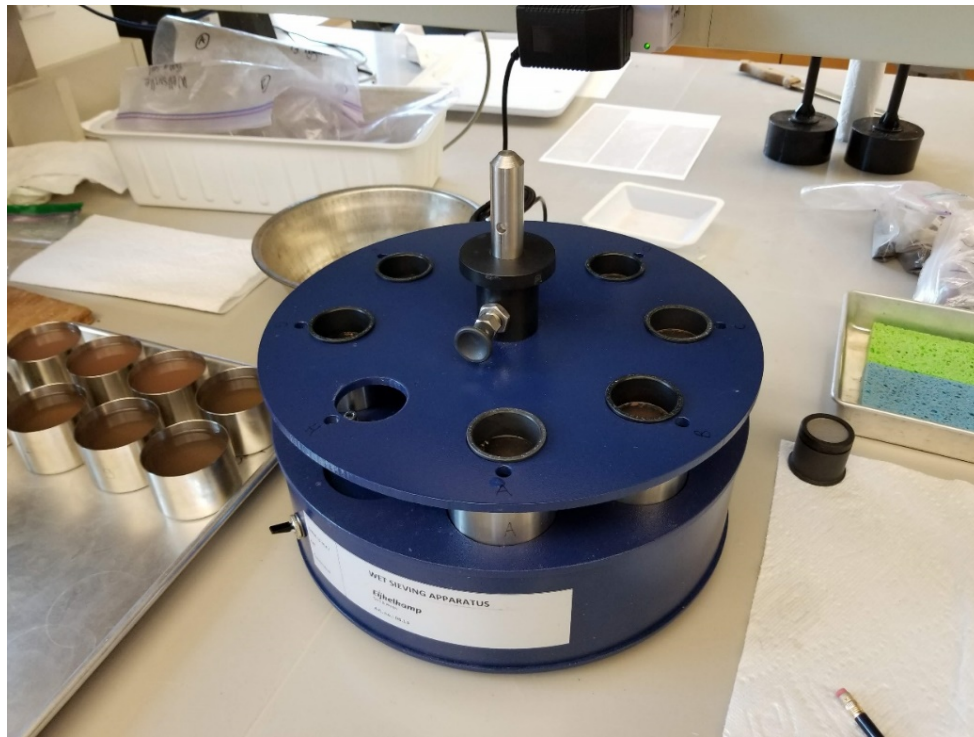


**Fig. 6. Aggregate stability being conducted with sieving apparatus being run, submerging aggregates.**





**Fig. 7. Aggregate stability results after sieving and prior to being placed in oven for final drying. The slake material (unstable aggregate) in the foreground, with the non-aggregate in the background.**

#### Chemical Soil Health Indicators

Data for soil pH, electrical conductivity, and sodium adsorption ratio were obtained via a saturated soil paste extract (distilled, deionized water (ddH<sub>2</sub>O)). Soil pH and EC<sub>e</sub> were measured using calibrated pH (HANNA HI 4522) and electrical conductivity (Vernier LabQuest) probes. Inductively-coupled plasma Spectrophotometer (Thermo Electron iCAP ICP) or ICP was performed by Utah State Analytical Laboratories to provide elemental concentrations. Samples used for the ICP analysis were obtained from saturated soil paste extracts. Using cation concentration (mmols L<sup>-1</sup>) results from the ICP analysis, sodium adsorption ratio was calculated as follows:

$$SAR = \frac{[Na^+]}{\sqrt{[Ca^{2+}] + [Mg^{2+}]}}$$

Exchangeable sodium percentage is calculated from the SAR. The calculation used is as follows:

$$ESP = \frac{100(-0.0126 + [0.01475 \times SAR])}{1 + (-0.0126 + [0.01475 \times SAR])}$$

Equations for calculating SAR and ESP were provided by Handbook 60 from the USDA Salinity Lab (USDA – ARS, 1954).

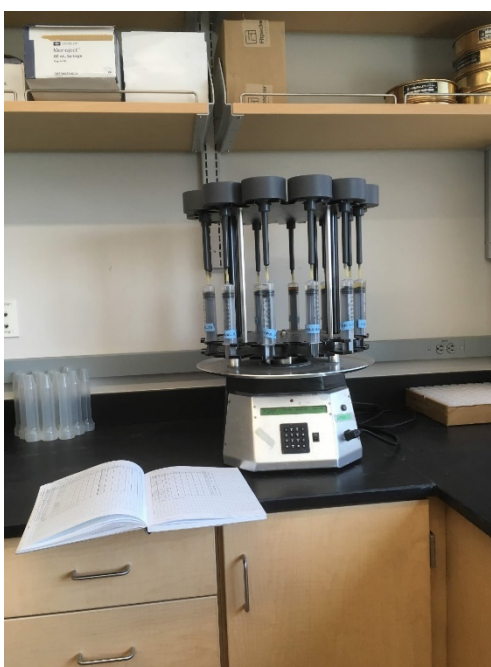


**Fig. 8. Soil saturated paste extracts being extracted for pH, EC<sub>e</sub>, and SAR.**

The method used for measuring soil organic carbon (SOC) was dry combustion (Shimadzu SSM-5000A). Dry combustion burns off the carbon in the soil sample and measures the quantity of carbon with a nondispersive infrared (NDIR) detector. Since the pH of the soils tested were greater than 7, the inorganic carbon needs to be accounted for and subtracted from the sample, providing the organic carbon fraction (Stott, 2019). Soil organic carbon was measured by subtracting the amount of inorganic carbon (IC) by the

total amount of carbon (TC). Two samples are needed for each soil tested, one for total carbon and one for inorganic carbon. Soil samples used for soil organic carbon testing were oven dried at 105 °C. Two samples were taken from each soil and were weighed. The sample measuring TC (0.5000 (±0.01) grams) was analyzed by burning off all the present carbon by heating the sample to 900 °C. The sample measuring IC (0.2500 (±0.01) grams) was treated with 25% phosphoric acid and heated to 200 °C. The acid reacts with the carbonates and burns off all the inorganic carbon. A nondispersive infrared (NDIR) detector measured the amount of carbon for both the total carbon and the inorganic carbon samples. By subtracting the amount of inorganic carbon from the total carbon, the organic carbon is calculated.

$$TC - IC = OC$$

#### Biological Soil Health Indicators

By measuring CO<sub>2</sub> respiration of the soil, the amount of microbial activity can be estimated. Soil CO<sub>2</sub> respiration was measured with a dynamic gas flux chamber, causing minimal disturbance of the soil and the microbial community. Six measurements were taken on two pads and two adjacent rangelands (12 total measurements). The six measurement locations were selected based on EM<sub>H</sub> values, collected from electromagnetic induction. Locations were chosen in order to cover the variability in EM<sub>H</sub> values (2 high, 2 average, and 2 low).

The dynamic gas flux chamber was assembled at each sample sites. Metal rings were inserted into the soil and allowed to rest for 15 mins. A transparent, polycarbonate dome was attached to the metal ring after 15 minutes. The dome was connected to a trailer containing a Los Gatos Research (LGR) Greenhouse Gas Analyzer. Each

individual location was monitored for 30 minutes, with the LGR switching readings from inside and outside the dome chamber every 20 seconds. From these values, the CO<sub>2</sub> dynamic flux was calculated. The variables  $Q$  and  $S$  represent the flow rate and the surface area being measure, respectively.

$$Flux = \frac{(\Delta CO_2 \times Q)}{S}$$

Because microbial activity is temperature-sensitive and changes based on temperature (Davidson et al., 2006), adjustments were made to the dynamic CO<sub>2</sub> flux in order to normalize it for variations in temperature. Using an equation from the NRCS Soil Quality Test Kit Guide (1999), the dynamic CO<sub>2</sub> fluxes were adjusted to 25 °C. This equation is for adjusting temperatures ranging between 15 – 35 °C and is as follows:

$$Soil\ Respiration\ Rate = Soil\ Respiration \times 2^{(25-T)/10}$$

As temperature increases, CO<sub>2</sub> evolution rate increases by a constant factor referred to as “Q<sub>10</sub>.” Q<sub>10</sub> is the “factor by which respiration is multiplied when temperature increases by 10 °C” (Davidson et al., 2006, pg. 156). The above equation assumes a Q<sub>10</sub> value of 2, but using data collected from the dome and LGR, a new Q<sub>10</sub> value was calculated using the following equation:

$$Resp = R_{basal} \times Q_{10}^{(T-T_{basal})/10}$$

$$Q_{10} = (Resp_{T_2}/Resp_{T_1})^{10/(T_2-T_1)}$$

The new Q<sub>10</sub> values were used to adjust the soil temperature to 25 °C. These equations come from Davidson et al. (2006, pg. 156).



**Fig. 9. Dynamic CO<sub>2</sub> flux being measured on 2-35-8-18 with a polycarbonate flux chamber, with the hose running to the trailer containing the LGR greenhouse gas analyzer.**

Plant counts are important to this study as it is one of the main indicators to the BLM of proper land reclamation. Plant counts are considered a site evaluation and not a soil health indicator. Using the same grid layout used to collect soil samples, plant counts were performed, using a 1-meter square. Plant species were listed, along with their respective percent cover in the 1-meter square. Plant species were split into two groups; beneficial and invasive plants. Beneficial plants were those that were native, approved by the BLM, or provided quality forage for wildlife (Table 5). The percent cover was calculated for the beneficial and invasive plants and can be found on Table 1.



**Fig. 10. Plant counts being performed using a meter squared to measure plant cover on the rangeland adjacent to 12-11-9-18.**

### **Electromagnetic Induction**

Electromagnetic Induction (EMI) measurements were collected using a Geonics EM38DD instrument and a sub-meter GPS unit. The EM38DD is a commonly used electromagnetic induction probe for collecting apparent electrical conductivity (Heil and Schmidhalter, 2017). The grid system previously established and discussed in the soil sampling section of methods and materials, was followed, using GPS to ensure good coverage of the site. Soil samples were collected from two locations at each grid site (24 samples) to measure gravimetric soil moisture. Gravimetric soil moisture was measured by weighing the soil samples, then drying the samples in a 105 °C oven to remove all water, and re-weighing once completely dry. The weight of water loss is divided by the oven dried soil weight. Soil temperature was also measured at those 24 locations using a soil temperature probe. An average soil moisture (gravimetric) and temperature were



recorded from those two samples and used as the soil moisture and temperature for the measured areas.



**Fig. 11. Electromagnetic induction sensor (EMI) being carried across rangeland adjacent to 11-12-9-17.**

The EM38DD collected  $EM_H$  (horizontal electromagnetic reading) and  $EM_V$  (vertical electromagnetic reading) data, but only  $EM_H$  data was used. The  $EM_H$  values provide enough depth for what is desired for this study. Using the average soil temperature for each site,  $EM_H$  values were normalized to 25 °C using the following equation.  $OT$  is the original temperature and  $NT$  is the temperature normalized to 25 °C.

$$OT \times \{1 - [(OT - 25^\circ\text{C}) \times 0.02]\} = NT$$

After  $EM_H$  value outliers were removed, Cochran's equation (also referred to as Cochran's sample size equation) was used providing the number of sample sites necessary, providing accurate ground truthing. In Cochran's equation,  $n_0$  is the sample size,  $Z$  is the z-value from a Z table,  $e$  is the margin of error,  $p$  is the proportion of the population affected, and  $q$  is  $1 - p$ .

$$n_0 = \frac{Z^2 \times p \times q}{e^2}$$

The number of samples calculated were then split into percentile groups covering the whole range of  $EM_H$  values. Since soil samples had previously been collected from these locations, those soil samples were used for the ground truthing. Using Google Earth Pro Desktop, the ground truthing locations provided by the Cochran equation were compared to the locations of the soil samples taken from the establish grid system. This provided the closest soil samples to the ground truthing sites.

Since the grid soil samples are not the exact location calculated by the Cochran equation, the  $EM_H$  values associated with the ground truthing sites are not the same as those at the grid locations. Using inverse distance weighting (IDW) in ArcGIS, the  $EM_H$  values were estimated at those grid locations.

Those ground truthing samples (101) were compiled with the soil properties that could affect  $EM_H$  including: soil texture (sand, silt, and clay percentages), pH,  $EC_e$ , SAR, SOC, soil moisture, and soil temperature (Table 11). In order increase the sample size, all soil samples collected from the grid (240) were also compiled with their  $EM_H$  and other soil property values and ran separate from the ground truthing samples. This was done to see how a larger sample set would compare to the results provided from the ground truthing samples.

### **ArcGIS Modeling**

Esri ArcGIS for Desktop version 10.4, was used to make interpolation maps showing the distribution of different soil health indicators, including  $EM_H$ , SAR, plant cover, and  $EC_e$  (Fig. 37, 38, & 39). Using inverse distance weighting (IDW), the maps



were created to easily visualize key soil health indicators across the rangeland as well as the P&A well pads.

## RESULTS

### Soil Health

The soil health of each P&A well pad was compared to the adjacent undisturbed rangeland. The adjacent, undisturbed rangeland would be indicative of successful reclamation and optimal soil health for the given conditions. P&A well pads and adjacent undisturbed rangeland were compared using paired T-Tests (Microsoft Excel 2016) for each measured soil health indicator. A P-Value of  $<0.05$  was considered statistically significant for all measurements.

The six different locations are all independent of each other, each P&A well pad with the corresponding adjacent rangeland may have varying differences from location to location. Of the measured soil health indicators, soil texture, sodium adsorption ratio, and beneficial plant cover were significantly different between the P&A well pads and the adjacent undisturbed rangeland at all six locations. Specifically, the P&A well pads were statically higher in clay percentage, higher in SAR, and lower in beneficial plant cover than the adjacent rangeland. Soil texture and sodium adsorption ratio are indicative of soil health, while beneficial plant cover is vital to successful reclamation (Table 3 & 4).

#### Texture

There was an overall change in the soil texture of the disturbed P&A well pads and the undisturbed rangeland. P&A well pads had significantly higher amounts of clay at all six locations than the adjacent rangeland. P&A well pads had 30% more clay on average than the undisturbed rangeland (Fig. 13). This increase of clay on the P&A well pads changed the texture to a finer texture class (clay loam and sandy clay loam), while

the undisturbed, adjacent rangeland had higher amounts of sand (sandy loam and sandy clay loam) (Fig. 12).

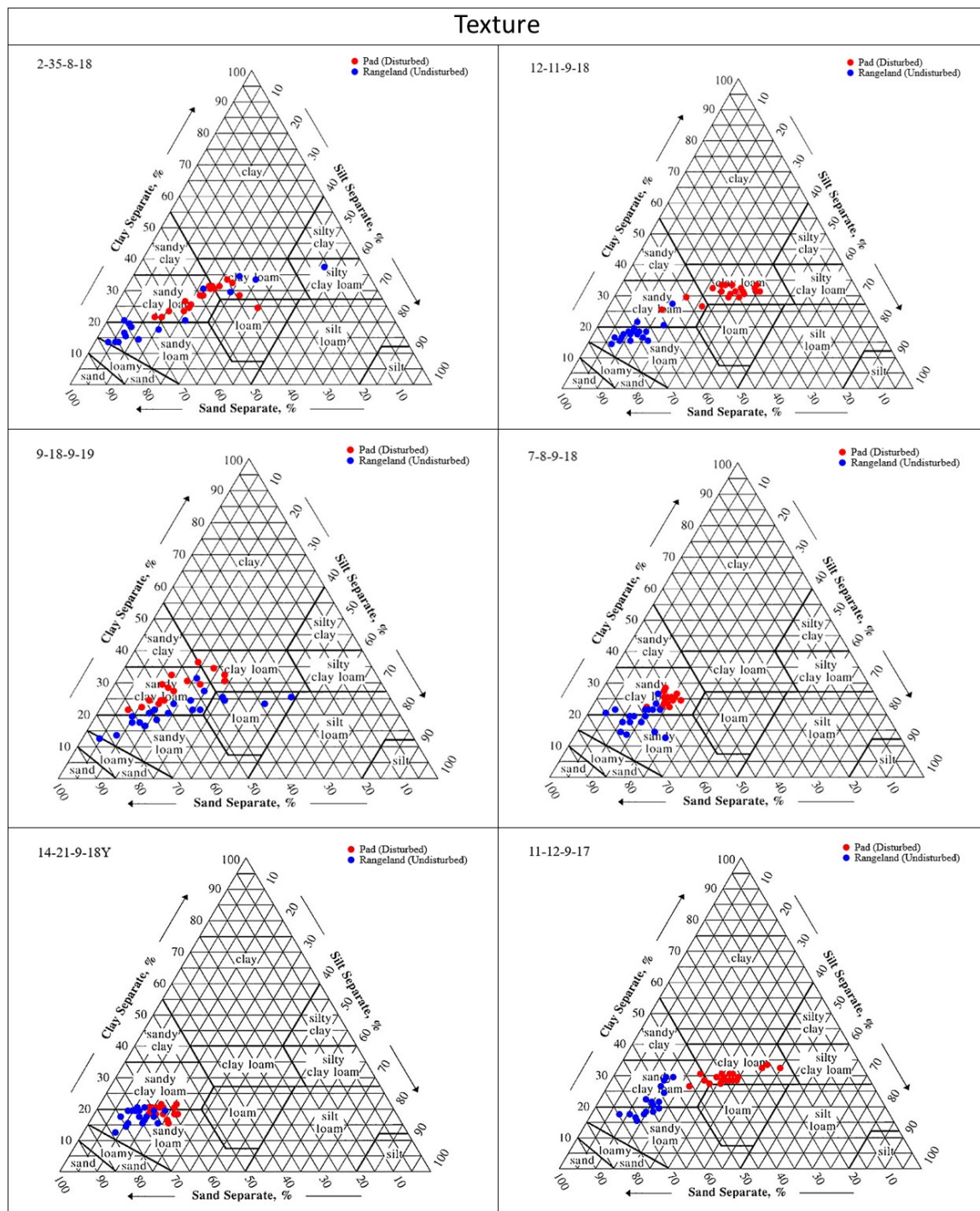


**Fig. 12. Texture triangle displaying each soil sample with the corresponding P&A well pad and rangeland.**

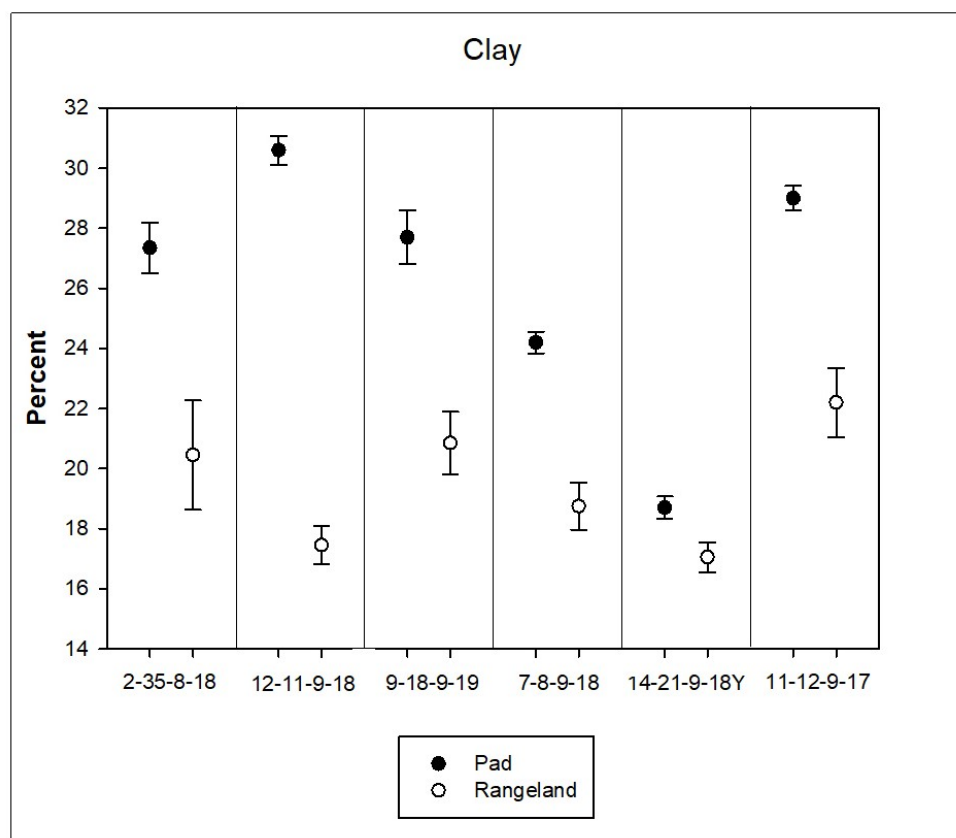


**Fig. 13. Percentage of clay with mean and error at all six locations.**

### Salinity

Salinity, measured by  $EC_e$ , was different between the disturbed P&A well pads and the adjacent rangeland at five of the six locations. P&A well pads had much higher levels of salinity than the undisturbed rangeland (Fig. 14 & 15). P&A well pads were 2 – 9 times greater in  $EC_e$  than the rangeland.

Location 14-21-9-18 was the only location not significantly different. This location has been left undisturbed for eight years (from when soil sample was taken), since it was declared plugged and abandoned (Table 6).

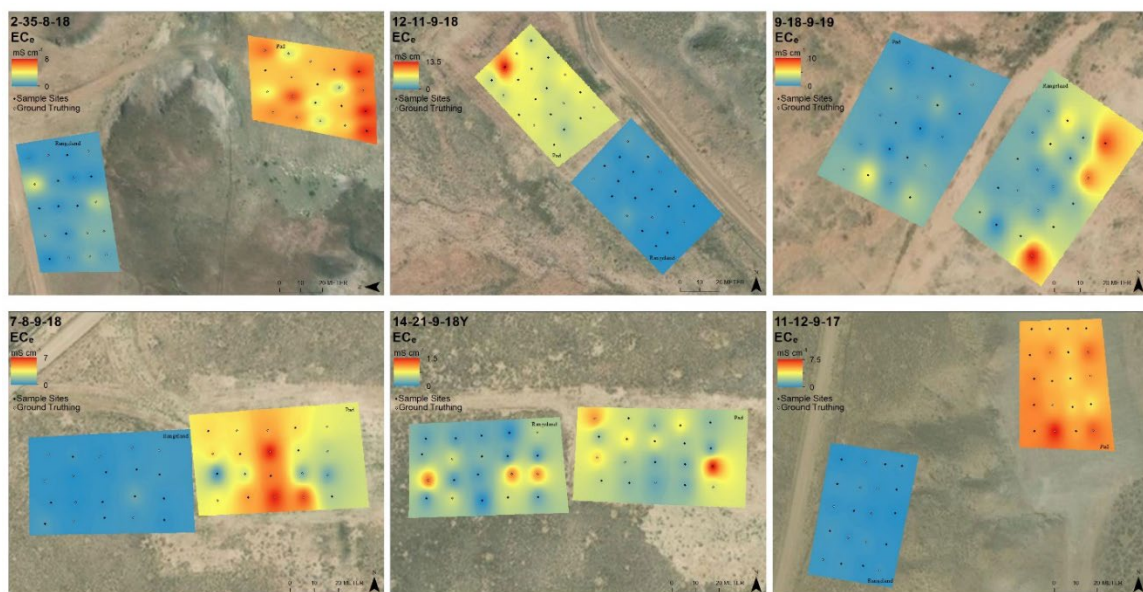


**Fig. 14. Interpolation map displaying  $EC_e$  values from all pads and the corresponding rangelands. Service Layer Credits: Source: Esri, DigitalGlobe, GeoEye, Earthstar Geographics, CNES/Airbus DS,a USDA, AeroGRID, IGN, and the GIS User Community.**

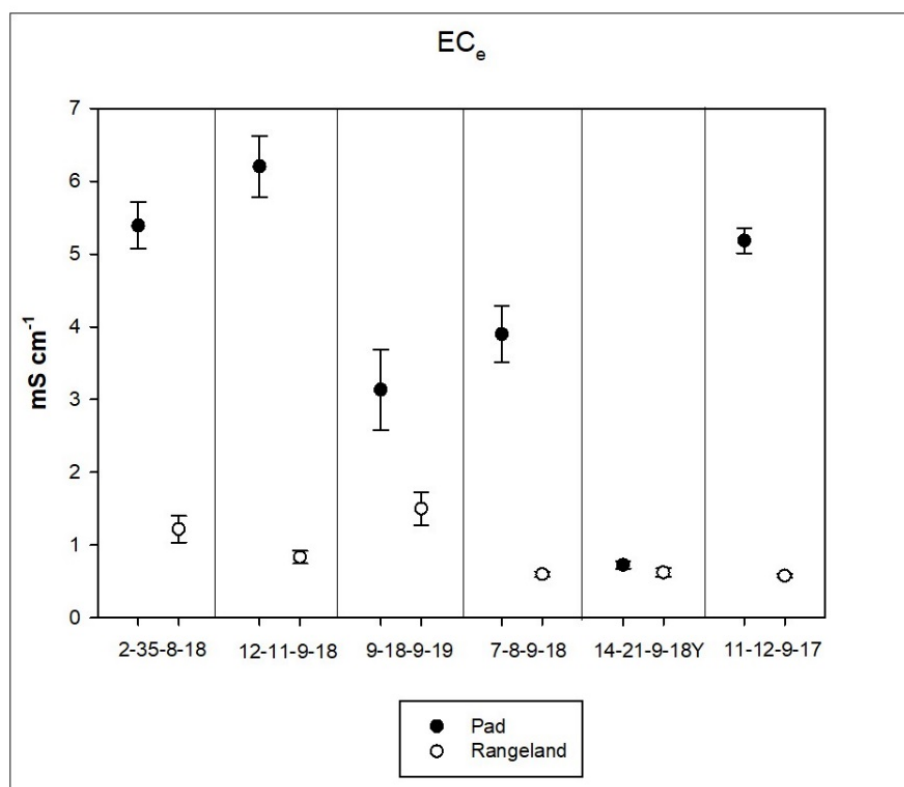


**Fig. 15. Electrical conductivity from a saturated paste extract ( $EC_e$ ) mean and error at all six locations.**

## Sodicity

P&A well pads had much higher levels of sodicity, measured by sodium adsorption ratio (SAR) than the undisturbed rangeland (Fig. 16 & 17). P&A well pads had 2 – 12.5 times greater SAR levels than the rangeland.

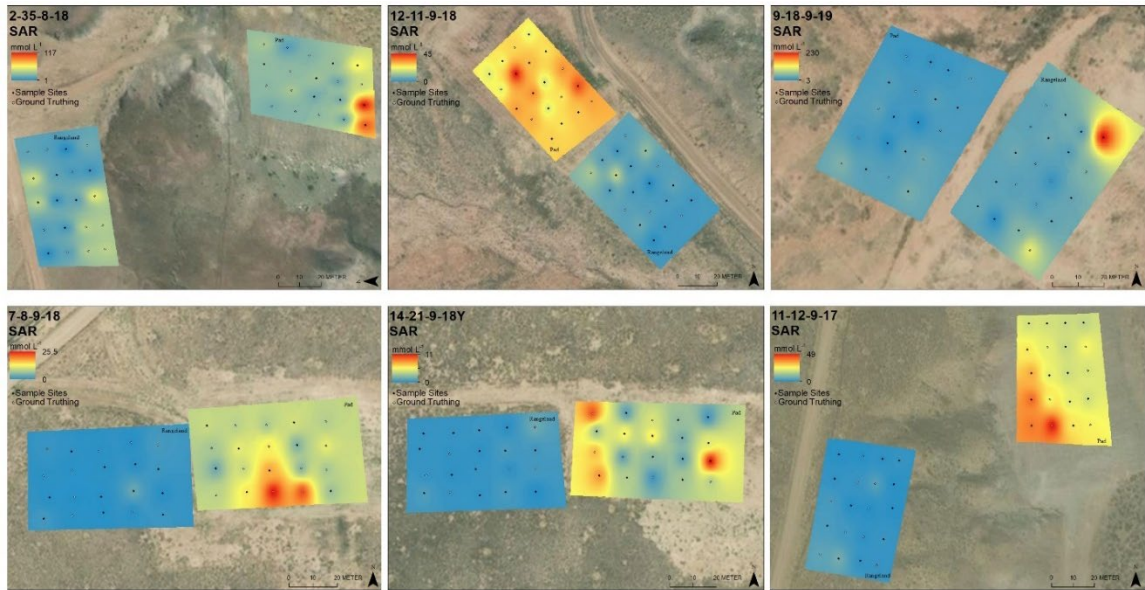


**Fig. 16. Interpolation map displaying SAR values from all pads and the corresponding rangelands. Service Layer Credits: Source: Esri, DigitalGlobe, GeoEye, Earthstar Geographics, CNES/Airbus DS,a USDA, AeroGRID, IGN, and the GIS User Community.**

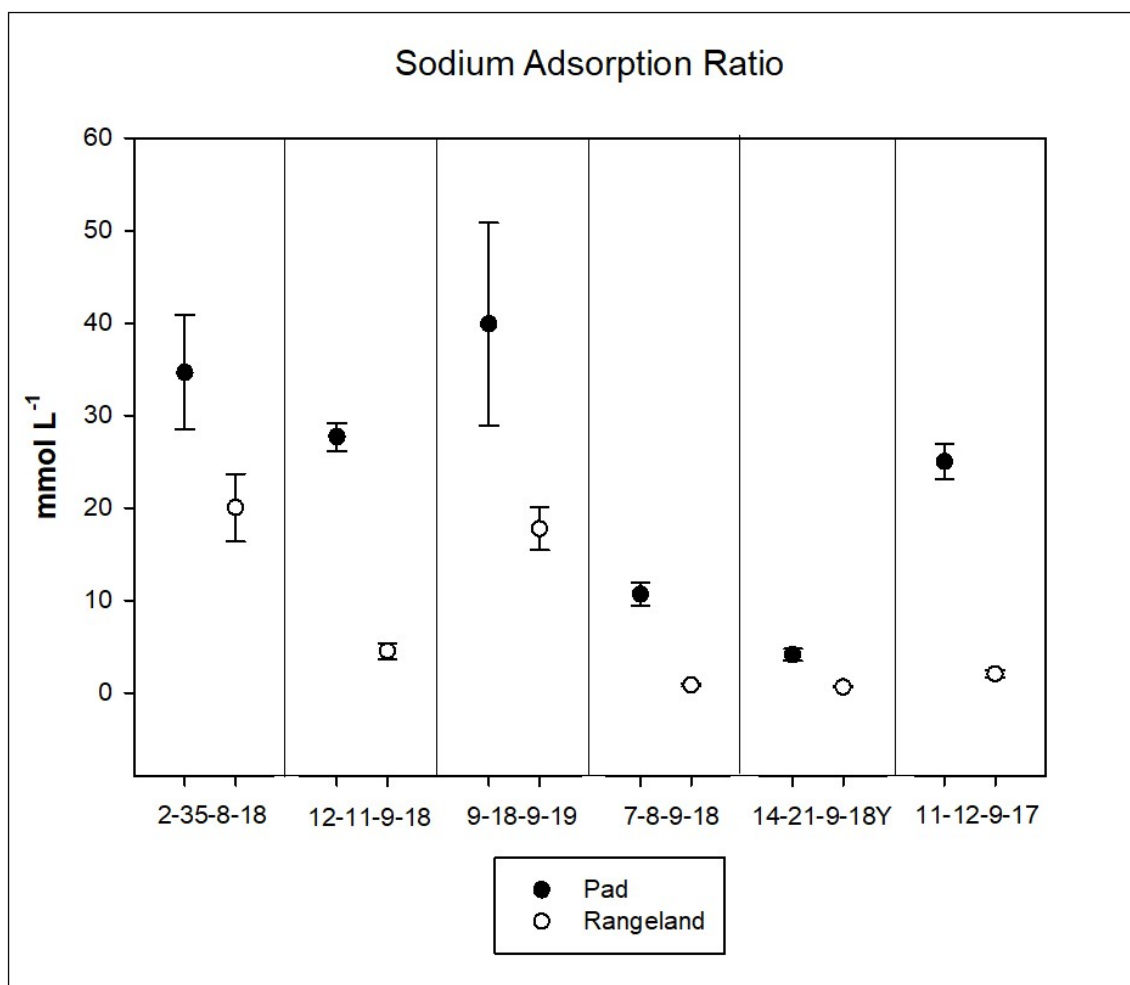


**Fig. 17. Sodium Adsorption Ratio (SAR) mean and error at all six locations.**

### Plant Cover

There was a higher percentage of beneficial plants on the rangeland compared to the P&A well pads at all six locations (Fig. 18).

The percent of plant cover of invasive plants was different at three locations. At locations 12-11-9-18 and 7-8-9-18, there was a higher percentage of invasive plants on the P&A well pad than the adjacent rangelands. At site 14-21-9-18Y there was a higher amount of invasive plants on the adjacent rangeland rather than the P&A well pad (Fig.



18). However, the adjacent rangeland at site 14-21-9-18Y still had more beneficial plant than invasive plants (Fig. 19).

There was a higher ratio of beneficial plants to invasive plants at all adjacent rangeland locations. There were also more invasive plants to beneficial plants on the P&A well pads at all locations, except at site 14-21-9-18Y, which had more beneficial plants than invasive plants (Table 1).

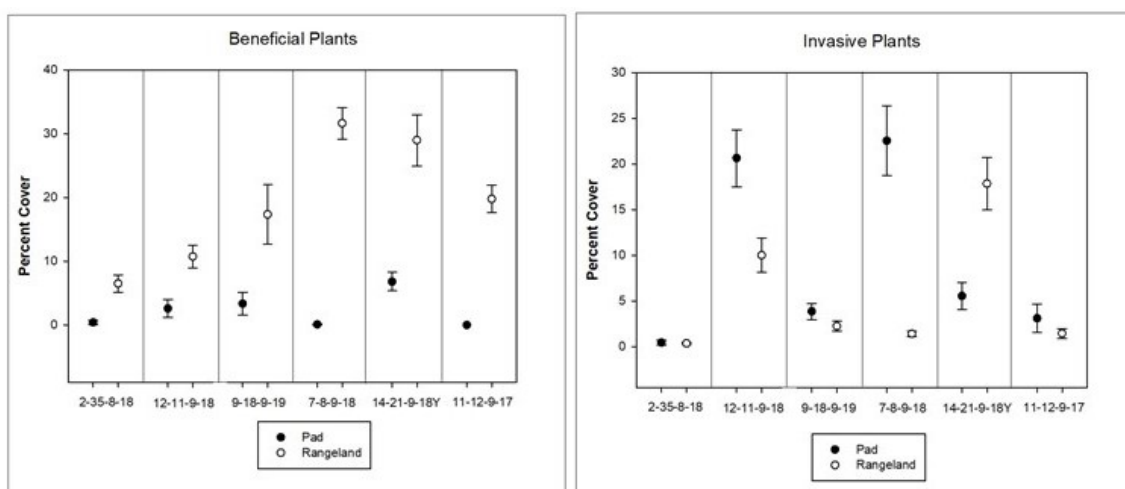


**Fig. 18. Percentages of plant cover for beneficial (left) and invasive (right) plants at all six locations with mean and error.**



**Table 1. The total percent cover from plant counts split into beneficial and invasive for P&A well pads (Pad) and the adjacent rangeland. Also included is the ratio of beneficial vs invasive plant cover.**

		Beneficial (% Cover)	Invasive (% Cover)	Ratio (Beneficial/Invasive)
2-35-8-18	Pad	8	9	0.89
	Rangeland	130	7	18.57
12-11-9-18	Pad	52	413	0.13
	Rangeland	215	200	1.08
9-18-9-19	Pad	67	77	0.87
	Rangeland	347	45	7.71
7-8-9-18	Pad	2	451	0.00
	Rangeland	633	28	22.61
14-21-9-18Y	Pad	136	111	1.23
	Rangeland	580	357	1.62
11-12-9-17	Pad	0	62	0.00
	Rangeland	396	29	13.66

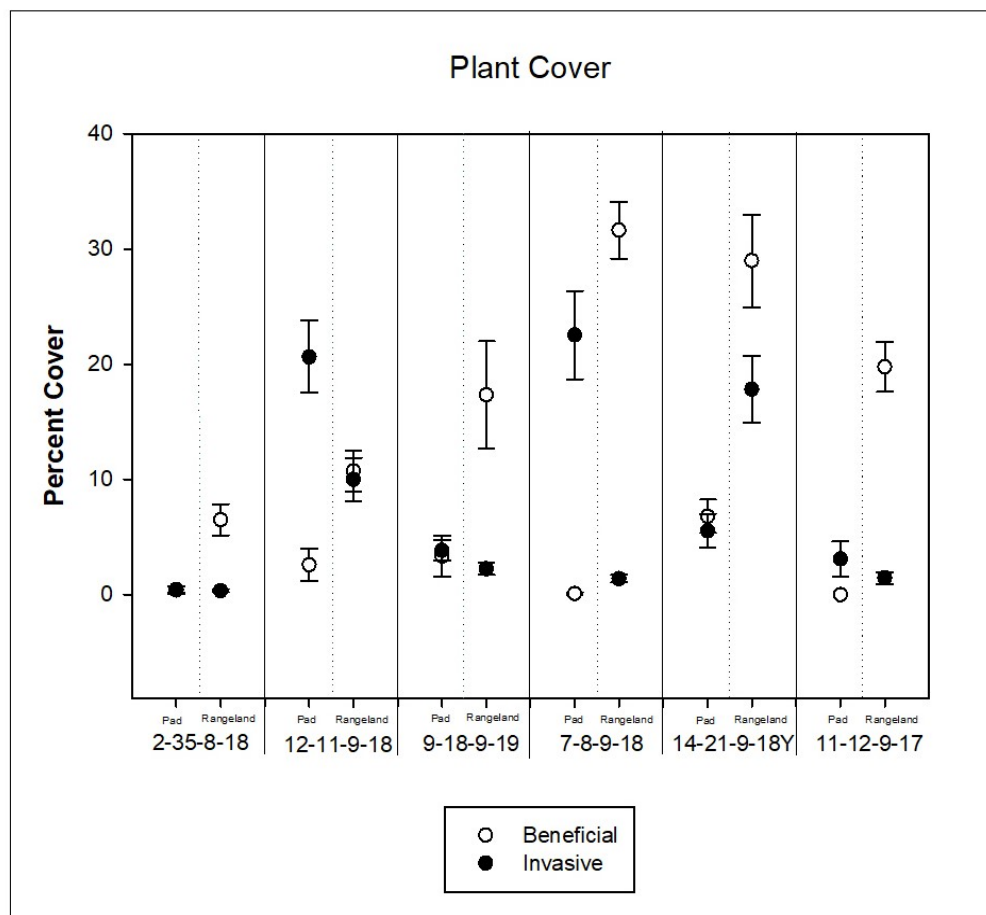


**Fig. 19. Percent plant cover of beneficial and invasive plants at all six locations with mean and error.**

### Aggregate Stability

Soil aggregate stability was measured at two locations: 12-11-9-18 and 9-18-9-19. There was a difference between the P&A well pads and the adjacent rangeland at one of the locations, 9-18-9-19. The aggregates from P&A well pad 9-18-9-19 were less stable and were more prone to slaking than the adjacent rangeland (Fig. 20). Soil aggregate stability had no significant correlation with SAR.

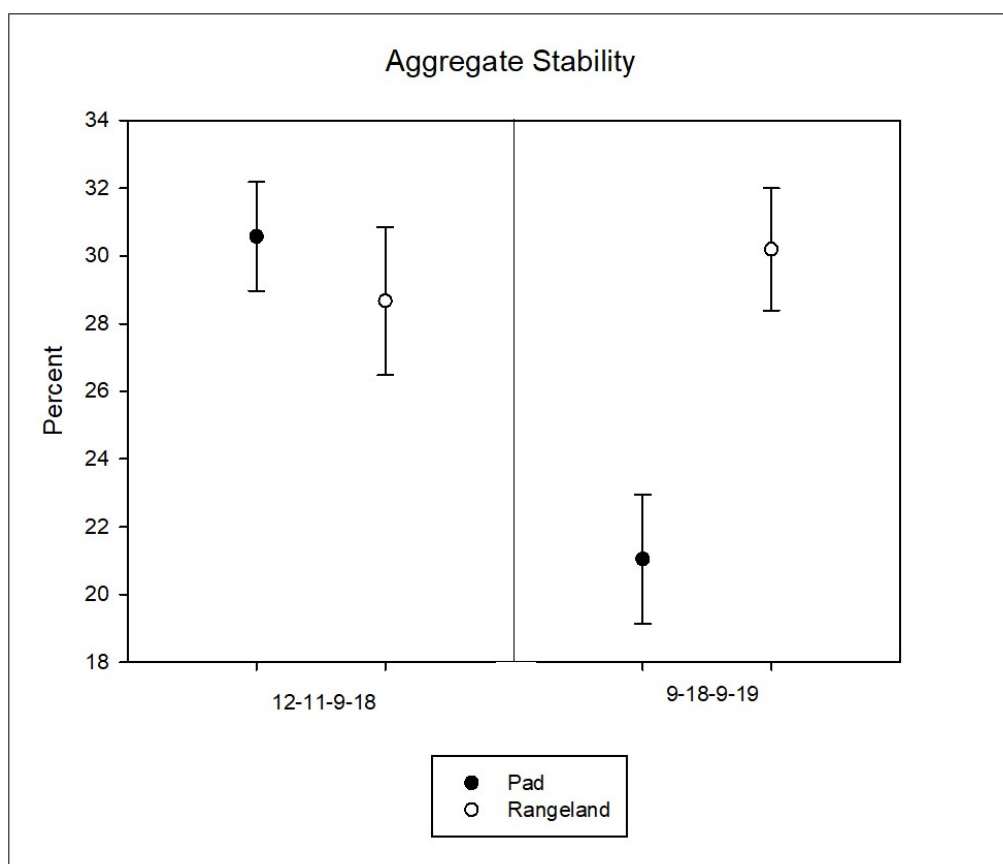


**Fig. 20. Aggregate Stability mean and error for the two locations tested.**

### Soil Microbial Activity

There was no measured difference in soil microbial activity, via CO<sub>2</sub> respiration between disturbed P&A well pads and undisturbed rangeland at the two locations

measured. Soil microbial activity was measured at two location: 2-35-8-18 and 12-11-9-18 (Fig. 21). There was no significant correlation between the amount of soil organic carbon and CO<sub>2</sub> respiration. This could be influenced by the seepage of methane, being broken down by methanotrophs into CO<sub>2</sub> prior to reaching the topsoil, where soil organic carbon samples were taken (Lyman et al., 2017; Lyman et al., 2020). Microbial CO<sub>2</sub> respiration, via subsurface methanotrophs, would not be accounted for in the soil organic carbon readings and would influence the correlation between soil organic carbon and CO<sub>2</sub> respiration.

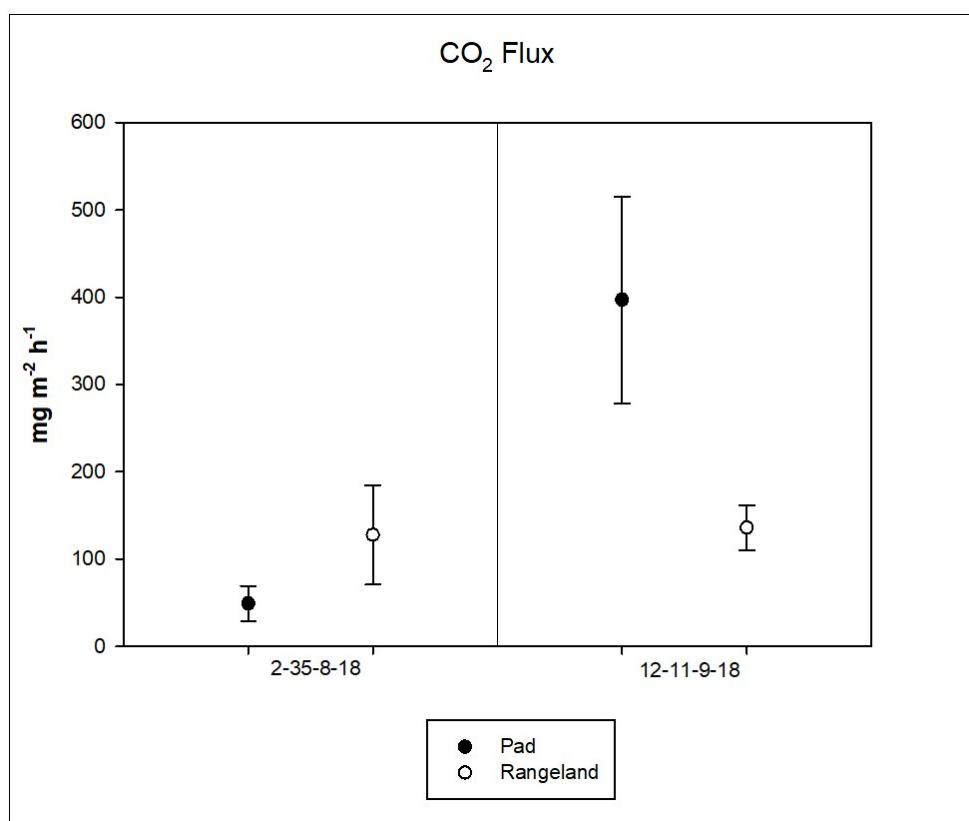


**Fig. 21. CO<sub>2</sub> Flux mean and error at the two locations measured. CO<sub>2</sub> flux is being used to measure soil CO<sub>2</sub> respiration.**

### Other Notable Differences

There was a difference in pH values at four of the locations (Fig. 29). At three of the locations: 2-35-8-18, 7-8-9-18, and 11-12-9-17, the adjacent rangeland had a higher pH than the P&A well pad. The rangeland at locations 14-21-9-18Y had a lower pH than the P&A well pad. This difference in soil pH was unexpected, as inherent soil indicator do not change rapidly.

Soil organic carbon was different at three locations: 2-35-8-18, 9-18-9-19, and 7-8-9-18. At P&A well pad 2-35-8-18, there was more soil organic carbon on the rangeland than the well pad (Fig. 30 & Table 3). At the other two locations, 9-18-9-19 and 7-8-9-18, there was more soil organic carbon on the P&A well pads than the adjacent rangeland. It was expected that if there was a difference in soil organic carbon, it would have been a similar to what was measured at 2-35-8-18, with the P&A well pads having less soil organic carbon than the adjacent rangeland. At site 9-18-9-19, this result could be due to the carbon treatments performing in 2014 – 2015, but that would also not account for the difference seen at location 7-8-9-18.

### **Electromagnetic Induction**

The multiple regressions performed used SAS Studio (SAS OnDemand for Academics) software, Version 9.4. SAS Studio software. The multiple regressions were used to determine those soil properties that impacted the  $EM_H$  values. Using the ground truthing sites (101 samples), SAR and soil moisture were determined to have had the greatest influence on  $EM_H$  (Tables 9 & 10). However, when all soil samples (240 samples) were included in the multiple regression, SAR, soil temperature, and soil

moisture had the greatest influence on  $EM_H$ , while pH and SOC also had an influence (Tables 7 & 8).

Another set of multiple regressions were performed, but only using the soil properties that had a significant impact on the  $EM_H$  values. These generated coefficients for the major influencing factors, from which a new equation was calculated and used to adjust the  $EM_H$  values, so only those factors that had the greatest impact on the EMI data.

Using the interpolated maps created via ArcGIS,  $EM_H$ ,  $EC_e$ , and SAR hot spots were identified on the P&A well pads and the adjacent rangeland. Interpolated maps were not created for soil moisture and soil temperature, as they were averaged for each location, removing variation. Both the rangeland and P&A well pads had SAR, soil moisture, and soil temperature as the major influences on  $EM_H$  values. Fig. 22 and 23 demonstrate a clear visual relationship between  $EM_H$  and SAR hotspots at the two locations (7-8-9-18 and 9-18-9-19) where it is most indicative. Where  $EM_H$  and SAR hotspots were visually similar,  $EC_e$  hotspots was also visually similar with  $EM_H$  (Fig. 24 & 25).

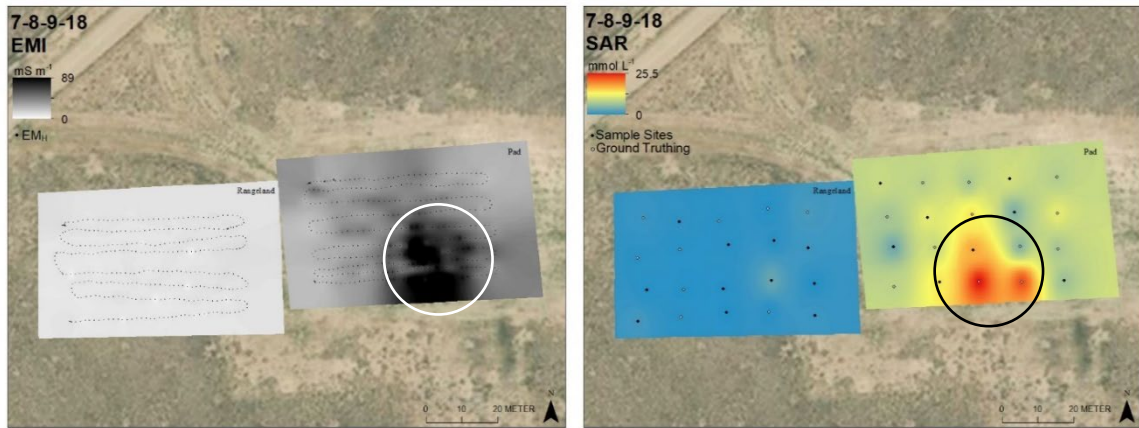


**Fig. 22. Interpolation map displaying the EM<sub>H</sub> (left) and SAR (right) values from pad 7-8-9-18 and its corresponding rangeland. Service Layer Credits: Source: Esri, DigitalGlobe, GeoEye, Earthstar Geographics, CNES/Airbus DS, USDA, AeroGRID, IGN, and the GIS User Community.**

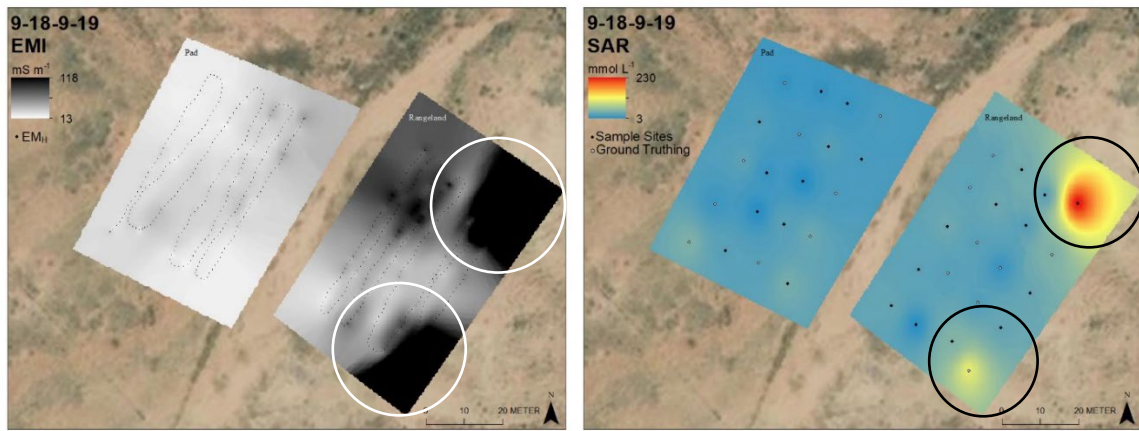


**Fig. 23. Interpolation map displaying the EM<sub>H</sub> (left) and SAR (right) values from pad 9-18-9-19 and its corresponding rangeland. Service Layer Credits: Source: Esri, DigitalGlobe, GeoEye, Earthstar Geographics, CNES/Airbus DS, a USDA, AeroGRID, IGN, and the GIS User Community.**

There was no visual relationship between EM<sub>H</sub> and SAR hotspots with the other 4 locations (2-35-8-18, 12-11-9-18, 14-21-9-18Y, 11-12-9-17) (Fig. 24 & 25). There were visual relationships between EM<sub>H</sub> and some other soil health properties hotspots. Location 12-11-9-18 showed a visual relationship between EM<sub>H</sub> and EC<sub>e</sub> hotspots (Fig. 24). Location 11-12-9-17 had a visual relationship between EM<sub>H</sub> and invasive plant cover

hotspots (Fig. 25). The increase in plant cover at this location might indicate an increase in soil moisture. Locations 2-35-8-18 and 14-21-9-18Y had no visual relationships between EM<sub>H</sub> and other soil health properties hotspots (Fig. 24 & 25).



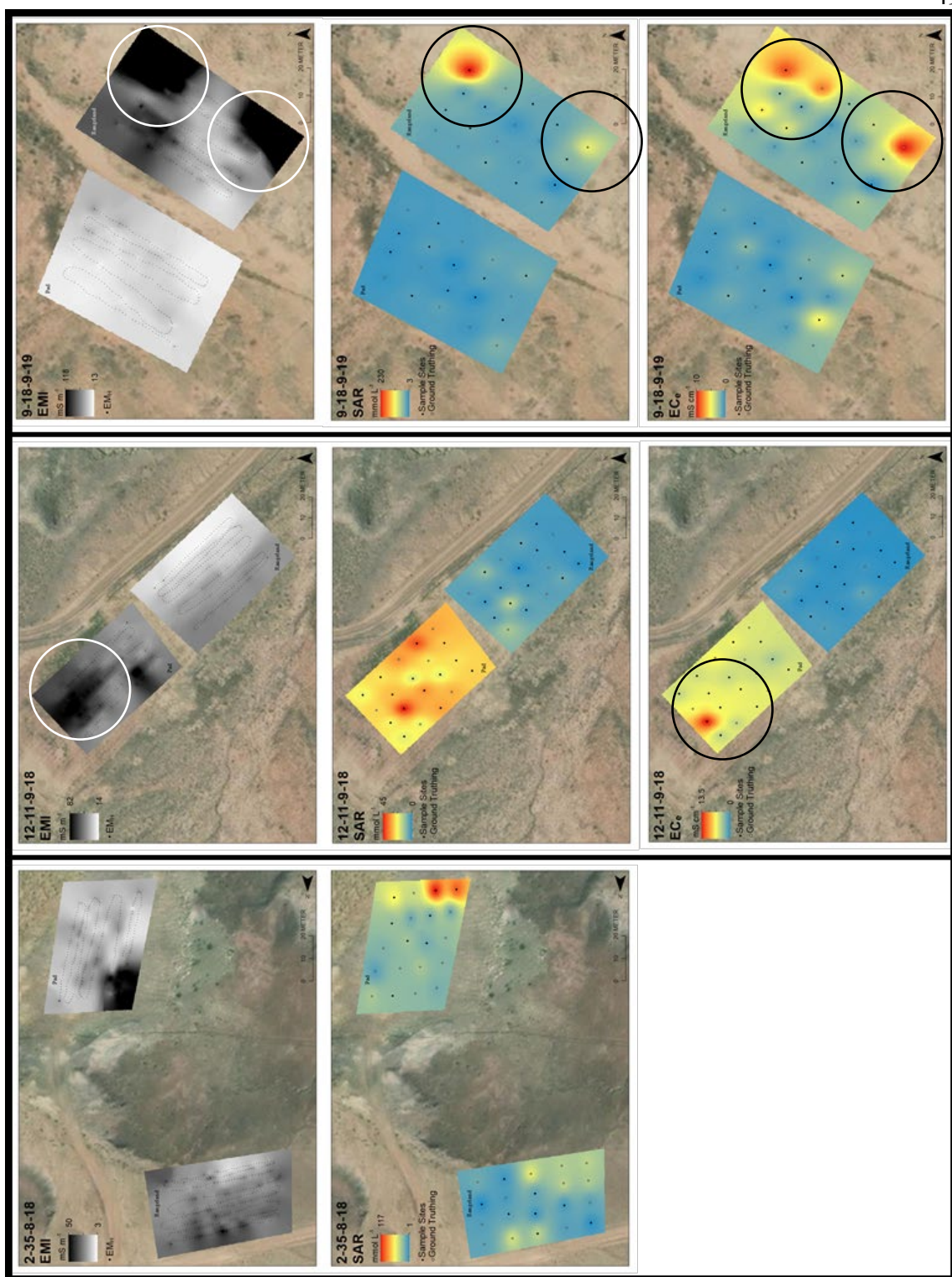


**Fig. 24. Interpolation maps displaying the EM<sub>H</sub>, SAR, and other values from P&A well pads; 2-35-8-18, 12-11-9-18, & 9-18-9-19 and the corresponding rangelands.**  
 Service Layer Credits: Source: Esri, DigitalGlobe, GeoEye, Earthstar Geographics, CNES/Airbus DS, a USDA, AeroGRID, IGN, and the GIS User Community.



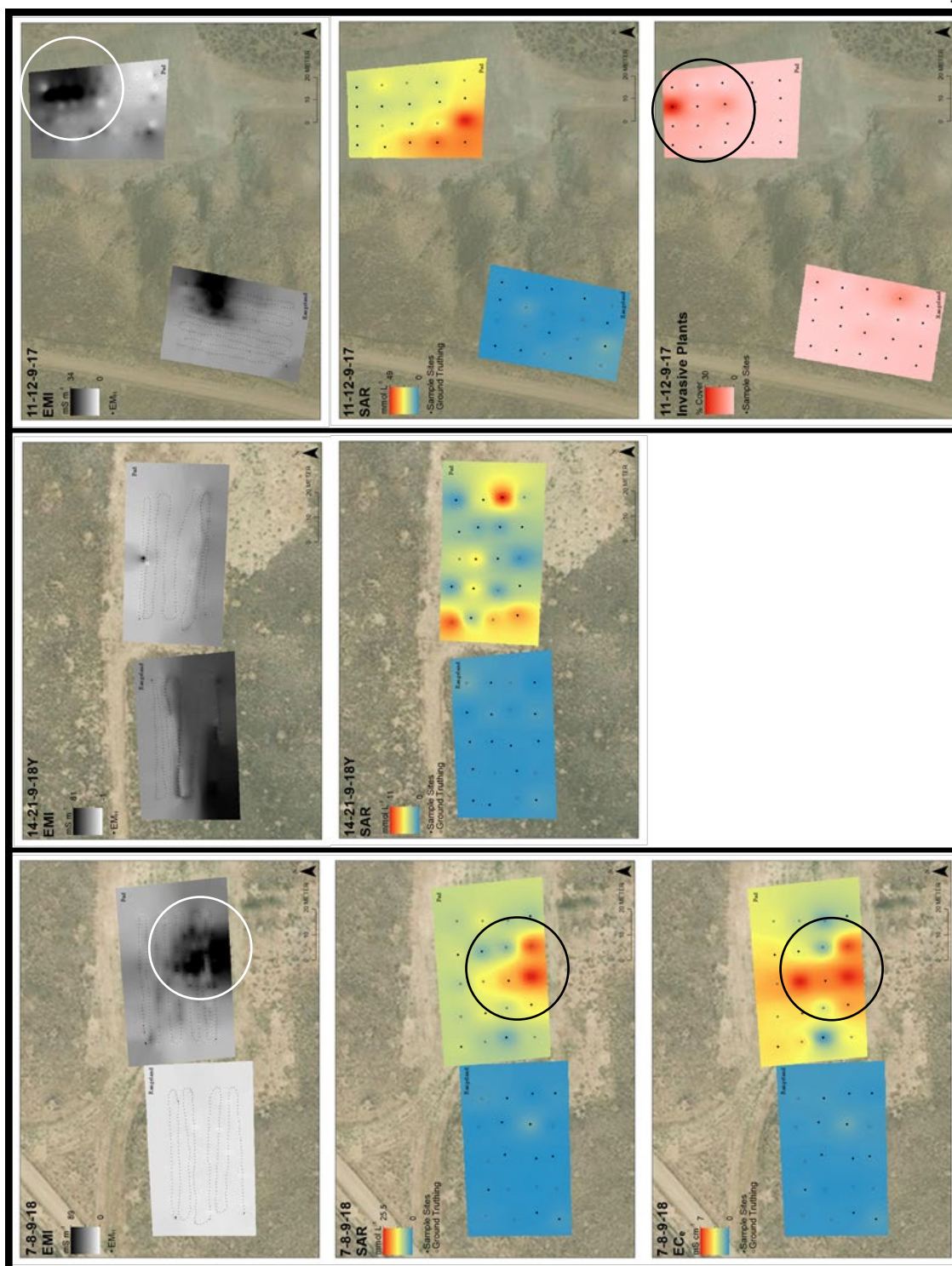


**Fig. 25. Interpolation maps displaying the EM<sub>H</sub>, SAR, and other values from P&A well pads; 7-8-9-18, 14-21-9-18Y, & 11-12-9-17 and the corresponding rangelands. Service Layer Credits: Source: Esri, DigitalGlobe, GeoEye, Earthstar Geographics, CNES/Airbus DS,a USDA, AeroGRID, IGN, and the GIS User Community.**

**DISCUSSION**

## Soil Health

Every location is unique when it comes to reclamation and soil health. Locations should be assessed on an individual basis with the adjacent rangeland. However, several soil health differences were found at all six disturbed P&A well pads. The P&A well pads had higher percentages of clay, higher amounts of sodium (SAR), and lower amounts of beneficial plant cover. And overall,  $EC_e$  was higher on P&A well pads, while pH was higher at three locations and lower at one, on the rangeland, compared to the P&A well pads.

Initially, it was thought that only dynamic soil health indicators would be influenced by oil and gas exploration, development, and extraction, specifically,  $EC_e$ , SAR, aggregate stability, and soil organic carbon. However, several inherent soil health indicators were different between P&A well pads and the adjacent, undisturbed rangeland, with soil texture being the most notable.

The presence of higher amounts of finer soil particles (clay and silt), sodium, and salts could be a result of subsoil being mixed into the topsoil, while the pad is initial being prepared for development or when the salvaged soil was placed back onto the well pad. Soil pH also varies depending on the soil horizon. Jones et al. (2017) measured differing soil pH between soil horizons (topsoil and subsoil) on the Pariette Bench. The change in soil pH could also be an indication of topsoil being mixed with subsoil.

A study on P&A well pads within the Pariette Bench by Grossl (2017) showed that salinity increased with depth on undisturbed soils, with salinity being higher on P&A well pads (Fig. 64). A soil profile described by Jones (2017) on a Pariette Bench undisturbed soil showed an increase in clay, salinity ( $EC_e$ ), and sodicity (SAR) with

depth. These studies show that there might be a mixing of topsoil and subsoil during pad development and pad reclamation. However, further research would be necessary to confirm the mixing of topsoil and subsoil, by measuring texture, salinity, and sodicity through the entire soil profile depth on both the rangeland and the P&A well pads.

If the topsoil and subsoil are being mixed prior to reclamation, land managers may find it best to change the procedure in which topsoil and subsoil are collected, stored, and redistributed. The addition of more organic matter could also prove beneficial by increasing the amount of organic carbon in the soil. While only one location measured had significantly less soil organic carbon, the addition of more organic matter could help alleviate some issues created by the increase in clay content, salts, and exchangeable sodium. Soil organic carbon can improve water and air infiltration and prevent sodic crusts from forming. Soil organic carbon can also increase aggregate stability as well as microbial activity, in those locations where those are a concern.

In conclusion, there was a clear difference between the soil health on the P&A well pads compared to the undisturbed, adjacent rangeland. P&A well pads are not as “healthy” as the undisturbed, adjacent rangeland. There is an overall difference in soil texture and sodicity, which impacts plant growth and that can prevent or delay successful P&A well pad reclamation.



**Fig. 26. Well pad with salvaged topsoil.**

### **Electromagnetic Induction**

Electromagnetic induction may prove helpful to land managers in order to locate potential saline/sodic hotspots to create a targeted reclamation plan. However, due to the many variables that can impact the  $EM_H$  values, each location may be different. Taking samples for ground truthing is required in order to understand which soil properties have the greatest influence, but even with ground-truthing, there is no certainty that the  $EM_H$  values will directly indicate the salinity or sodicity on P&A well pads.

Interpolated maps can provide beneficial information to help visualize certain soil properties, but their value should only be used as an informational tool and not exact values.

## CHAPTER 3: SUMMARY

There was a difference between the soil health between plugged and abandoned (P&A) well pads and adjacent, undisturbed rangeland. The P&A well pads had significantly lower soil health than adjacent rangeland.

While each location measured is independent of the others, there were common differences between the P&A well pads and the undisturbed rangeland segments, at all the sites measured. Those common differences include: soil texture, sodium adsorption ratio, exchangeable sodium percentage,  $EC_e$ , and beneficial plant cover (Table 3; Fig. 12, 13, 14, 15, 16, 17, & 18). All six locations had a significant difference in soil texture, with the P&A well pads having a finer soil texture and the rangeland having a coarser soil texture (Table 3; Fig. 12 & 13). The P&A well pads had higher amounts of sodium (SAR and ESP) at all six sites measured as well as having higher amounts of salts ( $EC_e$ ) at five of the locations (Table 3; Fig. 14, 15, 16, & 17). And while not a soil health indicator, plant counts provide important information on the P&A well pad's progress towards successful reclamation. At all locations, the undisturbed adjacent rangeland had more beneficial plant cover as well as having a greater ratio of beneficial than invasive plant cover (Tables 3 & 5; Fig. 18 & 19).

Electromagnetic induction can be influenced by several different soil properties. Some of the soil properties that influence electromagnetic induction are soil health indicators. The soil health indicators that can influence electromagnetic induction and that were measured in this study include: soil texture (sand, silt, and clay percentages), soil organic carbon (SOC), pH,  $EC_e$ , and sodium adsorption ratio (SAR).

The factors that had the greatest influence on the electromagnetic induction were SAR, soil temperature, and soil moisture. Sodium adsorption ratio (SAR) is a soil health indicator, but soil temperature and soil moisture are not soil health indicators.

There were no correlations between any tested soil health indicators and the  $EM_H$  value from electromagnetic induction so no information can be directly obtained about the soil health from just  $EM_H$  values. While not directly correlated with  $EM_H$ , SAR had a strong influence on the  $EM_H$  values, leading to two locations (9-18-9-19, 7-8-9-18) where  $EM_H$  and SAR hotspots were visually similar (Fig. 22 & 23).

Since  $EM_H$  values can be influenced by some soil health indicators, information can be obtained, as long as those soil health indicators have a significant influence on the  $EM_H$  reading. By performing multiple regressions, any possible soil health indicator that impacts the  $EM_H$  can be identified, and information about the soil health can be estimated.

## REFERENCES

- Abiven, S., S. Menasseri, and C. Chenu. 2009. The effects of organic inputs over time on soil aggregate stability – A literature analysis. *Soil Biol. Biochem.* 41:1–12.
- Adamchuk, V.I., J.W. Hummel, M.T. Morgan, and S.K. Upadhyaya. 2004. On-the-go soil sensors for precision agriculture. *Comput. Electron. Agric.* 44:71–91.
- Arias, M.E., J.A. Gonzales-Perez, F.J. Gonzalez-Vila, and A.S. Ball. 2005. Soil Health – A new challenge for microbiologists and chemists. *Int. Microbiol.* 8:13–21.
- Armstrong, A.S., and T.W. Tanton. 1992. Gypsum applications to aggregated saline-sodic clay topsoils. *J. Soil Sci.* 43:249–260.
- Carter, M.R., E.G. Gregorich, D.W. Anderson, J.W. Doran, H.H. Janzen, and F.J. Pierce. 1997. Concepts of Soil Quality and Their Significance. In: E.G. Gregorich and M.R. Carter, editors, *Soil Quality for Crop Production and Ecosystem Health*. p. 1–19.
- Davidson, E.A., I.A. Janssens, and Y. Luo. 2006. On the variability of respiration in terrestrial ecosystems: moving beyond  $Q_{10}$ . *Global Change Biol.* 12:154–164.
- Diaz, E., A. Roldan, A. Lax, and J. Albaladejo. 1994. Formation of stable aggregates in degraded soil by amendment with urban refuse and peat. *Geoderma* 63:277–288.
- Doolittle, J.A., and E.C. Brevik. 2014. The use of electromagnetic induction techniques in soils studies. *Geoderma* 223:33–45.
- Doran, J.W. 2002. Soil health and global sustainability: translating science into practice. *Agric., Ecosyst. Environ.* 88:119–127.
- Dose, H.L., A. Fortuna, L.J. Cihacek, J. Norland, T.M. DeSutter, D.E. Clay, and J. Bell. 2015. Biological indicators provide short term soil health assessment during sodic soil reclamation. *Ecol. Indic.* 58:244–253.
- Ekwue, E.I. 1990. Organic-Matter Effects on Soil Strength Properties. *Soil Tillage Res.* 16:289–297.
- Gregorich, E.G., M.R. Carter, J.W. Doran, C.E. Pankhurst, and L.M. Dwyer. 1997. Biological Attributes of Soil Quality. In: E.G. Gregorich and M.R. Carter, editors, *Soil Quality for Crop Production and Ecosystem Health*. p. 81–113.
- Grossl, P.R. 2017. Reclamation of Disturbed Arid Lands Study in Utah (Agreement No. BLM# L10AC20369).

- Heil, D., and G. Sposito. 1997. Chemical Attributes and Processes Affecting Soil Quality. In: E.G. Gregorich and M.R. Carter, editors, *Soil Quality for Crop Production and Ecosystem Health*. p. 59–79.
- Heil, K., and U. Schmidhalter. 2017. The Application of EM38: Determination of Soil Parameters, Selection of Soil Sampling Points and Use in Agriculture and Archaeology. *Sensors* 17(2540):1–44.
- Herrick, J.E., W.G. Whitford, A.G. de Soyza, J.W. Van Zee, K.M. Havstad, C.A. Seybold, and M. Walton. 2001. Field soil aggregate stability kit for soil quality and rangeland health evaluations. *Catena* 44:27–35.
- Jones, C.P., P.R. Grossl, M.C. Amacher, J.L. Boettinger, A.R. Jacobson, and J.R. Lawley. 2017. Selenium and salt mobilization in wetland and arid upland soils of Pariette Draw, Utah (USA). *Geoderma* 305:363–373.
- Karlen, D.L., S.S. Andrews, B.J. Wienhold, and T.M. Zobeck. 2008. Soil Quality Assessment: Past, Present and Future. *J. Integr. Biosci.* 6(1):3–14.
- Karlen, D.L., C.A. Ditzler, and S.S. Andrews. 2003. Soil quality: why and how? *Geoderma* 114:145–156.
- Kemper, W.D., and R.C. Rosenau. 1986. Aggregate stability and size distribution. In: A. Klute et al., editors, *Methods of soil analysis. Part 1*. 2nd ed. Agron. Monogr. 9. ASA and SSSA, Madison, WI. p. 425–442.
- Lloyd, J., and J.A. Taylor. 1994. On the Temperature Dependence of Soil Respiration. *Funct. Ecol.* 8(3):315–323.
- Lyman, S.N., C. Watkins, C.P. Jones, M. L. Mansfield, M. McKinley, D. Kenney, and J. Evans. 2017. Hydrocarbon and carbon dioxide fluxes from natural gas well pad soils and surrounding soils in Eastern Utah. *Environ. Sci. Technol.* 51(20):11625–11633.
- Lyman, S.N., H.N.Q. Tran, M.L. Mansfield, R. Bowers, and A. Smith. 2020. Methane fluxes from natural gas well pad soils exhibit strong temporal variability. Under review for *Atmospheric Pollution Research*.
- Lyman, S.N., M.L. Mansfield, H.N.Q. Tran, J.D. Evans, C. Jones, T. O’Neil, R. Bowers, A. Smith, and C. Keslar. 2018. Emissions of organic compounds from produced water ponds I: Characteristics and speciation. *Sci. Total Environ.* 619–620:896–905.



- Makky A.A., A. Alaswad, D. Gibson, S. Song, and A.G. Olabi. 2018. A numerical and experimental study of a new design of closed dynamic respiration chamber. *Computers and Electronics in Agriculture*. 145:326–340.
- Moebius-Clune, B.N., D.J. Moebius-Clune, B.K. Gugino, O.J. Idowu, R.R. Schindelbeck, A.J. Ristow, H.M. van Es, J.E. Thies, H.A. Shayler, M.B. McBride, K.S. M Kurtz, D.W. Wolfe, and G. S. Abawi. 2016. *Comprehensive Assessment of Soil Health – The Cornell Framework*, 3.2 ed. Cornell University, Geneva, NY.
- Mzezewa, J., J. Gotosa, and B. Nyamwanza. 2003. Characterisation of a sodic soil catena for reclamation and improvement strategies. *Geoderma*. 113:161–175.
- Raiesi, F., and A. Beheshti. 2015. Microbiological indicators of soil quality and degradation following conversions of native forests to continuous croplands. *Ecol. Indic.* 50:173–185.
- Rhoades, J.D. 1974. Drainage for Salinity Control. In: J. van Schilfgaarde, editors, *Drainage for Agriculture*. Am. Agron. Soc. Monogr. 17. p. 433–462.
- SAS Institute. 2019. SAS user's guide. SAS Inst., Cary, NC.
- Seybold, C.A., and J.E. Herrick. 2001. Aggregate stability kit for soil quality assessments. *Catena* 44:37–45.
- Skaggs, R. 2008. Ecosystem services and western U.S. rangelands. *Choices*. 23(2):37–41.
- Stott, D.E. 2019. Recommended Soil Health Indicators and Associated Laboratory Procedures. Soil Health Technical Note No. 430-03. U.S. Department of Agriculture, Natural Resources Conservation Service.
- Tisdall, J.M., and J.M. Oades. 1982. Organic matter and water-stable aggregates in soils. *J. Soil Sci.* 33:141–163.
- USDA – ARS. 1954. *Diagnosis and Improvement of Saline and Alkali Soils*.
- USDA – NRCS. 1996a. *Soil Quality Indicators: Organic Matter*.
- USDA – NRCS. 1996b. *Soil Quality Indicators: Aggregate Stability*.
- USDA – NRCS. 1998. *Soil Quality Resource Concerns: Salinization*.
- USDA – NRCS. 1999. *Soil Quality Test Kit Guide*.
- USDA – NRCS. 2001a. *Rangeland Soil Quality – Organic Matter*.

USDA – NRCS. 2001b. Rangeland Soil Quality – Physical and Biological Soil Crusts.

USDA – NRCS. 2008a. Soil Quality Indicators: Aggregate Stability.

USDA – NRCS. 2008b. Soil Quality Indicators: Slaking.

USDI – BLM. 2007. Surface Operating Standards and Guidelines for Oil and Gas Exploration and Development.

USDI – BLM, Green River District. 2011. Green River District Reclamation Guidelines. Bureau of Land Management Green River District, Vernal, Utah.

USDI – BLM, Vernal Field Office. 2012. Greater Uinta Basin: Oil and Gas Impacts Technical Support Document. Bureau of Land Management Vernal Field Office, Vernal, Utah.

USDI – USGS. The Public Land Survey System (PLSS). *USGS*, 18 January 2018, [http://nationalmap.gov/small\\_scale/a\\_plss.html](http://nationalmap.gov/small_scale/a_plss.html). Accessed 4 September 2019.

## APPENDICES

**Table 2. List of pad numbers and their corresponding information.**

Pad #	GPS Coordinates (DD)	API #	Well Type	Well Depth (ft)	Producing Date	P&A Completion Date
2-35-8-18	40.0757° -109.8625°	43-047-31455	Oil	6200	21-Nov-1984	9-Mar-2018
12-11-9-18	40.0437° -109.8679°	43-047-31029	Oil	5650	22-Jan-1982	27-Jul-2016
9-18-9-19	40.0362° -109.8163°	43-047-30063	Oil	4850	10-Oct-1969	29-Mar-1989
7-8-9-18	40.0475° -109.914°	43-047-31274	Oil	6070	4-Nov-1983	16-Mar-2017
14-21-9-18Y	40.0111° -109.9062°	43-047-32726	Oil	5350	10-Jun-1998	8-Feb-2010
11-12-9-17	40.0431° -109.9585°	43-047-35167	Oil	5770	7-Dec-2004	14-Dec-2017

**Table 3. All soil tests performed with mean and error values with corresponding site names. Pad indicates P&A well pad and RL indicates the adjacent rangeland.**

		2-35-8-18		12-11-9-18		9-18-9-19		7-8-9-18		14-21-9-18Y		11-12-9-17	
		Pad	RL	Pad	RL	Pad	RL	Pad	RL	Pad	RL	Pad	RL
Sand (%)	Mean	*50.20	64.60	***37.85	71.75	56.10	59.00	***57.45	67.35	***64.40	70.75	***39.80	64.00
	Error	1.90	4.56	1.73	1.24	1.90	3.28	0.50	1.13	0.60	0.88	1.51	1.40
Silt (%)	Mean	*22.45	14.95	***31.55	10.80	16.60	20.15	***18.35	13.90	***16.90	12.20	***31.20	13.80
	Error	1.36	2.85	1.42	0.78	1.15	2.51	0.39	0.99	0.63	0.72	1.20	0.51
Clay (%)	Mean	*27.35	20.45	***30.60	17.45	***27.70	20.85	***24.20	18.75	*18.70	17.05	***29.00	22.20
	Error	0.83	1.83	0.49	0.64	0.89	1.04	0.36	0.79	0.37	0.49	0.40	1.16
Aggregate Stability (%)	Mean	--	--	30.58	28.67	***21.04	30.20	--	--	--	--	--	--
	Error	--	--	1.61	2.19	1.90	1.80	--	--	--	--	--	--
pH	Mean	*8.15	8.36	7.89	7.98	8.24	8.33	***7.98	8.28	*8.19	7.96	***7.76	8.15
	Error	0.09	0.06	0.05	0.08	0.08	0.04	0.07	0.03	0.06	0.06	0.06	0.04
EC <sub>e</sub> (mS cm <sup>-1</sup> )	Mean	***5.39	1.22	***6.21	0.83	*3.13	1.50	***3.90	0.60	0.72	0.62	***5.19	0.58
	Error	0.32	0.18	0.42	0.09	0.55	0.23	0.39	0.04	0.05	0.06	0.17	0.02
SAR (mmol L <sup>-1</sup> )	Mean	*34.68	20.04	***27.73	4.54	*39.92	17.77	***10.68	0.85	***4.12	0.65	***25.04	2.08
	Error	6.16	3.65	1.53	0.85	10.94	2.32	1.26	0.16	0.65	0.07	1.90	0.41
ESP (%)	Mean	*30.01	19.62	***28.05	4.95	*30.40	18.89	***12.26	0.35	***4.46	0.08	***25.76	1.81
	Error	2.91	3.09	1.10	1.04	3.44	2.10	1.32	0.19	0.85	0.06	1.37	0.54
Total Carbon (%)	Mean	*1.00	1.36	*1.23	1.00	1.39	0.88	***2.30	0.99	***2.22	1.43	1.23	1.32
	Error	0.04	0.19	0.06	0.05	0.30	0.05	0.13	0.07	0.07	0.04	0.05	0.05
Inorganic Carbon (%)	Mean	*0.78	0.63	***0.85	0.61	0.50	0.57	***1.66	0.59	***1.74	0.95	0.91	0.97
	Error	0.03	0.07	0.03	0.03	0.02	0.03	0.08	0.07	0.07	0.03	0.04	0.04
Soil Organic Carbon (%)	Mean	***0.22	0.73	0.38	0.39	*0.89	0.30	*0.64	0.40	0.47	0.48	0.32	0.34
	Error	0.02	0.14	0.05	0.04	0.29	0.05	0.09	0.03	0.05	0.05	0.02	0.03
CO <sub>2</sub> Flux (mg m <sup>-2</sup> h <sup>-1</sup> )	Mean	49.06	127.56	397.23	135.84	--	--	--	--	--	--	--	--
	Error	20.30	56.78	118.40	25.79	--	--	--	--	--	--	--	--
Beneficial Plant Cover (%)	Mean	***0.40	6.50	***2.60	10.75	*3.35	17.35	***0.10	31.65	***6.80	29.00	***0.00	19.80
	Error	0.35	1.37	1.37	1.78	1.77	4.65	0.10	2.47	1.45	4.02	0.00	2.18
Invasive Plant Cover (%)	Mean	0.45	0.35	*20.65	10.00	3.85	2.25	***22.55	1.40	***5.55	17.85	3.10	1.45
	Error	0.27	0.11	3.13	1.88	0.90	0.53	3.83	0.31	1.47	2.89	1.52	0.52

\*Significant at the 0.05 probability level

\*\*\* Significant at the 0.001 probability level

**Table 4. List of tested soil attributes and the P&A well pad/rangeland, with the associated T-Stat and P-Value, showing significant differences between the P&A well pad and rangeland.**

		2-35-8-18	12-11-9-18	9-18-9-19	7-8-9-18	14-21-9-18Y	11-12-9-17
Sand	T-Stat	-2.75	-18.80	-0.57	-7.11	-5.68	12.19
	P-Value	6.61E-03	1.40E-13	0.29	6.35E-07	1.08E-05	1.95E-10
Silt	T-Stat	2.10	13.91	-1.28	3.61	4.43	-15.27
	P-Value	2.52E-02	2.26E-11	0.11	9.90E-04	1.63E-04	4.79E-12
Clay	T-Stat	3.56	17.27	4.58	5.45	2.36	-5.44
	P-Value	1.12E-03	5.99E-13	1.15E-04	1.79E-05	1.49E-02	1.79E-05
Aggregate Stability	T-Stat	--	0.67	-3.77	--	--	--
	P-Value	--	0.26	3.77E-04	--	--	--
pH	T-Stat	-1.75	-0.73	-0.60	-4.67	2.79	5.42
	P-Value	4.83E-02	0.24	0.28	9.53E-05	6.01E-03	1.88E-05
EC <sub>e</sub>	T-Stat	9.40	12.17	3.29	7.81	1.34	-25.44
	P-Value	1.14E-08	2.01E-10	2.04E-03	1.73E-07	9.91E-02	7.29E-16
SAR	T-Stat	2.20	15.55	2.19	7.42	5.30	-11.18
	P-Value	2.02E-02	1.46E-12	2.07E-02	2.50E-07	2.05E-05	7.79E-10
ESP	T-Stat	2.28	17.11	3.44	8.21	4.88	-15.18
	P-Value	1.74E-02	6.98E-13	1.44E-03	8.47E-08	6.05E-05	5.29E-12
Total Carbon	T-Stat	-1.99	3.57	1.66	9.33	10.52	1.08
	P-Value	3.09E-02	1.09E-03	5.72E-02	1.28E-08	2.04E-09	0.15
Inorganic Carbon	T-Stat	1.74	7.04	-1.53	10.83	10.50	0.85
	P-Value	4.91E-02	7.16E-07	7.13E-02	1.29E-09	2.09E-09	0.20
Soil Organic Carbon	T-Stat	-3.64	-0.23	1.99	2.30	-0.14	0.68
	P-Value	9.39E-04	0.41	3.12E-02	1.68E-02	0.45	0.25
CO <sub>2</sub> Flux	T-Stat	1.46	0.11	--	--	--	--
	P-Value	0.11	5.50E-02	--	--	--	--
Desirable Plant Cover	T-Stat	-4.60	-4.26	-2.65	-12.05	-4.59	-8.65
	P-Value	1.10E-04	2.37E-04	8.21E-03	2.36E-10	1.15E-04	3.99E-08
Invasive Plant Cover	T-Stat	0.40	2.93	1.52	5.65	-4.64	0.97
	P-Value	0.35	4.52E-03	7.32E-02	1.15E-05	1.02E-04	0.17

**Table 5. List of plants found during plant counts and split into either beneficial or invasive.**

Beneficial		Invasive	
Name	Common Name	Name	Common Name
<i>Achnatherum hymenoides</i>	Indian Ricegrass	<i>Halogeton glomeratus</i>	Halogeton
<i>Atriplex confertifolia</i>	Shadscale Saltbush	<i>Bromus tectorum</i>	Cheatgrass
<i>Atriplex corrugata</i>	Mat Saltbush	<i>Salsola tragus</i>	Russian Thistle
<i>Chrysothamnus Greenei</i>	Greene's Rabbitbrush	<i>Lappula occidentalis</i>	Western Stickseed
<i>Bassia prostrata</i>	Forage Kochia	<i>Bassia scoparia</i>	Kochia
<i>Atriplex gardneri</i>	Gardner Saltbush	<i>Brassica rapa</i>	Field Mustard
<i>Sphaeralcea munroana</i>	Munro's Globemallow	<i>Lepidium campestre</i>	Field Pepperweed
<i>Sarcobatus vermiculatus</i>	Greasewood	<i>Machaeranthera canescens</i>	Hoary Aster
<i>Hesperostipa comata</i>	Needle and Thread Grass		
<i>Plantago patagonica</i>	Woolly Plantain		
<i>Artemisia nova</i>	Black Sagebrush		
<i>Tetradymia spinosa</i>	Shortspine Horsebrush		
<i>Agropyron cristatum</i>	Crested Wheatgrass		
<i>Tetradymia nuttallii</i>	Nuttall's Horsebrush		
<i>Opuntia polyacantha</i>	Plains Pricklypear		
<i>Artemisia pygmaea</i>	Pygmy Sagebrush		
<i>Cryptantha kelseyana</i>	Kelsey's Cryptantha		
<i>Ericameria nauseosa</i>	Rubber Rabbitbrush		
<i>Sporobolus cryptandrus</i>	Sand Dropseed		
<i>Sphaeralcea coccinea</i>	Scarlet Globemallow		

**Table 6. Site names with corresponding GPS coordinates, dates sampled, and number of days since the start of reclamation. Site 9-18-9-19 has been used for previous studies and has been disturbed multiple times since reclamation was started.**

Site ID	GPS Coordinates (DD)	Date Soil Sample Collected	Days Under Reclamation	Date CO <sub>2</sub> Measured	Date Soil Aggregate Stability Collected
2-35-8-18	40.0757° -109.8626°	23-May-2018	76	19-Sep-2018	--
2-35-8-18_RL	40.0768° -109.8629°	23-May-2018	--	19-Sep-2018	--
12-11-9-18	40.0437° -109.8678°	23-May-2018	666	20-Sep-2018	22-April-2019
12-11-9-18_RL	40.0432° -109.8673°	23-May-2018	--	20-Sep-2018	22-April-2019
9-18-9-19	40.0362° -109.8163°	23-May-2018	10,648	--	22-April-2019
9-18-9-19_RL	40.0364° -109.8169°	23-May-2018	--	--	22-April-2019
7-8-9-18	40.0475° -109.9147°	24-May-2018	435	--	--
7-8-9-18_RL	40.0474° -109.9157°	24-May-2018	--	--	--
14-21-9-18Y	40.0111° -109.9062°	24-May-2018	3,028	--	--
14-21-9-18Y_RL	40.0111° -109.9070°	24-May-2018	--	--	--
11-12-9-17	40.0430° -109.9573°	24-May-2018	162	--	--
11-12-9-17_RL	40.0425° -109.9585°	24-May-2018	--	--	--

**Table 7. SAS Studio software output for multiple regression for EM<sub>H</sub> with all 240 sample sites and all soil properties that could impact EM<sub>H</sub>. Significant factors include: SAR, soil temperature, soil moisture, soil organic carbon, and soil pH.**

<b>The REG Procedure</b> <b>Model: MODEL1</b> <b>Dependent Variable: EMh</b>			
Number of Observations Read	241		
Number of Observations Used	240		
Number of Observations with Missing Values	1		

Analysis of Variance					
Source	DF	Sum of Squares	Mean Square	F Value	Pr > F
Model	9	18358	2039.75878	11.17	<.0001
Error	230	42012	182.66149		
Corrected Total	239	60370			

Root MSE	13.51523	R-Square	0.3041
Dependent Mean	24.16481	Adj R-Sq	0.2769
Coeff Var	55.92938		

Parameter Estimates				
Variable	DF	Parameter Estimate	Standard Error	t Value Pr >  t
Intercept	1	-133.33410	392.06467	-0.34 0.7341
Sand	1	1.72790	3.90560	0.44 0.6586
Silt	1	1.25066	3.92498	0.32 0.7503
Clay	1	1.65814	3.90221	0.42 0.6713
SOC	1	0.05170	0.01843	2.81 0.0055
pH	1	-7.07772	3.07662	-2.30 0.0223
ECe	1	-0.29407	0.73090	-0.40 0.6878
SAR	1	0.26412	0.06217	4.25 <.0001
Temp	1	0.97745	0.24507	3.99 <.0001
Moisture	1	6.58463	1.37980	4.77 <.0001

**Table 8. SAS Studio software output for multiple regression for EM<sub>H</sub>, with all 240 sample sites and soil properties that had the greatest influence from the original multiple regression (Table 7). SAR had the greatest influence out of the five soil properties.**

<b>The REG Procedure</b> <b>Model: MODEL1</b> <b>Dependent Variable: EMh</b>			
Number of Observations Read	241		
Number of Observations Used	240		
Number of Observations with Missing Values	1		

Analysis of Variance					
Source	DF	Sum of Squares	Mean Square	F Value	Pr > F
Model	5	14615	2923.02522	14.95	<.0001
Error	234	45755	195.53353		
Corrected Total	239	60370			

Root MSE	13.98333	R-Square	0.2421
Dependent Mean	24.16481	Adj R-Sq	0.2259
Coeff Var	57.86649		

Parameter Estimates				
Variable	DF	Parameter Estimate	Standard Error	t Value Pr >  t
Intercept	1	36.77758	27.61820	1.33 0.1843
SOC	1	0.06336	0.01854	3.42 0.0007
pH	1	-6.73888	3.04612	-2.21 0.0279
SAR	1	0.17679	0.04413	4.01 <.0001
Temp	1	0.84093	0.24345	3.45 0.0007
Moisture	1	4.11707	1.13480	3.63 0.0004



**Table 9. SAS Studio software output for multiple regression for EM<sub>H</sub>, using the ground truthing (101) sample sites and all soil properties that could impact EM<sub>H</sub>. Significant factors include: SAR and soil moisture.**

<b>The REG Procedure</b> <b>Model: MODEL1</b> <b>Dependent Variable: EMh</b>			
Number of Observations Read	128		
Number of Observations Used	101		
Number of Observations with Missing Values	27		

Analysis of Variance				
Source	DF	Sum of Squares	Mean Square	Pr > F
Model	9	8466.71818	940.74646	4.85 < .0001
Error	91	17652	193.97391	
Corrected Total	100	26118		

Root MSE	13.92745	R-Square	0.3242
Dependent Mean	23.85643	Adj R-Sq	0.2573
Coeff Var	58.38029		

Parameter Estimates				
Variable	DF	Parameter Estimate	Standard Error	t Value
Intercept	1	32.39983	499.85775	0.06
Sand	1	-0.16394	4.99044	-0.03
Silt	1	-0.72781	5.01116	-0.15
Clay	1	-0.75518	5.00209	-0.15
SOC	1	0.05918	0.03613	1.64
pH	1	-1.39962	4.85875	-0.29
ECe	1	0.58580	1.24076	0.47
SAR	1	0.51655	0.16632	3.11
Temp	1	0.55309	0.41354	1.34
Moisture	1	5.82174	2.15807	2.70

**Table 10. SAS Studio software output for multiple regression for EM<sub>H</sub>, using the ground truthing (101) sites and soil properties that had the greatest influence from the original multiple regression (Table 9). SAR had the greatest influence between SAR and soil moisture.**

<b>The REG Procedure</b> <b>Model: MODEL1</b> <b>Dependent Variable: EMh</b>			
Number of Observations Read	102		
Number of Observations Used	101		
Number of Observations with Missing Values	1		

Analysis of Variance				
Source	DF	Sum of Squares	Mean Square	Pr > F
Model	2	4200.20903	2100.10451	9.39 0.0002
Error	98	21918	223.65444	
Corrected Total	100	26118		

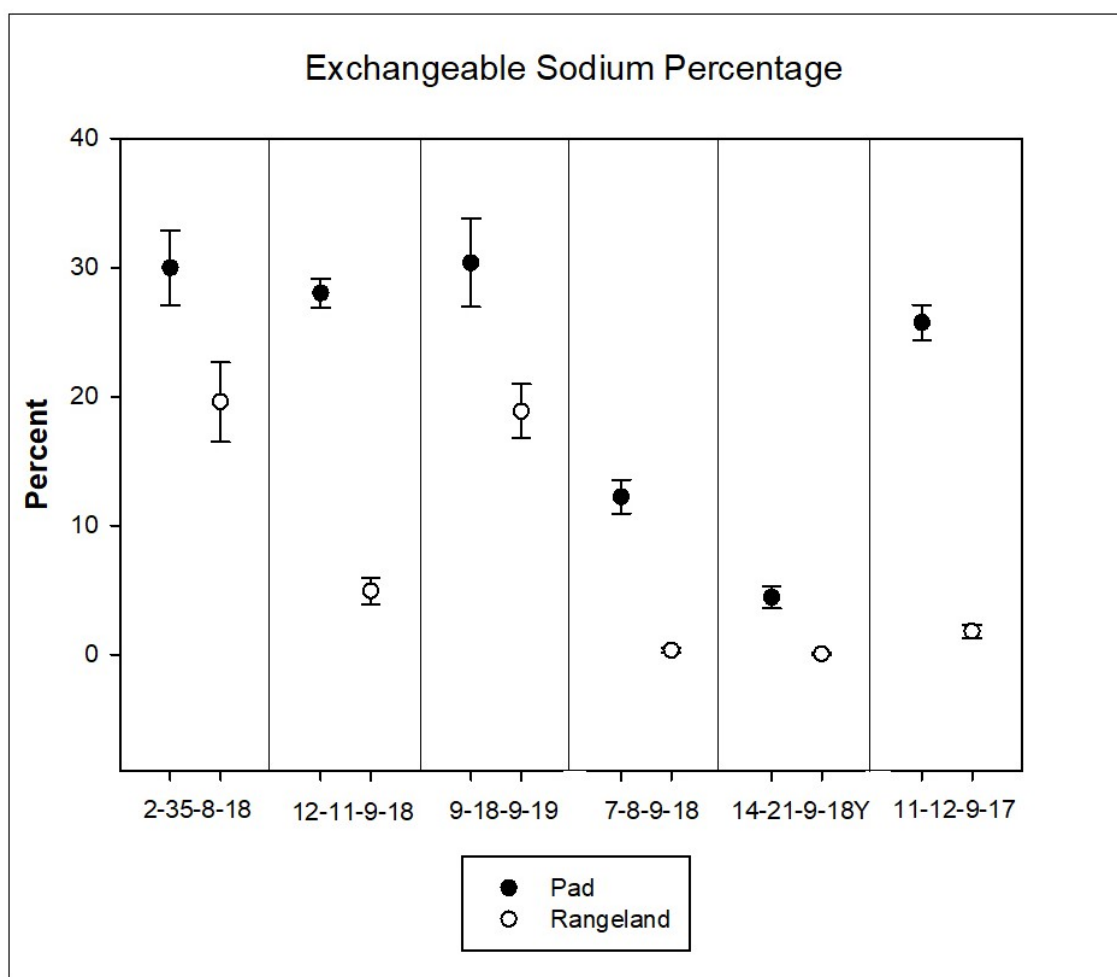
Root MSE	14.95508	R-Square	0.1608
Dependent Mean	23.85643	Adj R-Sq	0.1437
Coeff Var	62.68785		

Parameter Estimates				
Variable	DF	Parameter Estimate	Standard Error	t Value
Intercept	1	10.16528	3.86962	2.63
SAR	1	0.33030	0.09415	3.51
Moisture	1	3.43173	1.30633	2.63

**Table 11. Dates, soil moisture, soil temperature, and the number of ground truthing for each location for EMI.**

Pad #	Date EM <sub>H</sub> Measured	Soil Moisture (%)	Soil Temperature (C°)	# of Ground Truthing Samples
2-35-8-18	21-May-2018	1.7	34.5	12
2-35-8-18_RL	21-May-2018	1.6	36.5	12
12-11-9-18	21-May-2018	4.0	30.5	6
12-11-9-18_RL	21-May-2018	1.8	38	6
9-18-9-19	18-Sep-2018	1.8	35.5	8
9-18-9-19_RL	18-Sep-2018	1.5	34.5	9
7-8-9-18	21-May-2018	4.8	24	12
7-8-9-18_RL	18-Sep-2018	1.9	31.5	9
14-21-9-18Y	21-May-2018	2.4	28.5	6
14-21-9-18Y_RL	21-May-2018	2.3	29	6
11-12-9-17	21-May-2018	3.9	28	6
11-12-9-17_RL	18-Sep-2018	2.1	21.5	9



**Fig. 27. Exchangeable Sodium Percentage (ESP) mean and error at all six locations.**

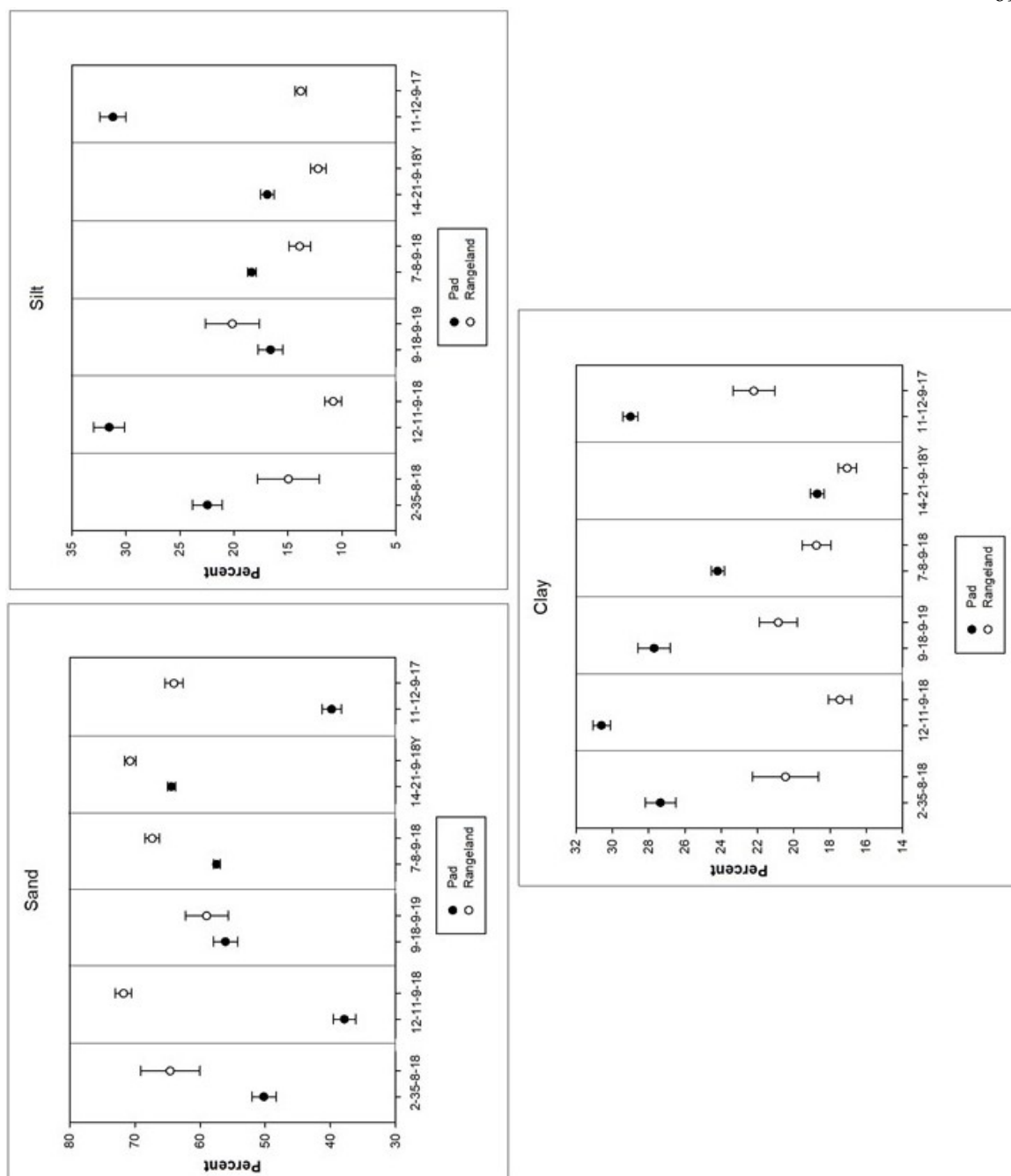


**Fig. 28. Percentages of sand (top left), silt (top right), and clay (bottom) with mean and error at all six locations.**

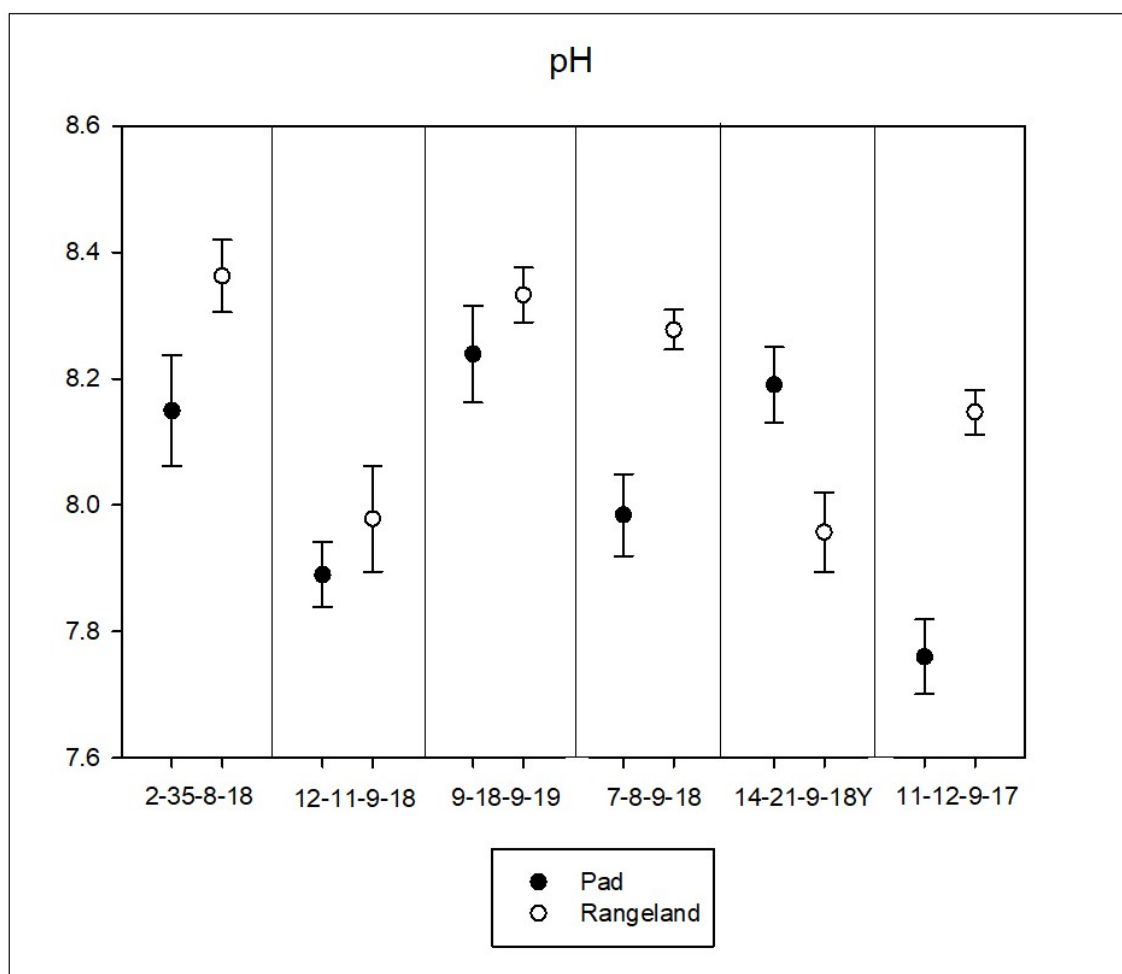


**Fig. 29. Soil pH mean and error at all six locations.**

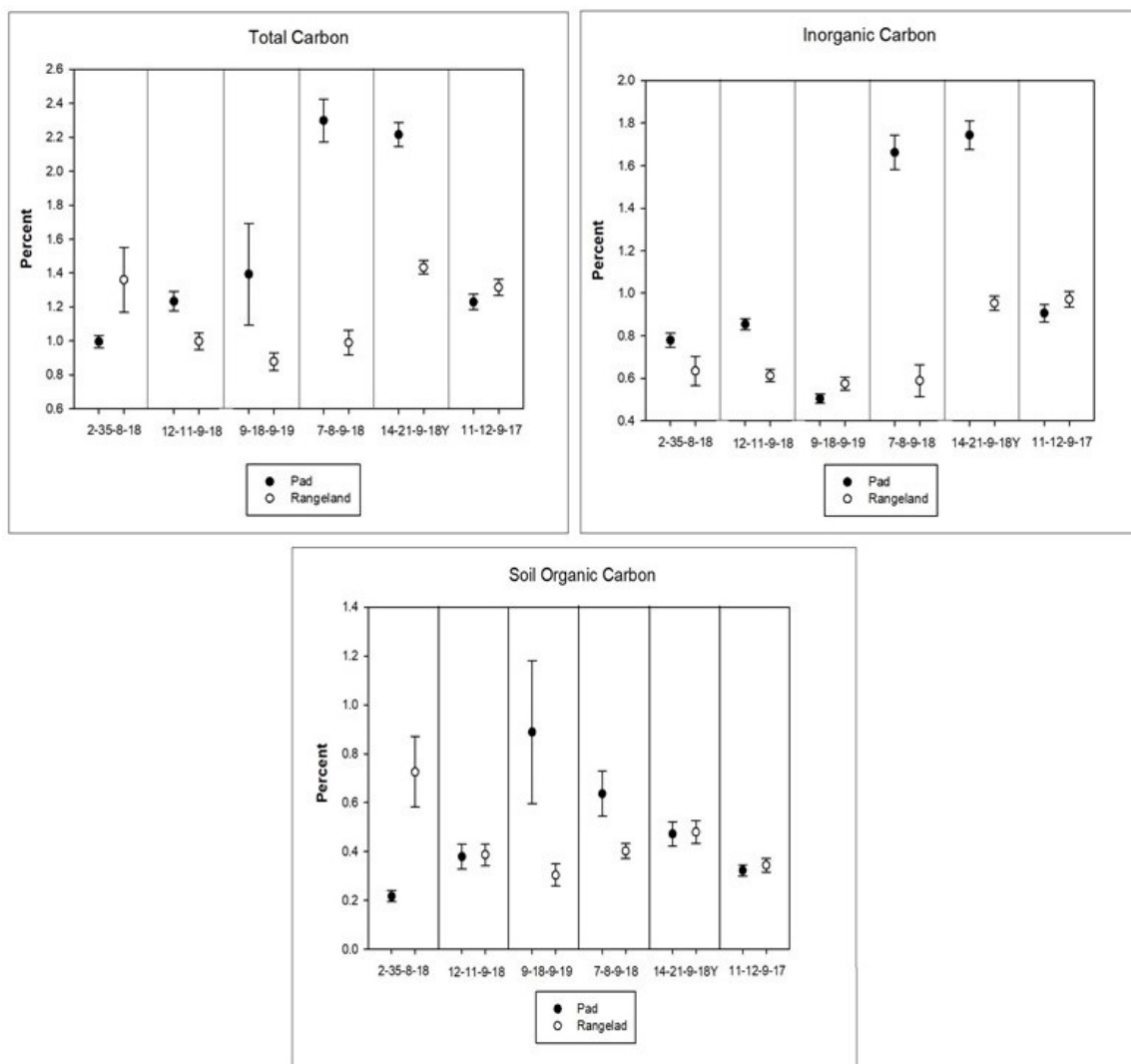


**Fig. 30. Percentages of total carbon (TC), inorganic carbon (IC), and soil organic carbon (SOC) with mean and error at all six locations.**

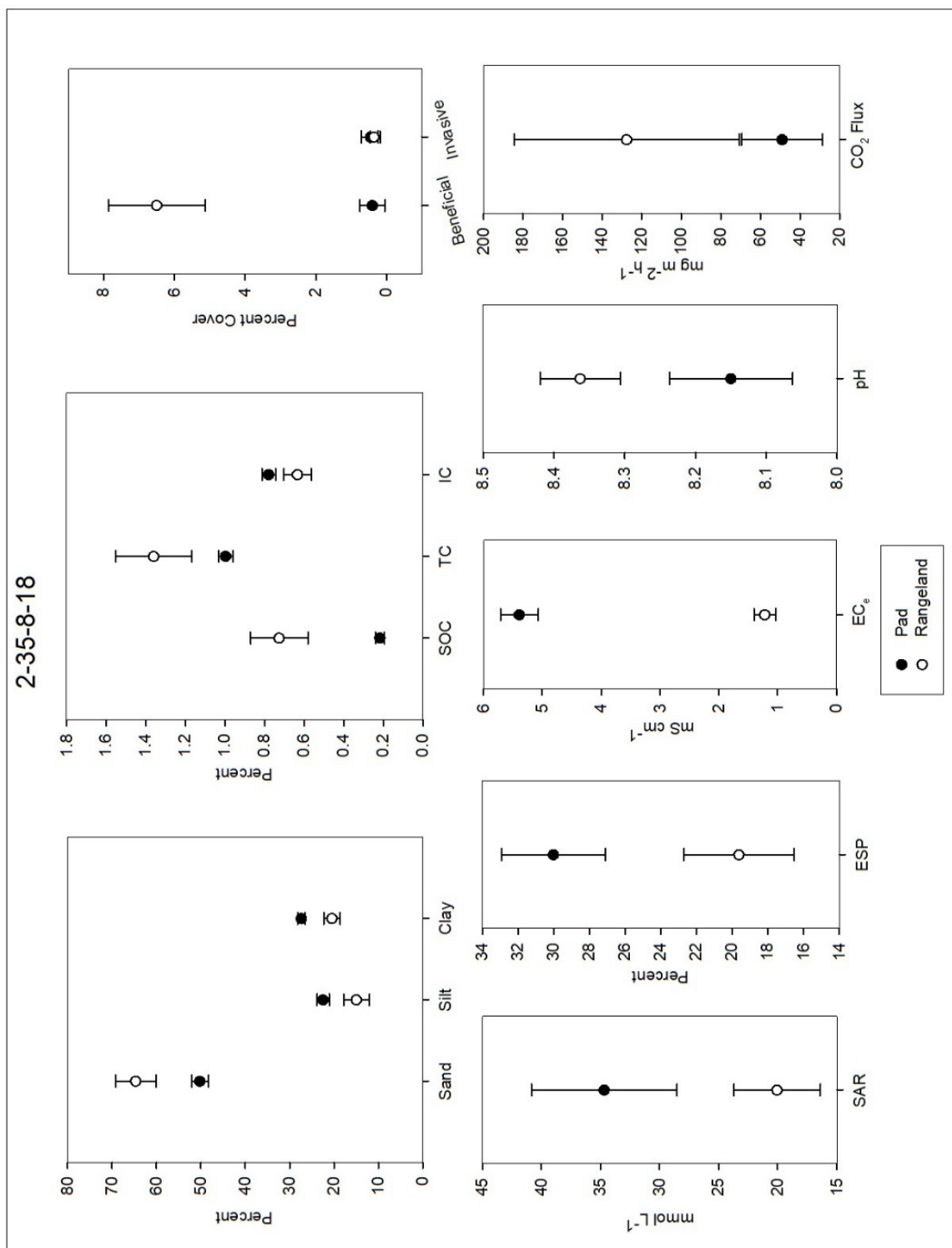


**Fig. 31. Compilation of mean and error for all soil tests performed between P&A well pad 2-35-8-18 and the adjacent rangeland.**

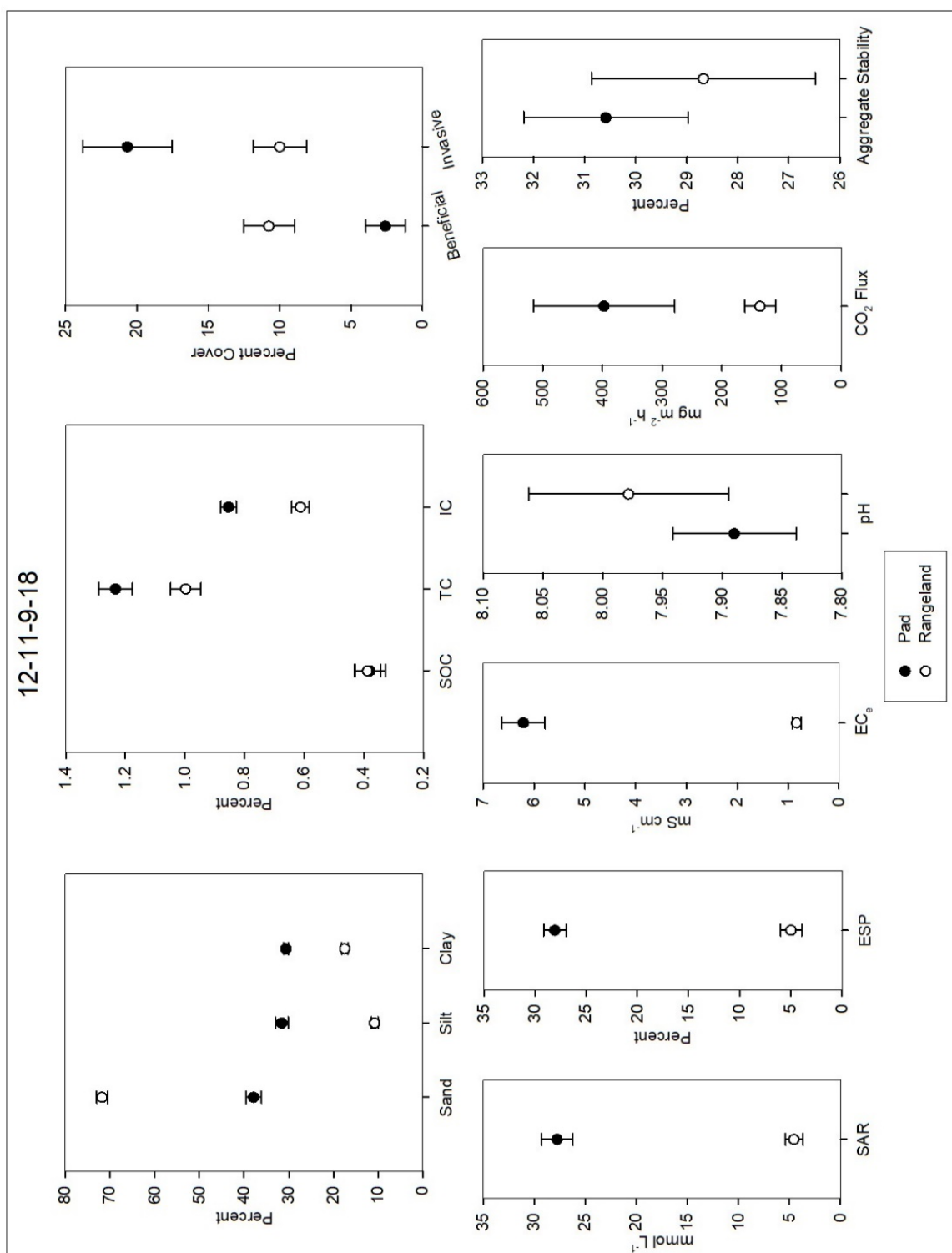


**Fig. 32. Compilation of mean and error for all soil tests performed between P&A well pad 12-11-9-18 and the adjacent rangeland.**



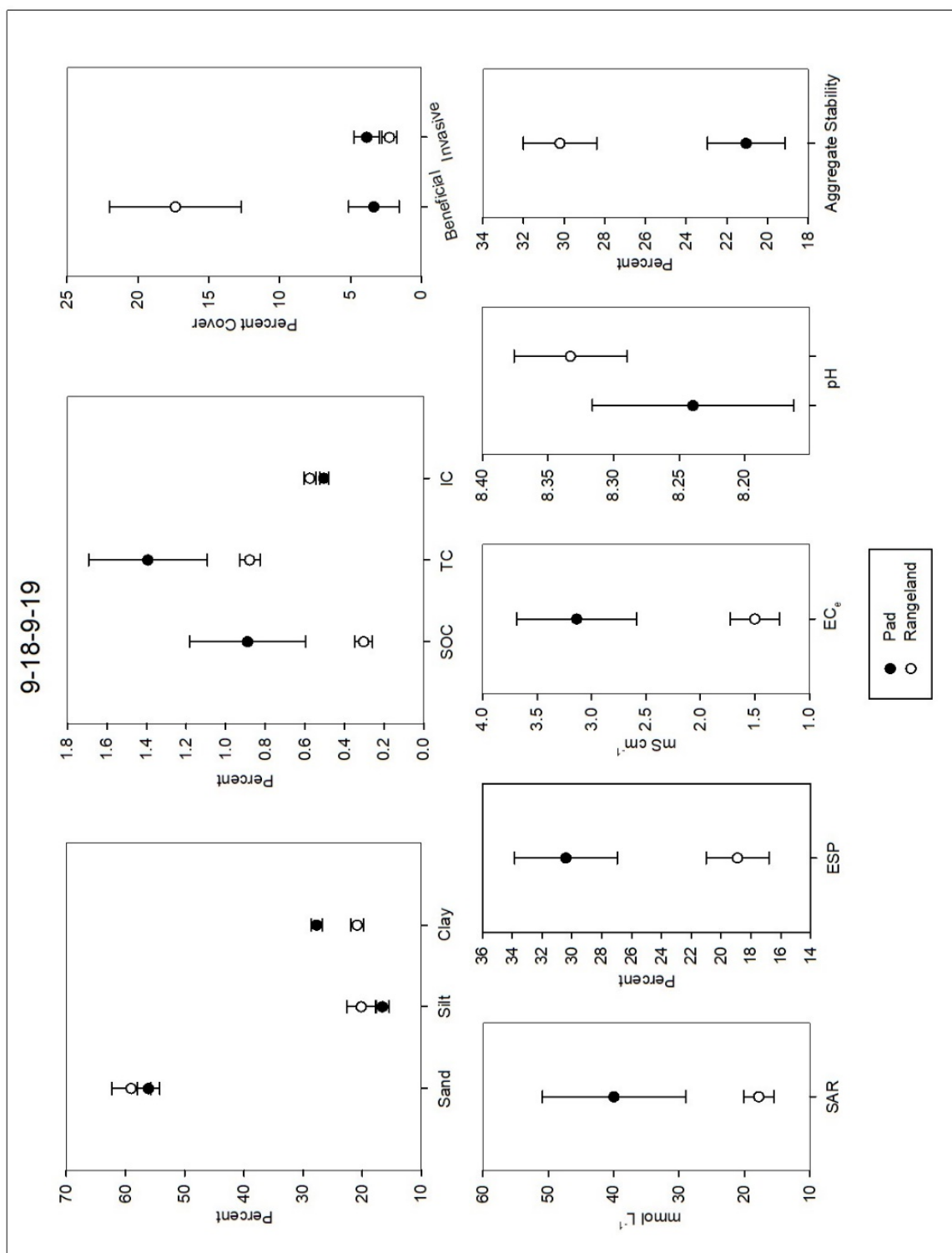


**Fig. 33.** Compilation of mean and error for all soil tests performed between P&A well pad 9-18-9-19 and the adjacent rangeland.

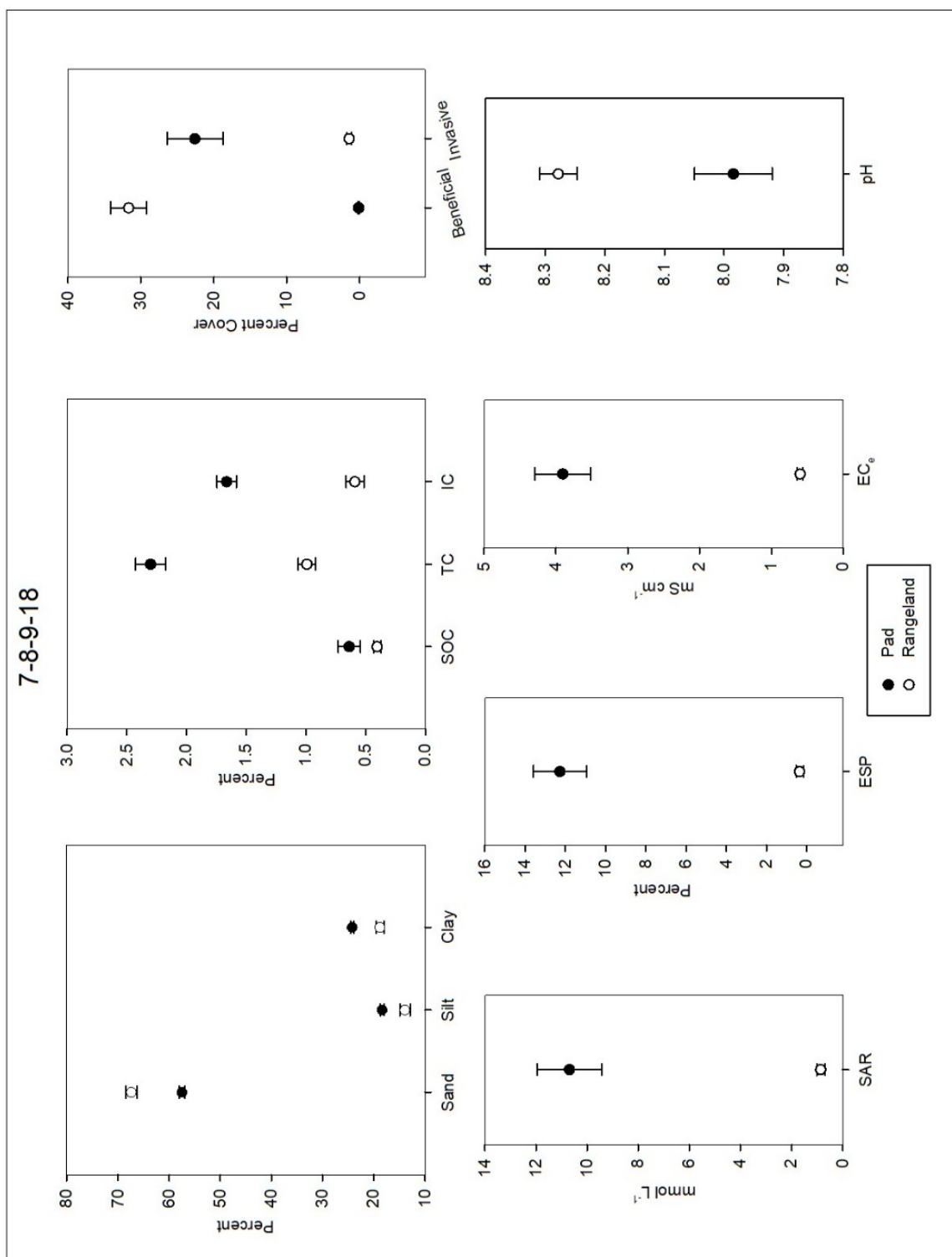


**Fig. 34. Compilation of mean and error for all soil tests performed between P&A well pad 7-8-9-18 and the adjacent rangeland.**

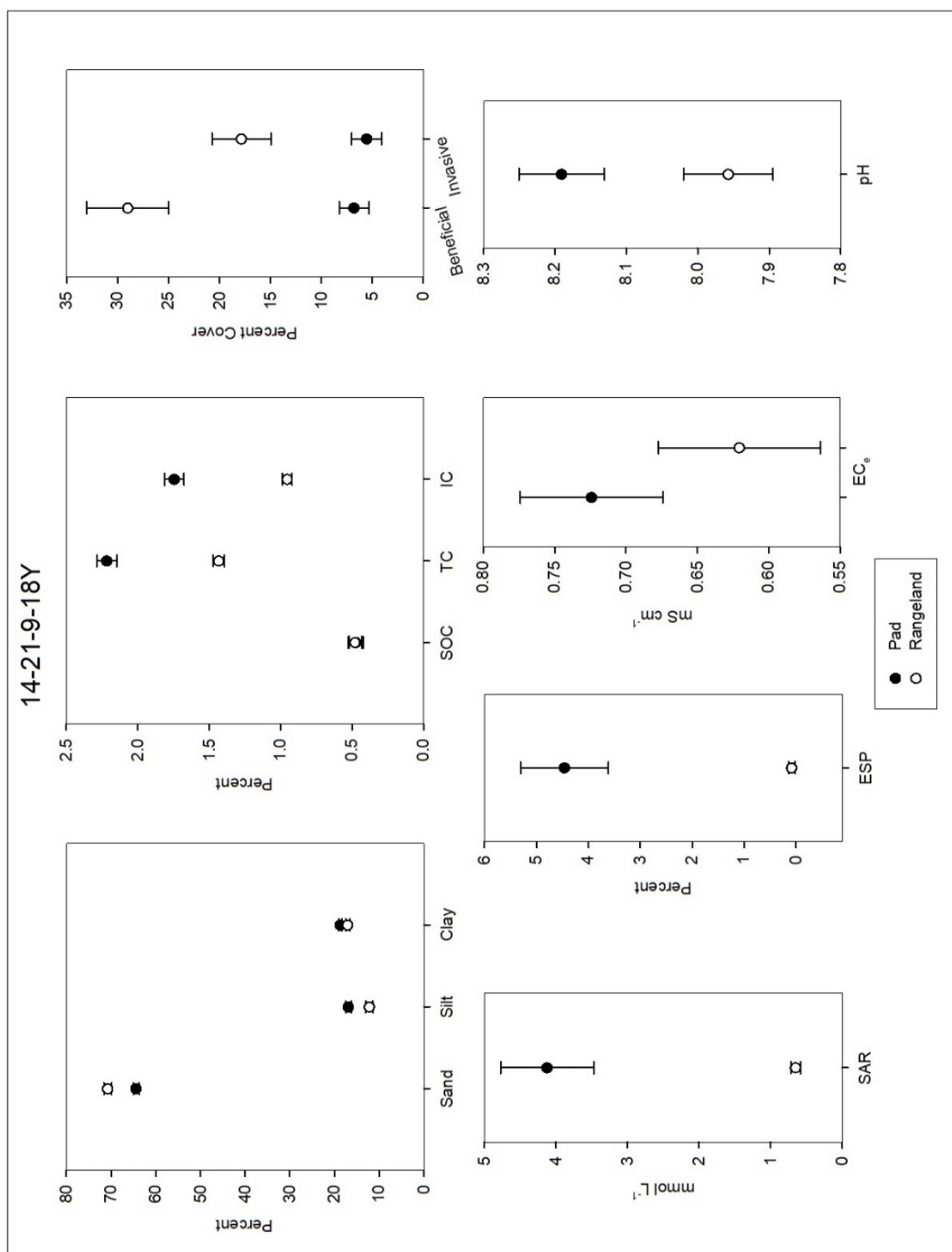
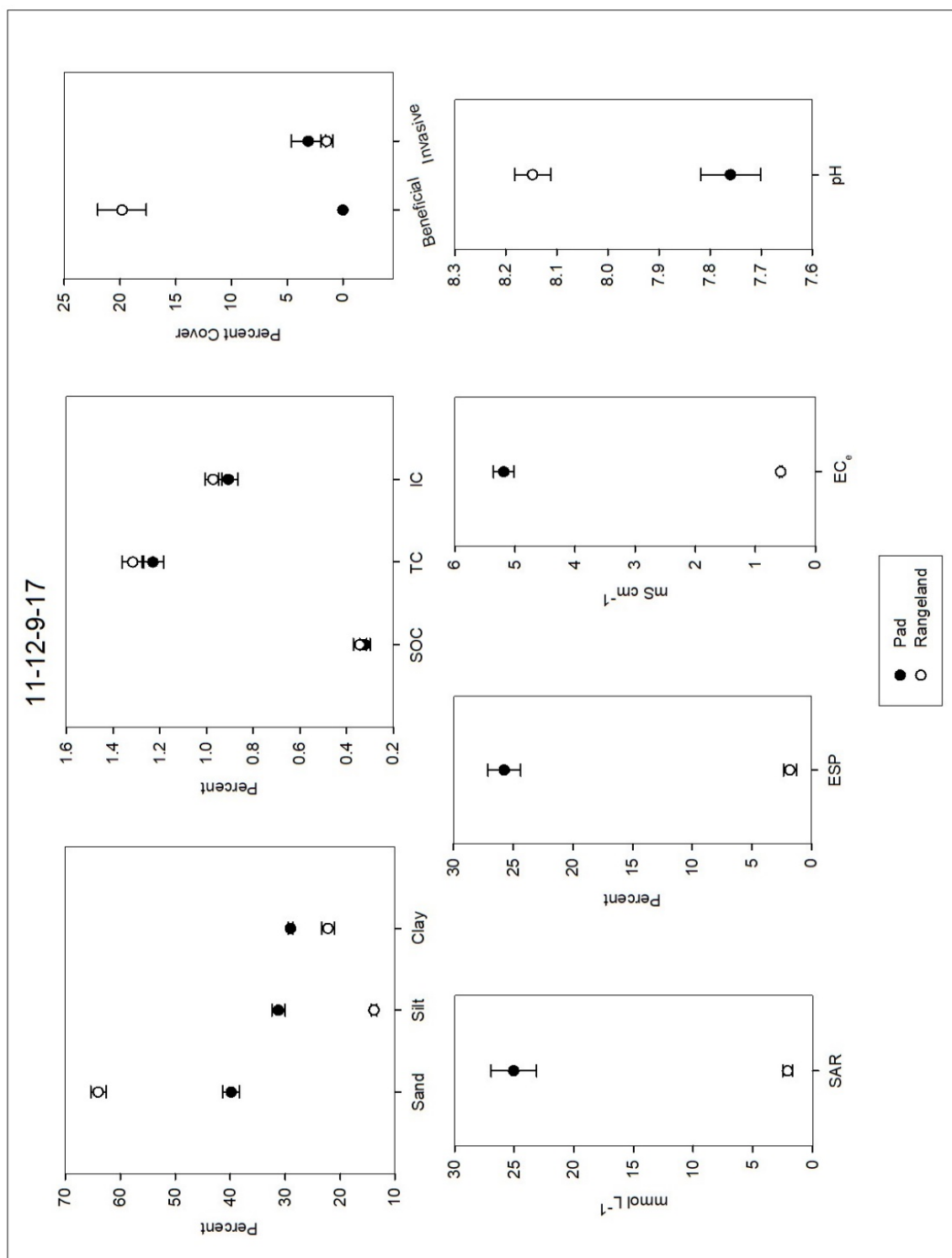
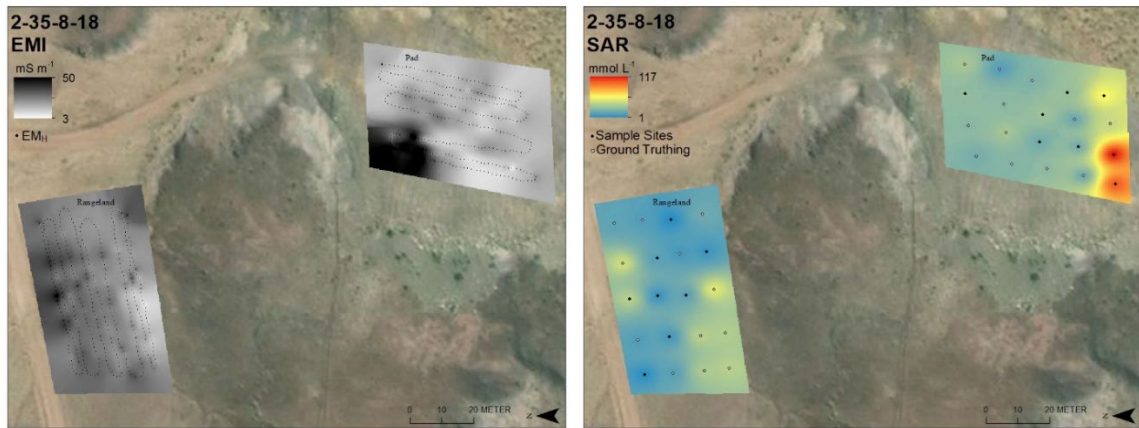


Fig. 35. Compilation of mean and error for all soil tests performed between P&A well pad 14-21-9-18Y and the adjacent rangeland.



**Fig. 36. Compilation of mean and error for all soil tests performed between P&A well pad 11-12-9-17 and the adjacent rangeland.**



**Fig. 37. Interpolation map displaying the EM<sub>H</sub> (left) and SAR (right) values from pad 2-35-8-18 and its corresponding rangeland. Service Layer Credits: Source: Esri, DigitalGlobe, GeoEye, Earthstar Geographics, CNES/Airbus DS, USDA, AeroGRID, IGN, and the GIS User Community.**

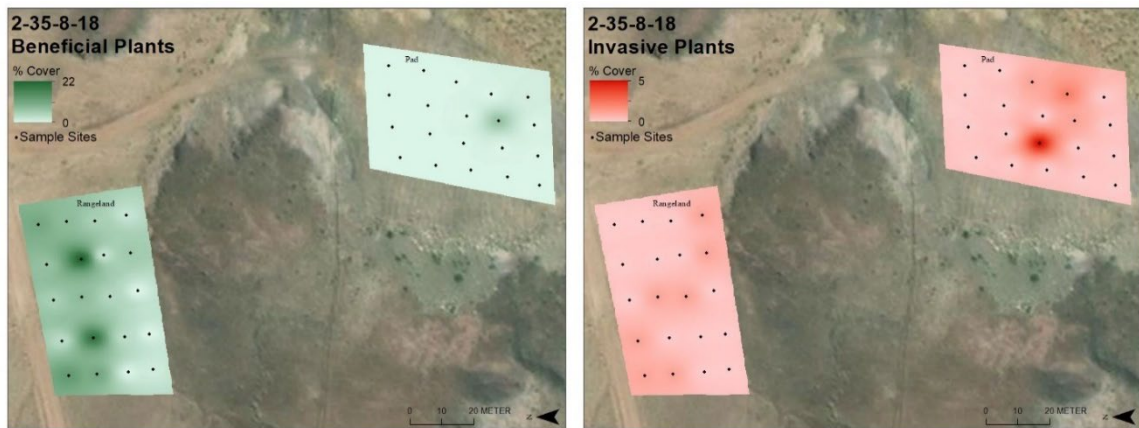


**Fig. 38. Interpolation map displaying the percent of plant cover of beneficial (left) and invasive (right) plants for pad 2-35-8-18 and its corresponding rangeland. Service Layer Credits: Source: Esri, DigitalGlobe, GeoEye, Earthstar Geographics, CNES/Airbus DS, USDA, AeroGRID, IGN, and the GIS User Community.**

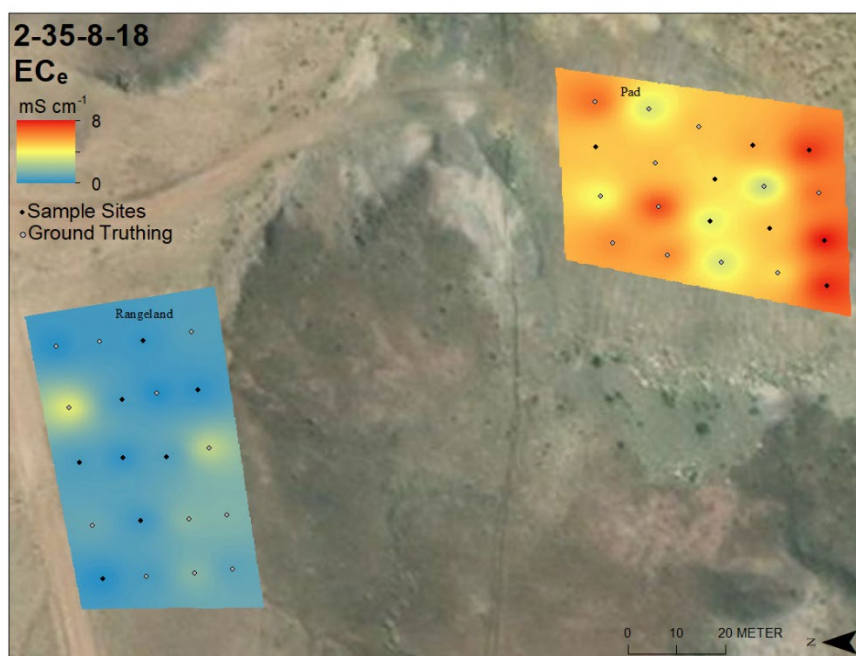


**Fig. 39. Interpolation map displaying the EC<sub>e</sub> values from pad 2-35-8-18 and its corresponding rangeland. Service Layer Credits: Source: Esri, DigitalGlobe, GeoEye, Earthstar Geographics, CNES/Airbus DS, USDA, AeroGRID, IGN, and the GIS User Community.**

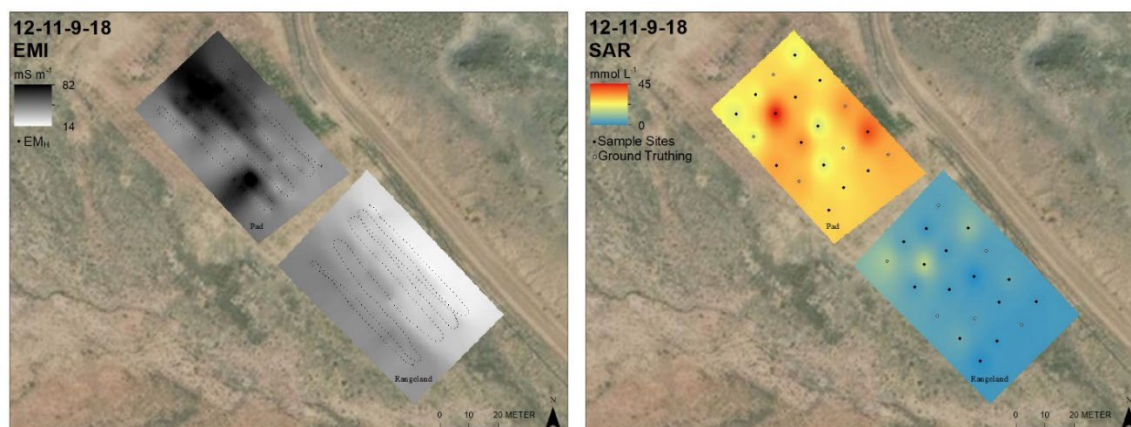


**Fig. 40. Interpolation map displaying the EM<sub>H</sub> (left) and SAR (right) values from pad 12-11-9-18 and its corresponding rangeland. Service Layer Credits: Source: Esri, DigitalGlobe, GeoEye, Earthstar Geographics, CNES/Airbus DS, USDA, AeroGRID, IGN, and the GIS User Community.**



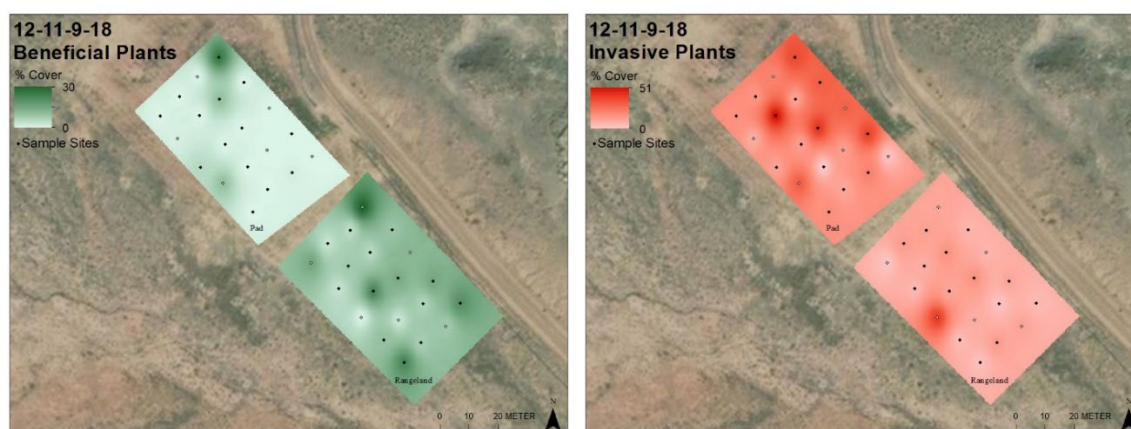


**Fig. 41. Interpolation map displaying the percent of plant cover of beneficial (left) and invasive (right) plants for pad 12-11-9-18 and its corresponding rangeland. Service Layer Credits: Source: Esri, DigitalGlobe, GeoEye, Earthstar Geographics, CNES/Airbus DS, USDA, AeroGRID, IGN, and the GIS User Community.**

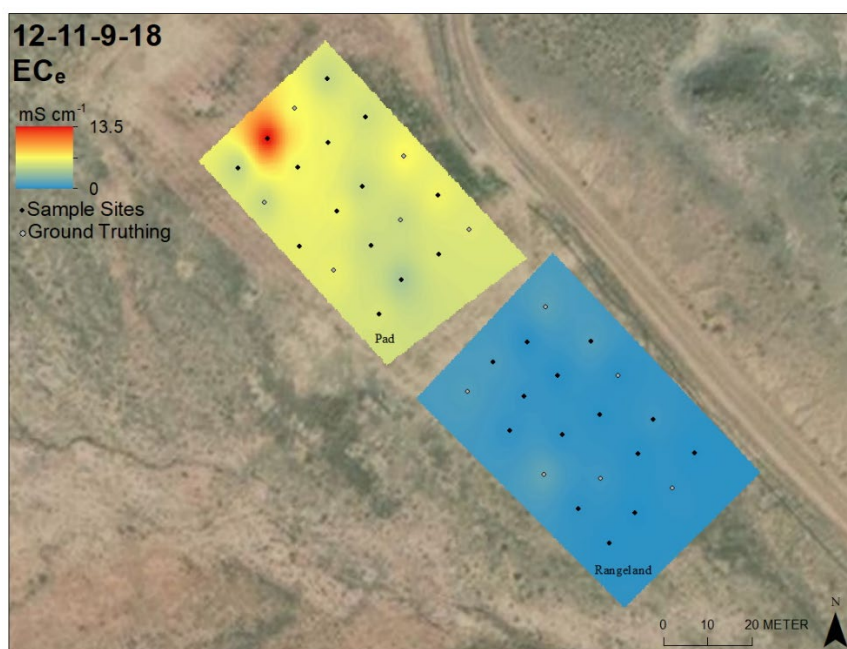


**Fig. 42. Interpolation map displaying the EC<sub>e</sub> values from pad 12-11-9-18 and its corresponding rangeland. Service Layer Credits: Source: Esri, DigitalGlobe, GeoEye, Earthstar Geographics, CNES/Airbus DS, USDA, AeroGRID, IGN, and the GIS User Community.**

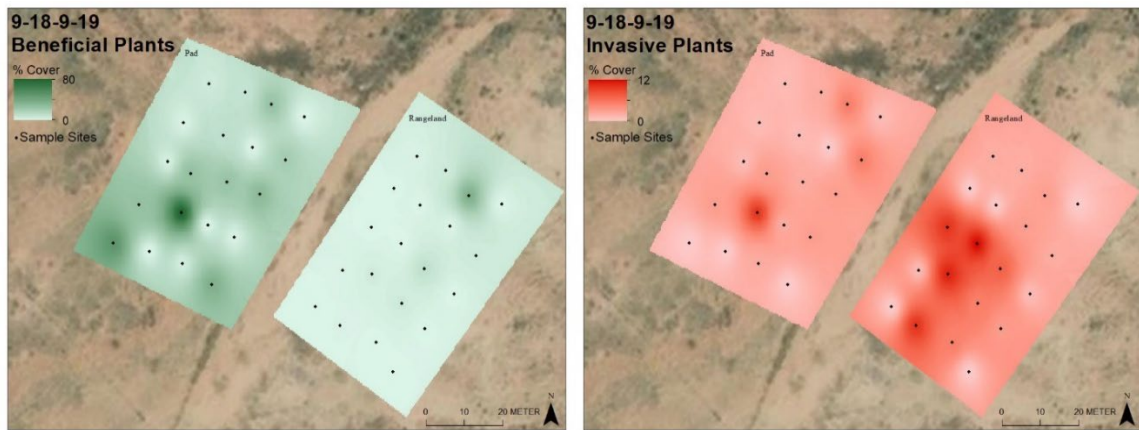


**Fig. 43.** Interpolation map displaying the percent of plant cover of beneficial (left) and invasive (right) plants for pad 9-18-9-19 and its corresponding rangeland. Service Layer Credits: Source: Esri, DigitalGlobe, GeoEye, Earthstar Geographics, CNES/Airbus DS, USDA, AeroGRID, IGN, and the GIS User Community.

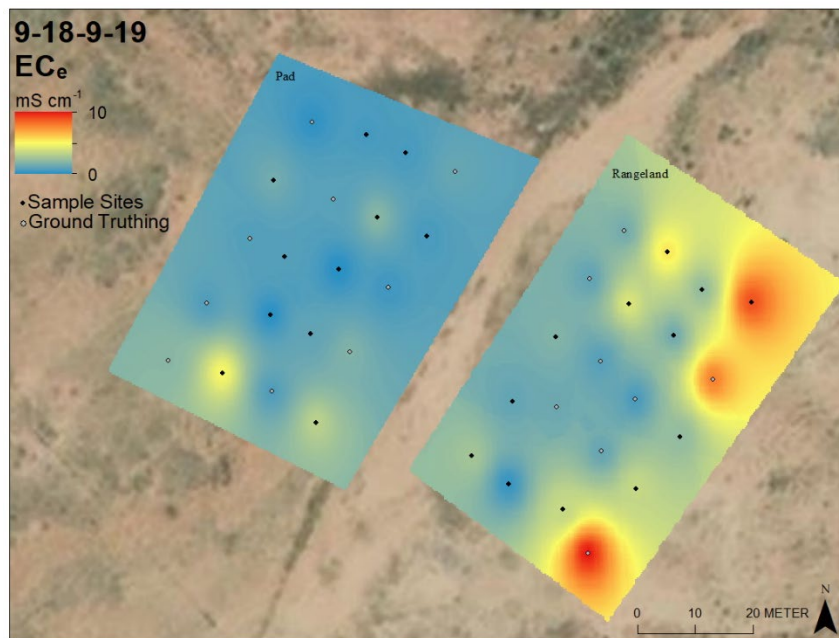


**Fig. 44.** Interpolation map displaying the EC<sub>e</sub> values from pad 9-18-9-19 and its corresponding rangeland. Service Layer Credits: Source: Esri, DigitalGlobe, GeoEye, Earthstar Geographics, CNES/Airbus DS, USDA, AeroGRID, IGN, and the GIS User Community.



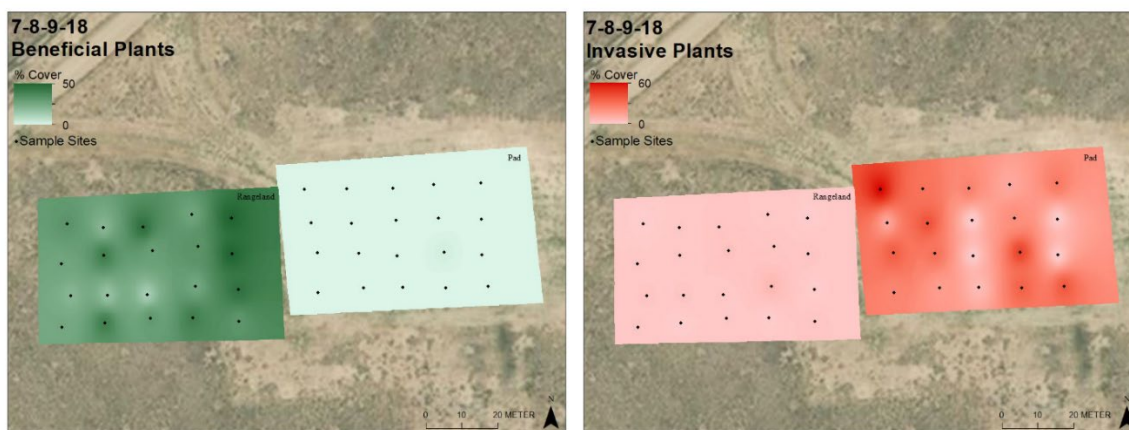


**Fig. 45. Interpolation map displaying the percent of plant cover of beneficial (left) and invasive (right) plants for pad 7-8-9-18 and its corresponding rangeland. Service Layer Credits: Source: Esri, DigitalGlobe, GeoEye, Earthstar Geographics, CNES/Airbus DS, USDA, AeroGRID, IGN, and the GIS User Community.**

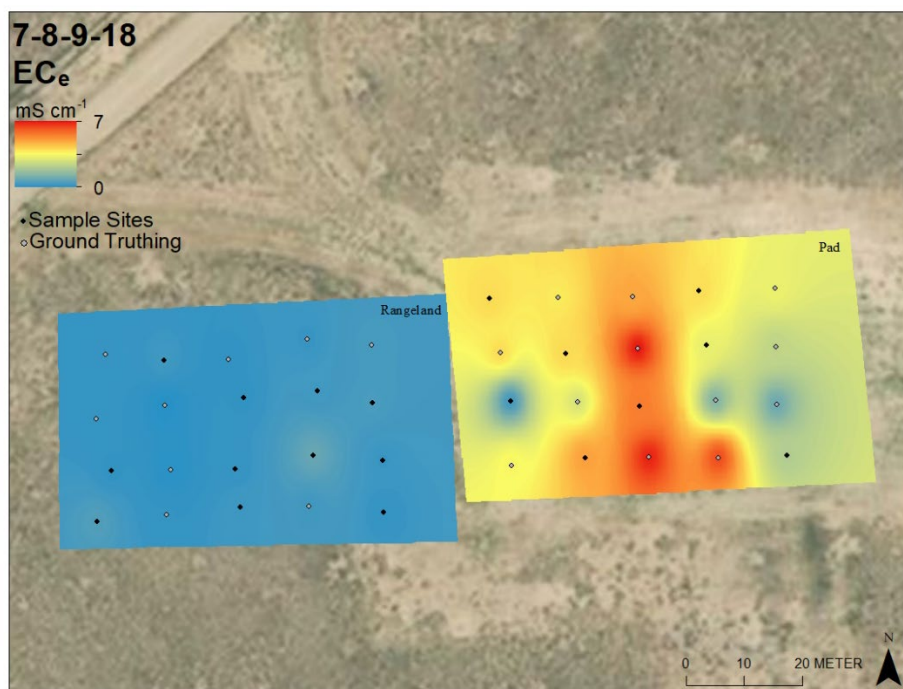


**Fig. 46. Interpolation map displaying the EC<sub>e</sub> values from pad 7-8-9-18 and its corresponding rangeland. Service Layer Credits: Source: Esri, DigitalGlobe, GeoEye, Earthstar Geographics, CNES/Airbus DS, USDA, AeroGRID, IGN, and the GIS User Community.**

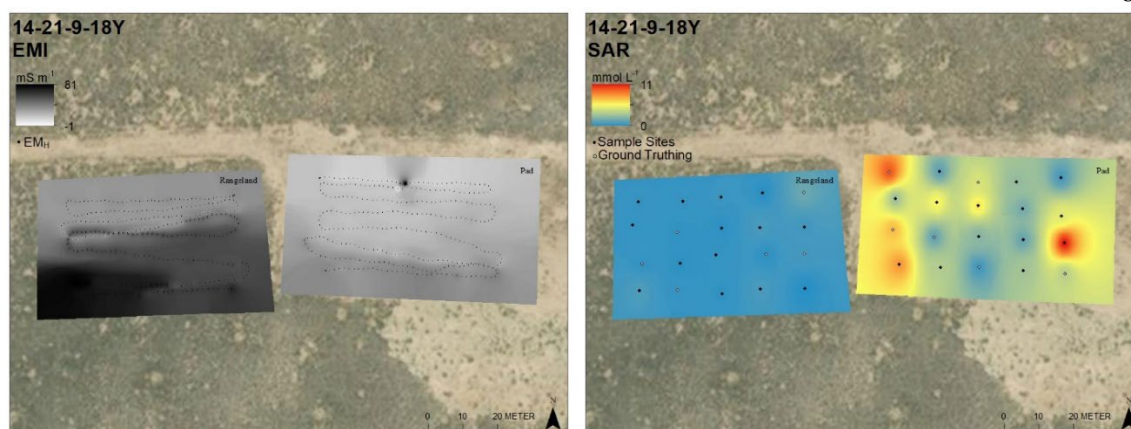


**Fig. 47.** Interpolation map displaying the EM<sub>H</sub> (left) and SAR (right) values from pad 14-21-9-18Y and its corresponding rangeland. Service Layer Credits: Source: Esri, DigitalGlobe, GeoEye, Earthstar Geographics, CNES/Airbus DS, USDA, AeroGRID, IGN, and the GIS User Community.

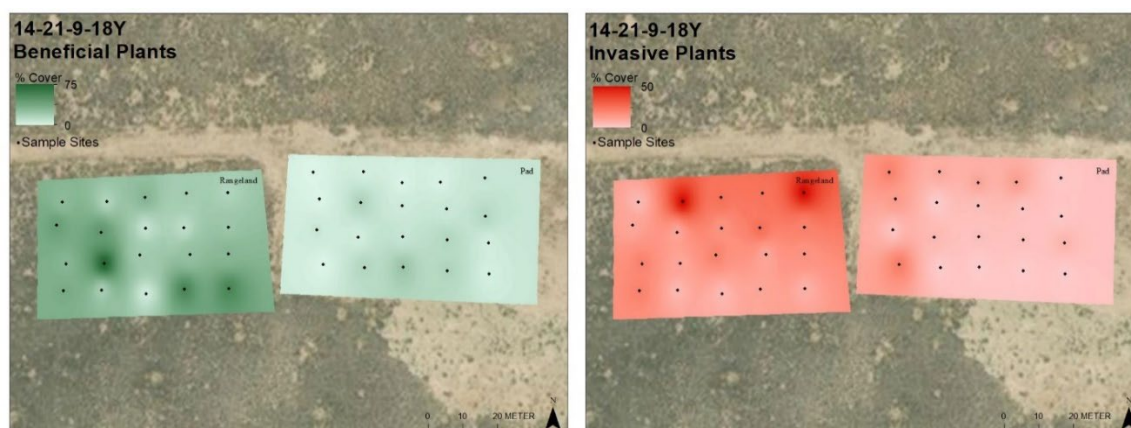


**Fig. 48.** Interpolation map displaying the percent of plant cover of beneficial (left) and invasive (right) plants for pad 14-21-9-18Y and its corresponding rangeland. Service Layer Credits: Source: Esri, DigitalGlobe, GeoEye, Earthstar Geographics, CNES/Airbus DS, USDA, AeroGRID, IGN, and the GIS User Community.

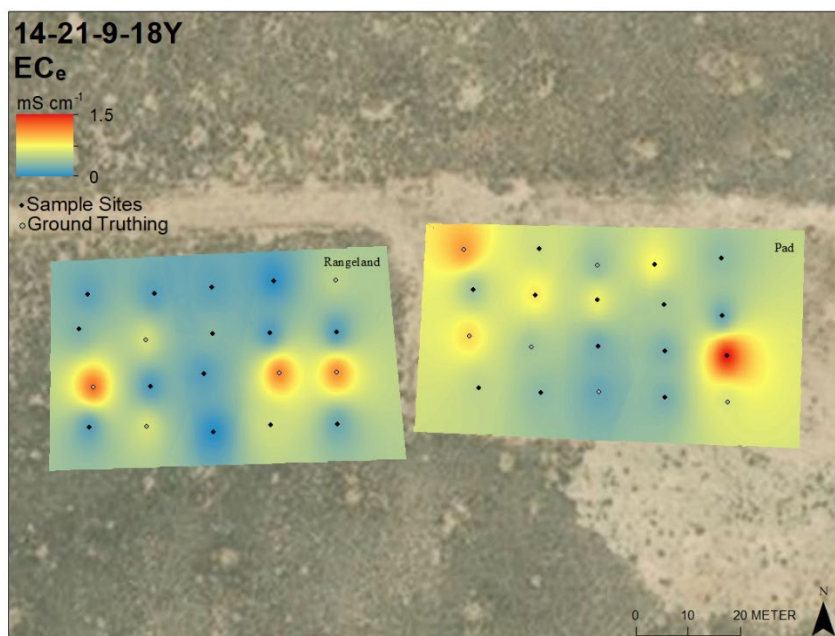


**Fig. 49. Interpolation map displaying the EC<sub>e</sub> values from pad 14-21-9-18Y and its corresponding rangeland. Service Layer Credits: Source: Esri, DigitalGlobe, GeoEye, Earthstar Geographics, CNES/Airbus DS, USDA, AeroGRID, IGN, and the GIS User Community.**

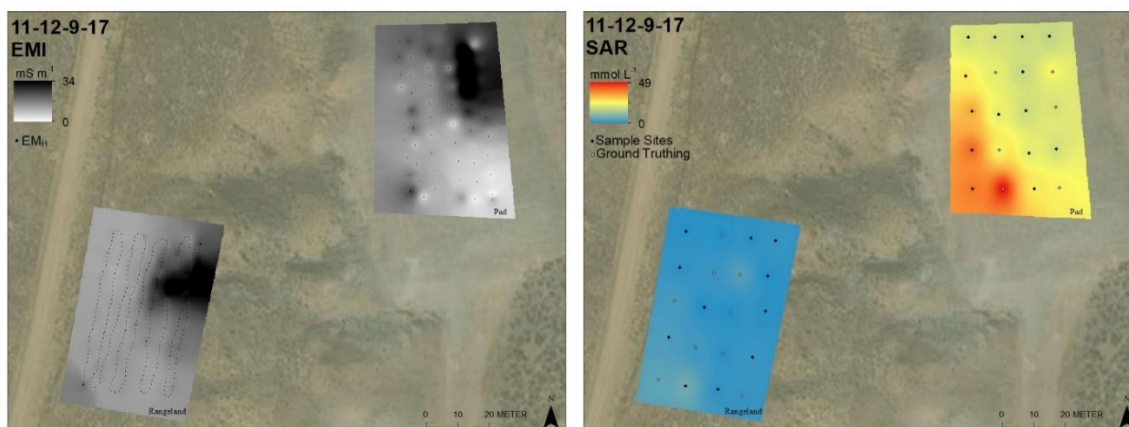


**Fig. 50. Interpolation map displaying the EM<sub>H</sub> (left) and SAR (right) values from pad 11-12-9-17 and its corresponding rangeland. Service Layer Credits: Source: Esri, DigitalGlobe, GeoEye, Earthstar Geographics, CNES/Airbus DS, USDA, AeroGRID, IGN, and the GIS User Community.**



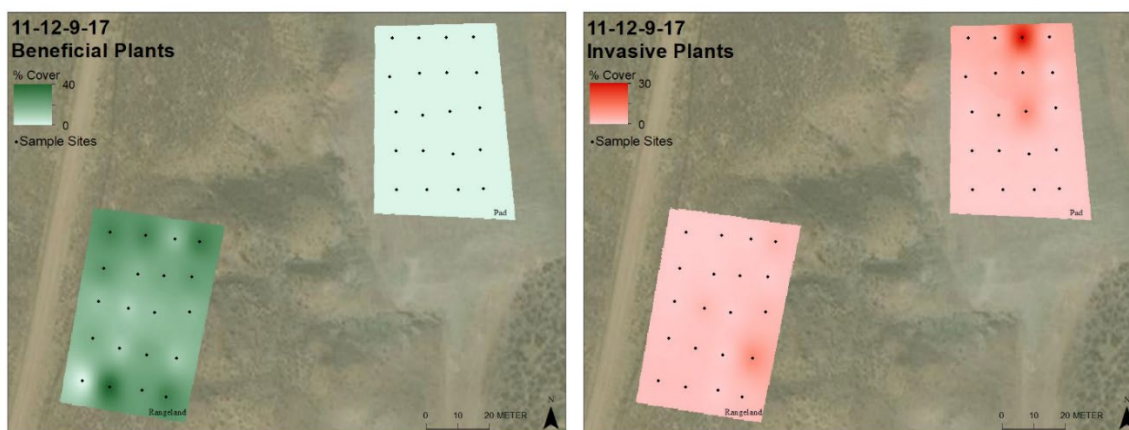


**Fig. 51. Interpolation map displaying the percent of plant cover of beneficial (left) and invasive (right) plants for pad 11-12-9-17 and its corresponding rangeland. Service Layer Credits: Source: Esri, DigitalGlobe, GeoEye, Earthstar Geographics, CNES/Airbus DS, USDA, AeroGRID, IGN, and the GIS User Community.**

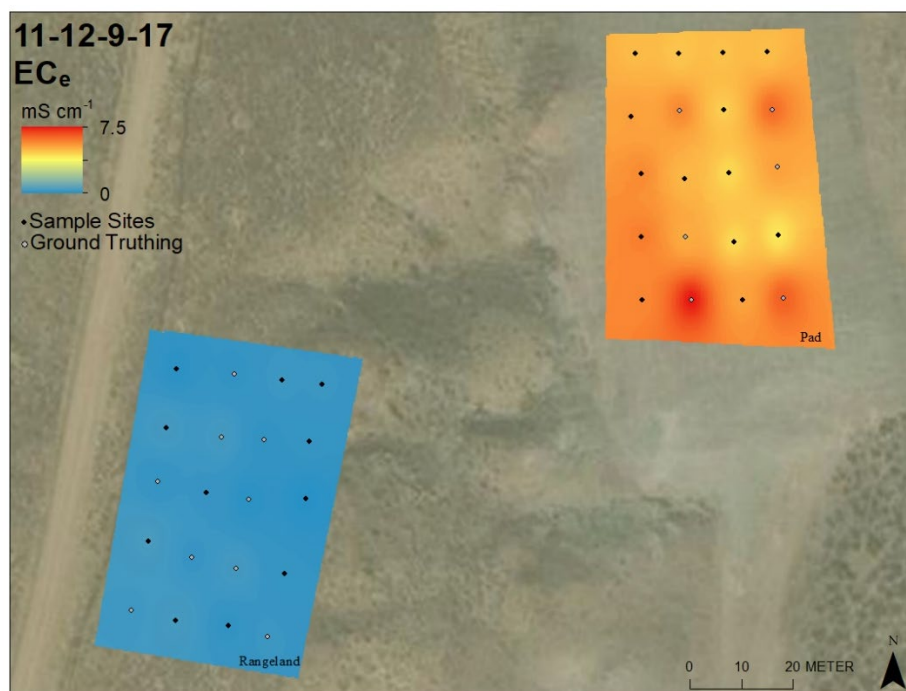


**Fig. 52. Interpolation map displaying the  $EC_e$  values from pad 11-12-9-17 and its corresponding rangeland. Service Layer Credits: Source: Esri, DigitalGlobe, GeoEye, Earthstar Geographics, CNES/Airbus DS, USDA, AeroGRID, IGN, and the GIS User Community.**



**Fig. 53. Plant counts being performed using a meter squared to measure plant cover on 12-11-9-18. Dynamic CO<sub>2</sub> flux being measured with a polycarbonate flux chamber, with the hose running to the trailer containing the LGR greenhouse gas analyzer.**



**Fig. 54. Dynamic CO<sub>2</sub> flux being measured on rangeland adjacent to 2-35-8-18 with a polycarbonate flux chamber.**





**Fig. 55. Dynamic CO<sub>2</sub> flux being measured on rangeland adjacent to 2-35-8-18 with a polycarbonate flux chamber.**



**Fig. 56. Plant counts being performed using a meter squared to measure plant cover on 2-35-8-18. Dynamic CO<sub>2</sub> flux being measured in the background with a polycarbonate flux chamber.**



**Fig. 57. Plant counts being performed using a meter squared to measure plant cover on 12-11-9-18.**



**Fig. 58. Plant counts being performed using a meter squared to measure plant cover on 2-35-8-18.**





**Fig. 59. Electromagnetic induction sensor (EMI) being carried across rangeland adjacent to 11-12-9-17.**



**Fig. 60. Well pad 9-18-9-19 with well marker present.**





**Fig. 61. Aggregate stability results after sieving and prior to being placed in oven for final drying. Tins containing non-aggregate fraction which remained after sieving and after stable aggregate was crushed and flushed out.**



**Fig. 62. Aggregate stability sieving apparatus, with aggregates being re-hydrated prior to sieving in the foreground.**



**Fig. 63.** Aggregate stability being conducted with sieving apparatus finished cycle. Slaked material (unstable aggregate) has now been collected in metal tins, while the non-aggregate and stable aggregate remain in the sieve.

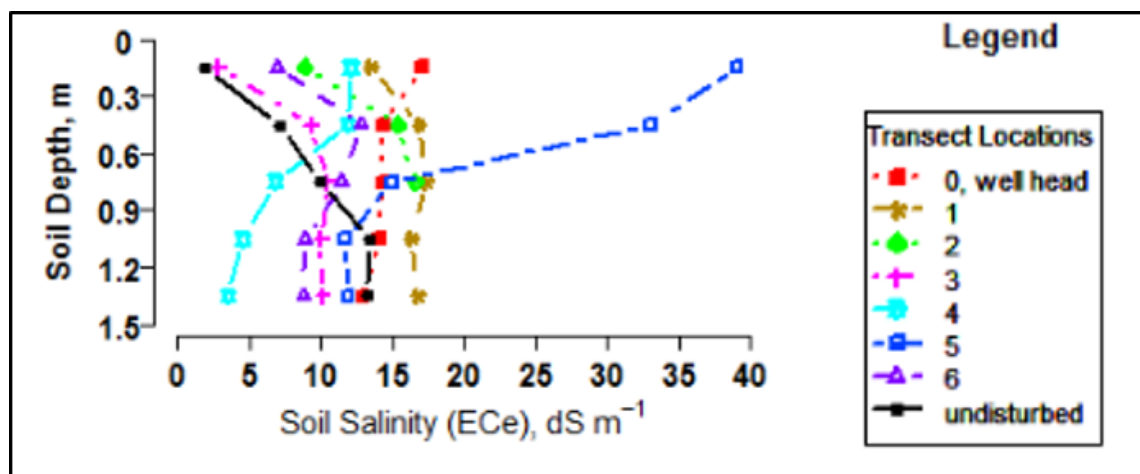


**Fig. 64.** Depth profile variation of  $EC_e$  at P&A well pad and undisturbed site (Grossl, 2017).